# UNIVERSITA' DEGLI STUDI DI TRIESTE

## XXIX CICLO DEL DOTTORATO DI RICERCA IN BIOMEDICINA MOLECOLARE

# Telomerase regulation by non-coding RNAs

Settore scientifico-disciplinare: **BIO11**


**DOTTORANDA**
Valentina Buemi

**COORDINATORE**
Prof.ssa Germana Meroni

**SUPERVISORE DI TESI**
Prof. Stefan Schoeftner


ANNO ACCADEMICO 2015 / 2016

# 1. INTRODUCTION

## 1.1 Telomeres

### 1.1.1 Historic background

Telomeres are specific nucleoprotein structures found at the end of each chromosome. Their fundamental role in the protection of the genome from degradation, unnecessary recombination and inter-chromosomal fusions has been deeply investigated in the last decades. The first insight into the existence of these protective structures is due to the eminent work of the two geneticists Herman J. Muller and Barbara McClintock that studied for the first time the unique role of telomeres. In 1938, Muller working with *Drosophila melanogaster* observed that X-ray irradiated chromosomes did not present any alterations such as deletions or inversions involving the natural ends of chromosomes. He concluded that a protective cap essential for chromosome homeostasis had to exist and he coined the term "telomere" from the Greek roots *telos* (end) and *meros* (part). Muller's analysis on alterations of chromosomes and the resulting finding of the existence of telomeres was independently complemented by the studies of Barbara McClintock on *Zea mays*. McClintock found that the breakage of chromosomes induced by X-ray irradiation caused the fusion of the two sister chromatid, thereby producing a dicentric chromosome (McClintock B. et al. 1939). This evidence supported Muller's hypothesis that telomeres play a pivotal role in chromosome protection and proper segregation of chromosomes during cell division.

Twenty years later, new evidences contributed to define the central role of telomeres in genome integrity preservation. In 1962, Leonard Hayflick and his colleague Paul Moorhead, overturning previous theories on the unlimited replicative potential of human and animal cells, discovered that human primary fibroblasts have a limited proliferative potential by demonstrating that human fibroblasts can double a finite number of times, after which they stop dividing (Hayflick L. et al. 1961). On the basis of this evidence, Hayflick and Moorhead classified the stages of cell culture into three different phases (Figure 1.1):

- Phase I is the primary culture
- Phase II is the exponential replication
- Phase III the period when cell replication ceases but metabolism continues (Hayflick L. et al. 1965). This growth arrest after a period of apparently normal cell proliferation is known as the Hayflick limit, Phase III phenomenon or replicative senescence (RS).

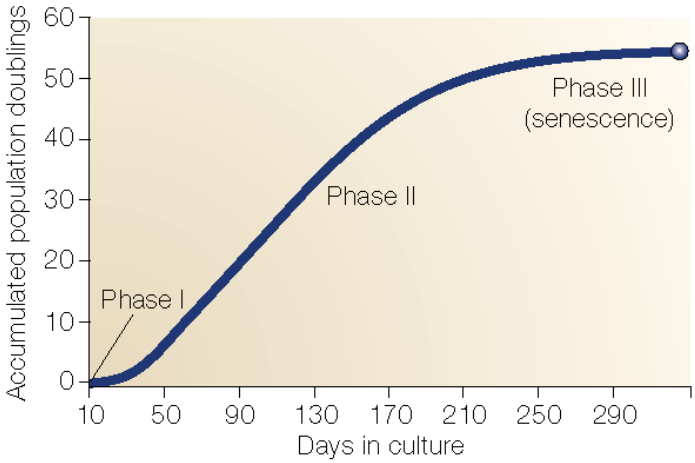


**Figure 1.1. Hayflick's classification of stages of cell culture.** Phase I is the primary culture; phase II represents subcultivated cells during the period of exponential replication. Phase III represents the period when cell replication ceases but metabolism continues. Cells may remain in this state for at least one year before death occurs. (Shay J.W. et al. 2012)

A decade later, James Watson identified the so-called "end replication problem".

The biochemical features of DNA polymerase preclude it from fully replicating the linear ends of DNA: DNA polymerase can synthesize long stretches of DNA in the 5' → 3' direction, instead the enzyme requires RNA primers to initiate synthesis of numerous Okazaki fragments in the 3' → 5' direction. After synthesis, the RNA primers are removed and the gaps are filled by a DNA polymerase. Because of the lack of DNA to serve as a template for a new primer at the end of a linear chromosome, the replication machinery is unable to synthesize the sequence complementary to the final priming event (Figure 1.2) (Watson J.D. 1972). Thus, the incapability of the DNA replication machinery to fully synthesize the lagging strand determines a progressive shortening of chromosome ends upon repeated mitotic cell division.

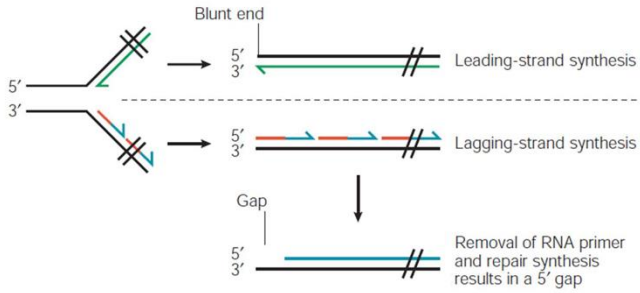


**Figure 1.2. The end replication problem.** The inability of DNA replication machinery to fill in the gap left from the removal of the RNA primer results in a loss of DNA in each round of DNA replication (adapted from **Vega L.R. et al. 2003**)

Concurrently, Alexsei Matveevich Olovnikov highlighted the crucial link between the "end replication problem", hypothesized by James Watson, and the cellular senescence described by Leonard Hayflick.

He postulated that because of the "end replication problem", telomeres undergo progressive shortening. In Olovnikov's hypothesis, this mechanism functioned as an internal clock to regulate the number of divisions that a cell could experience throughout its life thereby controlling organismal aging (Olovnikov A.M. 1973).

Oloknikov assumed that normal cells had a programme to maintain telomeric length during the normal replication of DNA.

The decisive step to understand the nature of this strategy came from the identification of telomeric DNA sequence and the telomerase reverse transcriptase. In 1978, Elizabeth H. Blackburn, working in Gall's laboratory at Yale, was investigating the DNA sequence that allowed the *Tetrahymena* and *Oxytricha* rDNA molecule to be maintained as a linear chromosome. Her work led to the finding that *Tetrahymena* and *Oxytricha* contain a micronucleus with normal chromosomes and a macronucleus with fragmented chromosomes consisting of multiple small segments of DNA that had the same coding region for ribosomal RNA (rDNA) (Blackburn E.H. and Gall J.G. 1978). Sequencing of the extra-chromosomal DNA showed that DNA termini contained multiple repetitions of the hexanucleotid CCCCAA/GGGGTT (Yao M.C. et al. 1981). Later, Jack W. Szostak and Elizabeth H. Blackburn were able to demonstrate that taking the hexanucleotidic sequence previously identified in *Tetrahymena* and coupling it with a mini-chromosome inserted in *Saccharomices cerevisiae*, stabilized the mini-chromosome, thus acting as telomere (Szostak J.W. and Blackburn E.H. 1982).

To verify the hypothesis that the function of repeated sequences is highly conserved in evolution, Szostak and Blackburn removed one *Tetrahymena* telomere by restriction enzyme digestion and added the yeast telomeres to the ends of *Tetrahymena* chromosomes (Shampay J. et al. 1984). They succeeded in the demonstration that yeast telomeres behaved as rDNA telomeres, providing a strong evidence for a high evolutionary conservation of the telomeric sequence and function.

In 1985, Blackburn and Carol Greider identified an enzyme capable of extending telomeric sequences (Greider C.W. and Blackburn E.H. 1985). Soon thereafter they found that the "terminal transferase" activity belonged to a ribonucleoprotein composed by a RNA molecule and a protein component that they termed "telomerase" (Greider C.W. and Blackburn E.H. 1987). The RNA component was complementary to the

sequence of the telomeric repeat, suggesting that it was acting as a template for repeat addition (Greider C.W. and Blackburn E.H. 1989).

### 1.1.2 Sequence and structural motifs

Telomere sequences of diverse species were deeply studied and it was revealed that telomeres consist of TG-rich tandem repeats, the sequence and size of which vary as a function of the species (Meyne J. et al. 1989) (Table 1).

| Species | Telomere length | Telomere sequence | Reference |
|---|---|---|---|
| Ciliates | | | |
| Protozoan (*T. thermophila*) | 120–420 bp | $T_2G_4$ | [6] |
| Yeast | | | |
| Baker's yeast (*S. cerevisiae*) | 200–300 bp | $TG_{2-3}(TG)_{1-6}$ | [76] |
| Vertebrates | | | |
| Humans | 5–15 kb | $T_2AG_3$ | [59] |
| Mice | Up to 150 kb | $T_2AG_3$ | [39] |
| Rats | 20–100 kb | $T_2AG_3$ | [17] |
| Birds | 5–20 kb | $T_2AG_3$ | [37] |
| Invertebrate | | | |
| Ants | 9–13 kb | $T_2AG_2$ | [50] |
| Plants | | | |
| Thale cress (*A. thaliana*) | 2–5 kb | $T_3AG_3$ | [68] |

**Table 1.** Telomere length and telomere sequence in different species (Oeseburg H. et al. 2010)

For istance, in mammals, telomeric sequences consist of the hexameric TTAGGG repeats, the so called G-rich strand, and a complementary CCCTAA sequence, termed C-rich strand (Fig.1.3) with a length of about 10-15 kilobases (kb) in humans and around 30-150 kb in mice (Palm W. and de Lange T. 2008). The termini of mammalian telomeres are not blunt-ended, but consist of a single-stranded protrusion of the G-strand, reffered to as the "G-overhang" that varies between 50-500 nt (McElligott R. and Wellinger R.J. 1997). Experiments focusing on the physical structure of chromosome ends in mouse and human revealed that protein-free DNA is organized in a large, looped structure called "T-loop" (Nikitina T. and Woodcock C.L. 2004) (Figure 1.3 A). In fact, the 3'-end of G-strand telomere (G-overhang) invades a region of telomeric double-stranded DNA (dsDNA) to form a displacement-loop (D-loop) and a looped region of double stranded telomere repeats (T-loop) (Nikitina T. and Woodcock C.L. 2004). On the functional level the T-loop structure masks the DNA terminus from

DNA double-stranded break (DSB) repair machinery and limits the access of telomerase (Griffith J.D. et al. 1999).

In contrast with the longstanding belief that telomeres are transcriptionally silenced, various evidences have shown that telomeres are actively transcribed by RNA polymerase II, producing a particular noncoding RNA containing telomeric repeats called TERRA (Azzalin C.M. et al. 2007; Schoeftner S. and Blasco M.A. 2008). Many aspects of TERRA biogenesis and functions still remain to be investigated. TERRA has already been connected with various pathways of telomere regulation: telomeric chromatin formation, telomere replication, the DNA damage response at telomeres and telomere length regulation. Based on the finding that TERRA interacts with several components of telomeric heterochromatin, a role of TERRA in the control of chromatin status at telomeres has been suggested. In particular, TERRA has been demonstrated to stabilize the interaction between TRF2 GAR domain and the origin recognition complex (ORC1), thus promoting heterochromatin formation and transcriptional silencing at telomere (Deng Z. et al. 2009).

Furthermore, TERRA is transcribed from telomeric C-rich strand, consequently its sequence is complementary to the RNA subunit of telomerase (hTR). This led to the hypothesis that TERRA may act as negative regulator of telomerase interacting with TERC. Experiments in vitro demonstrated that human TERRA is a potent inhibitor of telomerase by directly base-pairing to telomerase RNA template, but also interacting with the catalytic subunit hTERT (Schoeftner S. and Blasco M.A 2008). Moreover, newly synthesized TERRA transcripts can base-pair with their template DNA strand and form RNA:DNA hybrid structures, that trigger the formation of R-loops, three-stranded nucleic acid structures (Figure 1.3 B) (Arora R. and Azzalin C.M. 2015; Rippe K. and Luke B. 2015; Sagie S. et al. 2017). In these structures, nascent RNA transcript anneals with DNA template strand, displacing the non-template strand that remains unpaired (Aguilera A. and Garcia-Muse T. 2012). R-loops structures are prone to mutations, recombination, replication forks stalling and chromosome rearrangements (Aguilera A. and Garcia-Muse T. 2012). Accumulation of telomeric R-loop structures fosters homologous recombination-mediated telomere elongation as firstly demonstrated in yeast (Balk B. et al. 2013).

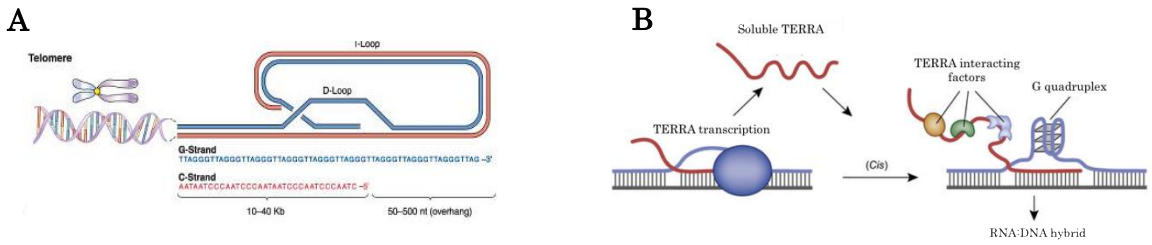


**Figure 1.3. Telomere sequence and structure:** Telomeres comprise TTAGGG repeats that varies in length. **A.** Telomeres contain a 50-500 bp long G-strand overhang. Telomeric 3'-overhang can fold up and invade the double-stranded DNA forming D-loop and T-loop structure. **B.** TERRA transcripts base-pair with the template DNA strand, forming RNA:DNA hybrid structures in cis. R-loop structure may be stabilized by a G-quadruplex forming at the displaced G-rich DNA strand (adapted from Rippe K. and Luke B. 2015).

## 1.2 Telomere homeostasis

### 1.2.1 The Shelterin complex

Telomeres exerts a crucial role in repressing DNA damage response at chromosome ends and double-strand break (DSB) repair pathways (Diotti R. and Loayza D. 2011). In particular, this protective role is performed by the protein complex Shelterin (de Lange T. 2005). Shelterin comprises six proteins: Telomere Repeat Binding Factors 1 and 2 (TRF1 and TRF2), Protection Of Telomeres 1 (POT1), TRF2- and TRF1-Interacting Nuclear protein 2 (TIN2), TPP1 (known as TINT1, PTOP, or PIP1) and RAP1 (the human ortholog of the yeast Repressor/Activator Protein 1).
TRF1 and TRF2 form homodimeric complexes that bind telomeric double-stranded DNA (dsDNA), while POT1 binds telomeric single-stranded DNA (ssDNA); TIN2 and TPP1 connect TRF1/TRF2 homodimers and POT1, whereas Rap1 is strictly associated with TRF2 (Figure 1.4).

The first mammalian shelterin protein identified was TRF1, isolated because of its *in vitro* specificity for double-stranded TTAGGG repeats (Chong L. et al. 1995). TRF2 was identified as a TRF1 paralog (Bilaud T. et al. 1997) and TIN2 and Rap1 were found in two-hybrid screens with TRF1 and TRF2, respectively (Li B. et al. 2000). TPP1 emerged from searches for TIN2-interacting proteins (Houghtaling D. et al. 2004). The most conserved component of shelterin, POT1, was identified due to its sequence homology to telomere end-binding factors in unicellular eukaryotes (Baumann P. 2001).

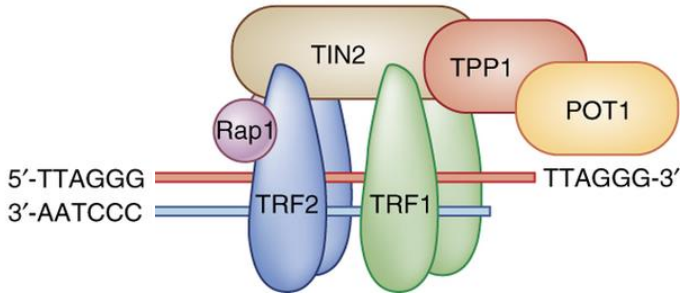


**Fig.1.4. Shelterin complex:** schematic representation of the Shelterin complex and its various interactions with the telomeric DNA (adapted from Sarek G. et al. 2015).

Key roles of Shelterin complex comprise the control of the access of telomerase to telomeres, end-resection at newly replicated telomeres and blocking DNA damage response pathway at telomeres (i.e., capping function) (Diotti R. and Loayza D. 2011).
In particular, TRF1 acts as negative regulator of telomere length maintenance by suppressing telomerase, whereas in cells that do not express telomerase activity and maintain telomere length via the homologous recombination-based ALT (Alternative Lengthening of Telomere) pathway, TRF1 is implicated as a positive mediator of ALT activity (Ho A. et al 2016). TRF1 plays a crucial role in the resolution of sister telomeres. Due to its interaction with SA1, a component of the cohesin complex, TRF1 tethers SA1 within telomeric sequence, controlling telomere cohesion (Lin J. et al. 2016). Moreover, conditional deletion of TRF1 induces the formation of fragile telomeres in S phase, a phenomena associated with replication dependent defects (McKerlie et al. 2013).
TRF2 homodimers play a pivotal role in the negative regulation of telomere length as well as in the protection of chromosome ends from inappropriate DNA damage response/repair activation, by controlling the formation and the stabilization of T-loops (Doksani Y. et al. 2013). Deletion of TRF2 leads to ataxia telangiectasia-mutated (ATM)-dependent DNA damage response at chromosome ends (i.e., telomere dysfunction-induced foci (TIFs)), which results in end-to-end telomere fusions mediated by the non-homologous end joining (NHEJ), DNA repair pathway (Denchi E.L. and deLange 2007).

The POT1/TPP1 heterodimer also plays a key role in protecting telomeres from DNA damage signalling activation, in the regulation of telomerase dependent telomere lengthening and in D-loop formation (Zhong F.L. et al. 2012). The mouse genome contains two different orthologs, Pot1a and Pot1b (Martinez P. et al. 2010). Deletion of Pot1a elicits DNA damage response at telomeres and early embryonic lethality, while Pot1b-deficient mice can survive to adulthood and only shows degenerative phenotypes like Diskeratosis Congenita patients (Wu L. et al. 2006; He H. et al. 2006).

TIN2 is a central player in the Shelterin complex because of its bridging role between TPP1/POT1 and the other components of the complex, but also because it can stabilize TRF1 and TRF2 on the duplex telomeric repeat array (Lei M. et al. 2004; Kim S. et al. 2004). TIN2 deletion results in the substantial activation of an ATR-dependent DNA damage response as a consequence of the displacement of TPP1/POT1a from telomeres and, though to a minor extent, in the impairment of TRF2-dependent repression of ATM signalling (Takai K.K. et al. 2011). TIN2 mutants elicit the phenotypes associated with POT1a and Pot1b deletion (Liuh-Yow et al. 2012): increase in the single stranded TTAGGG repeats and unprotected ends which leads to telomere fusions.

The POT1-TIN2 Organizing Protein or TPP1 is the Shelterin component that conjoins TIN2 and other shelterin units with POT1 thus suggesting that its impaired function can result in a weakened assembly of the shelterin complex and, consequently, deregulated telomere maintenance (O'Connor M.S. et al., 2006). TPP1 is involved in telomere length regulation because of its peculiar capability to recruit telomerase. Deletion of this Shelterin component results in the release of Pot1a and Pot1b from telomeres causing telomere dysfunction (Kibe T. et al. 2010).

RAP1 is a TRF2 interacting protein and because of this interaction is essential for the repression of homology-directed repair (HDR). It has been observed that Rap1 deletion from mouse telomeres causes HDR events in the absence of DNA damage foci (Sfeir A. et al. 2010). Unlike TRF1, TRF2 and POT1 this protein is not essential for telomere protection but it is fundamental to repress HDR at telomeres.

Altogether these studies demonstrate that by controlling the DNA damage and repair pathways, the Shelterin complex has a crucial role in maintaining telomere homeostasis.

### 1.2.2 Telomere in aging, disease and cancer

Telomeres shorten throughout an individual's lifetime as a result of the end replication problem. This progressive telomere shortening reach a critical point that can cause telomere dysfunction, leading to the the activation of a DNA damage response, cell cycle arrest and senescence (Fumagalli M. et al. 2012).

Excessive telomere shortening impairs the regenerative capacity of tissues and has been proposed as one of the molecular hallmarks of aging (Lo□pez-Oti□n et al. 2013). The first evidence that telomere attrition is one of the most relevant cause of age-related pathologies came from the study of telomerase deficient mice, which show premature aging phenotypes (Sahin E. and DePinho R.A. 2012; Jaskelioff M. et al. 2011).

Telomere attrition can occur prematurely because of germline mutations in genes involved in telomere maintenance and function causing the so-called telomeropathies or telomere syndromes (Table 2).

| Process/protein complex | Genes | Telomeropathies |
|---|---|---|
| Telomerase core components | *TERC* | DC, IPF, aplastic anemia, liver disease |
| | *TERT* | DC, HHS, IPF, aplastic anemia, liver disease |
| Telomerase biogenesis | *DKC1* | DC, HHS, IPF, aplastic anemia |
| | *NOP10* | DC, IPF, aplastic anemia |
| | *NHP2* | DC, IPF, aplastic anemia |
| Telomerase trafficking | *TCBA1* | DC |
| Shelterin components | *TIN2* | DC, HHS |
| | *TPP1* | DC, HHS, aplastic anemia |
| Telomeric DNA synthesis | *RTEL1* | HHS, IPF |
| | *CTC1* | DC |
| TERC RNA processing | *PARN* | DC, IPF |
| | *NAF1* | IPF |

**Table 2. Genes mutated in telomere syndromes:** a list of genes known to be mutated in telomeropathies with respective protein complexes and process they are involved with. (Martinez P. and Blasco M.A. 2017). DC: dyskeratosis congenita; IPF: idiopatic pulmonary fibrosis; HHS: Hoyeraal-Hreidarsson syndrome.

The symptoms of these disorders (Table 2) are broad and composite and the age of onset is highly variable (Holohan B. et al. 2014). However, the disorders share similar underlying molecular features, including critically short telomeres and impaired immune function due to the loss of bone marrow stem cell reserves, specific cancer types, pulmonary fibrosis, gastrointestinal disorders, neuropsychiatric condictions, diabetes, myocardiacal infarction, hair graying and skin pigmentation (Martinez P. and Blasco M.A. 2017).

Telomere homeostasis does not only play a crucial role in premature aging syndromes but also in tumour formation and progression. Telomere attrition in the presence of dysfunctional cell cycle checkpoints leads to major chromosomal aberrations (referred as to telomere crisis), which result in genomic instability, and consequently in neoplastic transformation (Artandi S.E. & DePinho R.A. 2010; Maciejowski J. et al. 2015). For instance, it has been recently reported that mutations in the shelterin complex component Pot1 gene correlate with telomeric protection defects and cause a specific glioma type (Walsh K.M. et al. 2015).

The escape from telomere crisis depends upon the reactivation of mechanisms that are able to reconstitute telomere function, thus allowing cells to recover proliferative capacity and leading to carcinogenesis and tumor progression.

In particular, two mechanisms of telomere maintenance were identified in mammalian cancer cells: the reactivation of the reverse transcriptase telomerase and the activation of ALT mechanisms (see paragraph 1.5).

This evidence suggests that maintenance of telomere homeostasis is a fundamental player in the control of carcinogenesis and tumor progression.

## 1.3 DNA damage control at telomeres

Telomere assembly can provide a solution to two major problems at chromosome ends: the “end replication problem” that finally leads to critical telomere shortening and the “end protection problem” that closely links telomeres to DNA damage response (DDR) and repair machineries.

The DNA damage response is a signal transduction pathway that senses DNA damage and sets in motion i) DNA repair mechanisms, ii) damage tolerance processes and iii) cell-cycle checkpoint pathways. Because of the high analogy between chromosome ends and DNA double strand breaks (DSBs), uncapped telomeres can be falsely sensed as DSBs, bound by the Mre11-Rad50-Nbs1 (MRN) complex and activate the ATM-dependent DNA damage response cascade. Once activated, ATM phosphorylates the histone variant H2AX on Ser139 at the site of DNA damage (Savic V. et al. 2009). The phosphorylated form of H2AX, known as γH2AX, spreads along the chromatin via the interaction with MDC1 (Turinetto V. and Giachino C. 2015), where it causes the accumulation of the DNA-damage mediator 53BP1 and the consequent activation of Chk2 downstream kinase (Lavin M.F. 2008).

Conversely, telomere single-stranded DNA (ssDNA) lesions coated by the Replication Protein A (RPA) specifically recruits and activates the complex composed of the ATR kinase and its partner ATRIP (Marechal A. and Zou L. 2015).

To avoid the recognition of telomeres as DSBs and to prevent the incongruous activation of DDR at the end of linear chromosomes, the Shelterin complex allows the formation of the unique T-loop structure ( Doksani et al. 2013). The Shelterin complex can protect telomere integrity not only by binding to the telomeric sites prone to DDR recognition but also by compacting telomeric chromatin, thus substantially reducing the accessibility of DDR signals (Bandaria J.N. et al. 2016).

Individual Shelterin proteins play a crucial role in telomere maintenance interacting with DNA damage sensors, repair, replication and transcription factors (Marti□nez P. and Blasco M. 2011). Importantly, it has been established that TRF2 can elicit telomere capping, inhibiting ATM-dependent DNA damage response (Celli G.B. and de Lange T. 2005; Denchi E.L. and de Lange T. 2007; Okamoto K. et al. 2013).

TPP1 and POT1 act as a complex in order to suppress ATR-dependent checkpoint activation by their specific binding to single-stranded telomeric DNA prevents the recruitment of RPA (Wu L. et al. 2006; Denchi E.L. and de Lange T. 2007). This crucial function is mediated by TIN2 which, by stabilizing the TPP1/POT1 complex at telomeres, represses ATR through RPA exclusion (Takai K.K. et al. 2011) (Figure 1.5).

Finally, conditional deletion of TRF1 in mouse embryonic fibroblasts (MEFs) also results in the activation of a DNA damage response as revealed by the occurrence of abundant TIFs and ATM/ATR activation at chromosome ends (Martìnez P. et al. 2009; Sfeir A. et al. 2009).

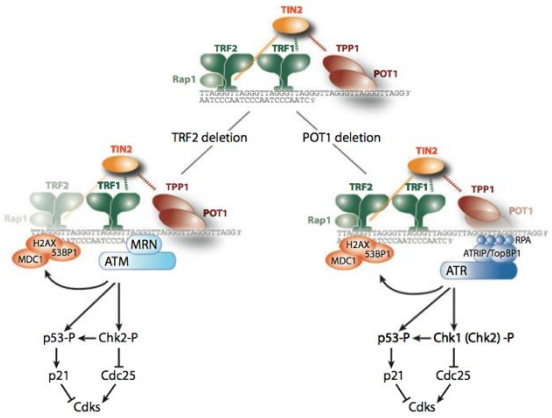


**Figure 1.5.** The DNA damage response at telomeres is regulated by the Shelterin complex.
TRF2 deletion induces the activation of ATM pathway due to the unprotected dsDNA at chromosome end; whereas POT1 deletion leads to RPA recruitment at 3' overhang eliciting the activation of ATR pathway (adapted from Palm W. and de Lange L. 2008).

## 1.4 The DNA damage repair at telomeres

Mammalian telomeres play a crucial role not only in the blockage of DNA damage response but also in protecting chromosome ends by the activation of the two most relevant DNA repair pathways: the Non-Homologous End Joining (NHEJ) and the Homology-Directed Repair (HDR) (Doksani Y. and de Lange T. 2014). NHEJ is essentially the predominant repair mechanism that induces direct relegation between two different ends. Conversely, HDR is a more complex process that uses a template sequence for repair, most often the sister chromatid in mitotic cells. At telomeres these pathways result in fundamentally different outcomes.

### 1.4.1 Non homologous end joining (NHEJ)

Short telomeres inadequately protected by the Shelterin complex (de Lange T. 2005) are recognized as DSBs and can elicit NHEJ repair. This pathway relies on KU70/80 and DNA ligase IV activity and can result in chromosomal, chromatid or sister chromatid fusions (Dimitrova N. and de Lange T. 2009; Hsiao S.J. and Smith S. 2009). The crucial Shelterin component that can control the repression of NHEJ is TRF2. Indeed, the protein is responsible of telomere capping by favoring the formation of the T-loop. However, TRF2 may be act in this context also through the action of its recently discovered iDDR domain (Okamoto et al. 2013). This small domain can interact with the MRN complex and the BRCC36 deubiquitylating enzyme, thus inhibiting the loading of 53BP1 at sites of DNA damage. Besides TRF2, TTP1 and POT1 have a pivotal role in the repression of NHEJ at telomeres. In fact, an extensive increase in chromosome end-to-end fusions has been observed in knockdown experiments for human POT1 or in POT1 knockout mouse cells. Moreover, telomere fusions occurred in cells depleted for TPP1, presumably because of its role in the recruitment of POT1 and in the stabilization of TRF2 at telomeres (Hockemeyer D. et al.2007)

### 1.4.2 Homology-Directed Repair (HDR)

In mammalian cells, Homologous Recombination (HR) activity at telomeres may seem less detrimental than that of NHEJ , though it can affect cellular survival when telomere length is altered.

HDR at telomeres can take place by three different major forms , as schematically reported in Figure 1.6 .

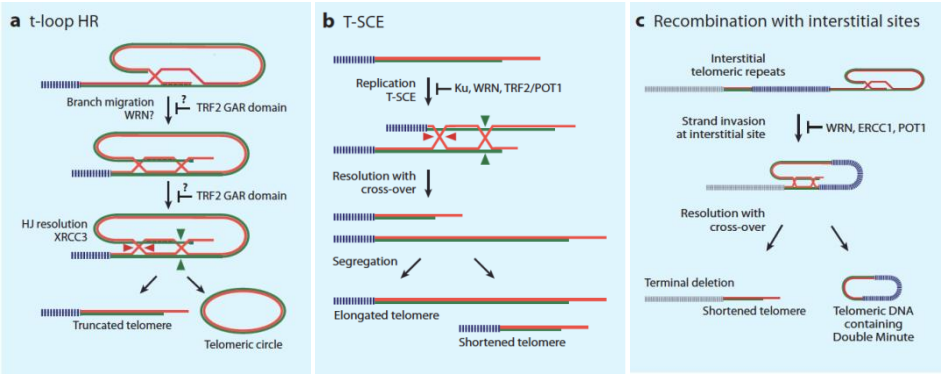


**Figure 1.6 Homology-directed repair mechanisms:** in mammalian cells, Homology-directed repair exists in three different forms. a) T-loop homologous recombination, b) Telomere sister chromatid exchange and c) Recombination with interstitial sites (adapted from Palm W. and de Lange T. 2008)

#### 1.4.2.1 T-loop homologous recombination (T-loop HR)

The T-loop structure results from the single stranded 3' overhang of telomeres invasion into telomeric double-stranded DNA that generates the so-called D-loop. Shelterin protein TRF2 is the main protein involved in the T-loop formation (Doksani Y. et al. 2013). TRF2 is able to induce topological changes in telomeres, but it can also bind Holliday junctions (HJ) stabilizing strand-invasion process (Poulet A. et al. 2009).

In particular, T-loop homologous recombination has been observed using a TRF2 allele lacking the N-terminal GAR domain (Wang R.C. et al. 2004). The cells with this construct showed telomere deletion and accumulation of circular telomeric DNA due to the formation of a Holliday junction (HJ) at the strand invasion point of the T-loop. This mechanism is dependent on XRCC3 resolvase and WRN responsible for branch migration in "T-loop HR" (Nora G.J. et al. 2010). These evidences demonstrate that

Shelterin components and in particular the GAR domain of TRF2 is important to repress HR event at telomeres.

#### 1.4.2.2 Telomeric sister chromatid exchange (T-SCE)

After replication, telomeres can recombine. These exchanges, referred to as telomeric sister chromatid exchanges or T-SCE, are harmless as long as they are equal. Unequal exchanges represent a threat to telomeres because they lead to the elongation of one telomere at the expense of another. Unequal T-SCE confers a proliferative advantage to a subset of cells that acquire longer telomeres, enabling their escape from cellular senescence (Hagelstrom R.T. et al. 2010).

Different factors, including those of the Shelterin complex, are able to repress recombination between sister telomeres. Two of the most relevant proteins that can safeguard controlled T-SCE are TRF2 and Ku70. Indeed, cells lacking both TRF2 and Ku70, show high frequency of T-SCE has been observed. Remarkably, the sole lack of TRF2 or Ku70 is not sufficient to induce T-SCE (Celli G.B et al. 2006), thus suggesting that these two proteins act in a synergistic manner in order to suppress T-SCE.

An increased frequency of T-SCE can be observed also in Ku70/80-deficient mice that also lacks POT1a and POT1b (Palm W. and de Lange 2008; Sfeir A. et al. 2010). POT1 binding to telomeric single-stranded DNA counteracts the loading of homologous recombination factors such as RPA and, subsequently, RAD51, thereby inhibiting recombination (Gu P. et al. 2017).

In addition, T-SCE frequency is tightly controlled by DNA helicases such as WRN or RTEL1. Telomerase deficient mouse cells that also lack WRN show critically shortened telomeres and high levels of T-SCE. WRN is a DNA helicase that normally resolves G-quadruplexes secondary structures during DNA replication, allowing replication fork progression and complete synthesis of telomeric DNA. Lack of WRN activity leads to stalled replication fork due to the accumulation of G-quadruplexes structures, with a consequent loss of the lagging strand telomeric DNA and an increase in T-SCE frequency (Laud P.R. et al. 2005). Similarly, RTEL1 is a helicase which plays a key role in telomere maintenance and DNA repair. It was shown that RTEL1 deficient mice show increased levels of T-SCE as the protein plays an important role in the resolution of common recombination intermediates in the presence of stalled or collapsed replication fork (Uringa E.J. et al. 2012).

These evidences denote a crucial role of Shelterin components in maintaining structure of telomere and DNA helicases in resolving aberrant structures controlling T-SCE,

suggesting that unprotected telomeres or accumulation of aberrant secondary structure at chromosome termini can elicit telomeric recombination.

#### 1.4.2.3 Homologous recombination with interstitial sites

Telomeres can partake in a third homology-directed repair pathway that involves internal portions of TTAGGG repeats. This pathway can be detrimental for telomeres as it can lead to terminal deletions of all sequence located distant to the interstitial TTAGGG repeats, thereby producing and extra-chromosomal element called double-minute chromosome (TDMs). These TDMs can contain telomeric sequences and have a variable size depending on the location of the interstitial sequences. TDMs have been frequently observed in immortalized mouse embryo fibroblast lacking the subunit ERCC1, an endonuclease usually recruited to telomere by the direct interaction with TRF2. On the molecular level ERCC1 prevents recombination of the telomere terminus by promoting the cleavage of the strand-invaded intermediates (Zhu X.D. et al 2003).
In addition, another contributor is the WRN helicase that counteracts TDMs formation in presence of short telomere (Laud P.R. et al. 2005). Finally, reduction of POT1a/b is strictly correlated with a high frequency of TDMs (He H. et al. 2006; Wu L. et al. 2006)

## 1.5 Regulation of telomere maintenance

Telomere integrity has important implications in cancer and aging: telomere attrition serves as a checkpoint in the control of cell proliferation by triggering replicative senescence, acting as tumor-suppressing mechanisms in order to avoid tumorigenesis.
Telomere length declines with each cell cycle and eventually, one or a few telomeres become sufficiently short and malfunction, presumably owing to loss of the protective structure. Dysfunctional telomeres trigger a DDR, to which cells respond by undergoing replicative senescence.
These events are best explained by a two-stage model for cellular senescence in which M1 and M2 represent independent mechanisms that can limit the proliferative potential of normal cells. Normal somatic cells can divide for limited number of cycles before entering senescence or mortality stage 1 (M1) phase. However telomeres can become shorter by the inactivation of oncosuppressor pathways, further shortening causes cell crisis or mortality stage 2 (M2) phase that finally can lead to apoptosis.

Rarely, cells can escape crisis becoming immortal by two different mechanisms: telomerase upregulation or activation of alternative lengthening of telomeres (Shay J.W. and Wright W.E. 2006).

90% of cancer cells can solve the end replication problem re-activating telomerase (Shay J.W. and Wright W.E. 2011).

On the other hand, approximately 10% of cancers employ a telomerase independent mechanism to maintain telomere length called Alternative Lengthening of Telomeres (ALT) pathway, that relies on homology-directed DNA recombination (Dilley R.L. and Greenberg R.A. 2015).

### 1.5.1 Telomerase: components and maturation

Telomerase is a ribonucleoprotein complex that is able to synthesize new telomeric DNA repeats (TTAGGG) at the 3' end of linear chromosome, counterbalancing the progressive loss of DNA from each round of replication.

Recent evidences have shown that telomerase, besides its classical role in telomere maintenance, is involved in various steps fundamental in the carcinogenesis process such as gene expression regulation, cell proliferation, apoptosis, NF-kB signaling, MYC-driven oncogenesis, cell adhesion and migration and epithelial–mesenchymal transition (Ghosh A. et al. 2012; Koh C.M. et al. 2015; Liu H. et al. 2016; Liu Z. et al. 2013)

The minimal ribonucleoprotein composition of active human telomerase can be assembled in a heterologous cell extract by expression or addition of two telomerase catalytic core subunits: telomerase RNA hTR and telomerase reverse transcriptase hTERT (Autexier C. and Lue N.F. 2006). The telomerase catalytic subunit (TERT) recognizes the 3'OH of the G-overhang and synthesizes TTAGGG repeats using the RNA component (hTR) as a template. In addition to TERT and hTR, other proteins that regulate the biogenesis and correct assembly of telomerase *in vivo* are part of the telomerase complex. Indeed, *in vivo*, the complete telomerase complex consists of hTERT, the telomerase RNA component, the RNA template used for the synthesis of new telomeric repeats, dyskerin (DKC1), NOP10, NHP2, Pontin, Reptin and GAR1 (Figure 1.7) (Fu D. and Collins K. 2003; Sauerwald A. et al. 2013; Low K.C. et al. 2013; Veinteicher A.S. et al. 2008).

In particular, the current model is that dyskerin, pontin and reptin actively recruit and stabilize hTR. Once this complex is formed, pontin and reptin are believed to dissociate

from the complex to release the catalytically active enzyme. In addition to the telomerase complex composition also the subnuclear localization of telomerase impacts on its function. The subcellular location of telomerase appears to be regulated by TCAB1, a protein that directs telomerase to specific subnuclear membraneless compartments, the Cajal Bodies which play a key role in telomerase maturation and recruitment to telomeres (Gomez D.E. et al. 2012; Zhong F. et al. 2011).

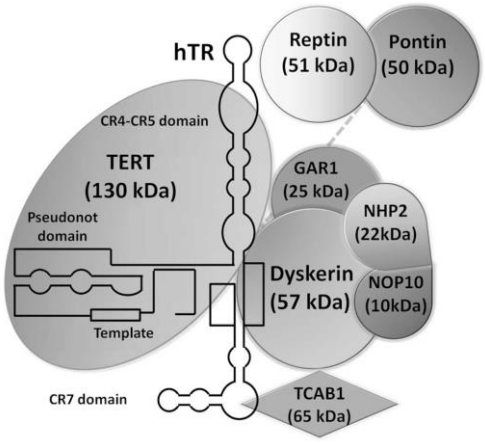


**Figure 1.7. Schematic representation of telomerase and its associated proteins:** two essential components compose telomerase: telomerase reverse transcriptase catalytic subunit (hTERT) and functional telomerase RNA (hTR), which serves as a template for the addition of telomeric repeats. Species-specific accessory proteins are associated to the core components of telomerase: dyskerin, Gar1, Nhp2, Nop10, Reptin and Pontin. (adapted from Gomez D.E. et al. 2012).

#### 1.5.1.1 hTERT structure and function

The human hTERT gene is located on chromosome 5 and consists of 16 exons and 15 introns spanning 35 kb (Bryce L.A. et al. 2000). hTERT represents the enzymatic component of the complex and it is divided in four conserved structural domains: the telomerase essential N-terminal (TEN) domain, the telomerase RNA-binding domain (TRBD), the reverse-transcriptase (RT) motif and the C-terminal (CTE) extension (Figure 1.8).

The central catalytic RT domain contains seven conserved motifs shared with conventional retrotranscriptases and reverse transcriptases. Mutations in conserved residues in the RT domain result in the loss of telomerase activity in vitro (Gillis A.J. et al. 2008). The telomerase CTE domain is able to bind to telomeric DNA, enhancing nucleotide polymerization and telomerase processivity (Nandakumar J. et al. 2013; Wyatt H.D. 2010).

While the RT and CTE domains are broadly conserved between hTERT and conventional reverse transcriptase, the TEN and TRBD domains are telomerase-specific and unique to the hTERT protein. In particular, the TEN domain is essential for the correct binding of telomerase to DNA and is critical for short duplex stabilization since it contains 'anchor' sites which specifically bind single-stranded telomeric DNA (Akiyama B.M. et al. 2015). Moreover, this domain can directly interact with the hTR template/pseudoknot domain through a low affinity binding site referred to as RNA interacting domain 1 (RID1) (Lai A.G. et al. 2017)

The TRBD contains mainly helical motifs and an RNA interacting domain 2 (RID2), which is a high affinity binding site for the hTR CR4/5 domain. The protein–RNA interactions through RID1 and RID2 are essential for telomerase assembly and processivity. disruptions of these domains abolish activity both in vitro and in vivo (Wu R.A. et al. 2017).

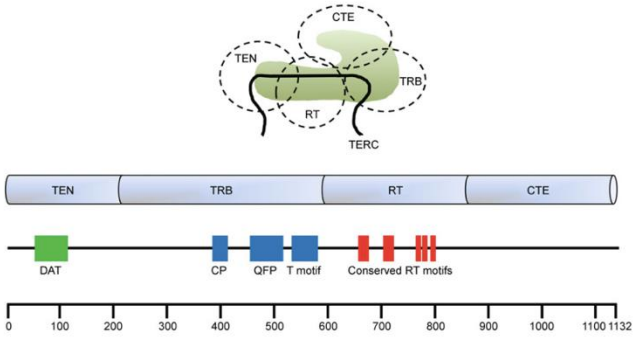


**Figure 1.8. hTERT structure:** Human TERT contains four key domains: the telomerase essential N-terminal (TEN) domain; the TERT RNA binding (TRB) domain; the reverse transcriptase (RT) domain and the C-terminal extension (CTE) domain. (Nicholls C. et al. 2011)

### 1.5.1.2 Telomerase RNA component structure and function

The second component of telomerase holoenzyme is the RNA component hTR that acts as a template to add telomeric repeats at chromosome termini. The human hTR gene is located at chromosome 3q26,3 and although telomerase RNA primary sequence differs among the vary vertebrate species, the secondary structure is well conserved,

suggesting a crucial role of RNA structure for telomerase activity (Figure 1.9) (Chen J.L. et al. 2000).

In particular, hTR from all species is characterized by two conserved structures: the template/pseudoknot domain (CR2/CR3), which contains several structural motifs that position the template in the active site and define the template boundary (Niederer R.O. and Zappulla D.C. 2015). The CR4/CR5 domain is distal from the template/pseudoknot domain and is able to stimulate telomerase activity and to bind to the TRBD (Blackburn E.H. and Collins K. 2011).

CR2/CR3 and CR4/CR5 domains are essential for telomerase activity, as suggested by the evidnece their excision from hTR and the combination in trans with the hTERT protein can generate an active telomerase enzyme in vitro (Mitchell J.R. and Collins K. 2000). The human telomerase RNA contains a third domain, the H/ACA motif which is characterized by two stem-loops separated by box H and box ACA moieties (Egan E.D. and Collins K. 2012). This H/ACA motif is dispensable for activity, although it is essential for in vivo biogenesis, accumulation, and RNP assembly.

hTR shares the H/ACA box motif with small nuclear (snRNA), small nucleolar RNA (snoRNA) and Small Cajal-body specific RNAs (scaRNA). The intacellular localization of snRNAs, snoRNA, scaRNA and hTR is essential for the maturation steps of these small RNAs that normally occur within Cajal bodies (CB). CBs are small subnuclear membraneless organelles that coordinate the assembly or modification of small nuclear ribonucleoprotein particles (snRNPs) (Cristofari G. et al 2007; Deryusheva S. et al. 2012) and are strictly involved in the maturation of hTR and assembly of the complete and active telomerase complex (see 1.5.1.5) (Nunes V.S. and Moretti N.S. 2016).

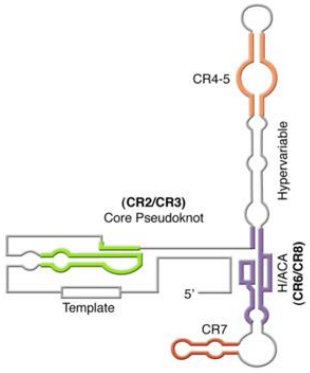


**Figure 1.9. hTR structure:** Secondary structure of human TR that contains a pseudoknot fundamental for interaction with hTERT (CR2/CR3), and a region used as a template for telomere elongation. hTR contains a small nucleolar H/ACA motif; box H/ACA refers to a region of small nucleolar RNAs (snoRNAs) carrying a conserved H motif (ANANNA where

N is any nucleotide) that ends with a single stranded 3' tail-encoded ACA. hTR can bind to other proteins, such as dyskerin, GAR, NHP2, and NOP10, through box H/ACA. (adapted from Calado R.T. et al. 2008).

#### 1.5.1.3 Telomerase RNA biogenesis and processing

The RNA component of telomerase varies across species with respect to sequence, length, structure, and synthesis (Podlevsky JD et al. 2008).

The precursor of hTR is transcribed from its own promoter by RNA polymerase II and undergoes further maturation steps (Egan E.D. and Collins K. 2012). The precursor form of telomerase RNA is produced as 3′ extended and polyadenylated form, processed post-transcriptionally into a mature form of 451 nucleotides (MacNeil D.E. et al. 2016).

After primary transcript synthesis by RNA-polymerase II, the precursor form of hTR and the 3' extended products after a crucial step of trimming is polyadenylated. The newly transcribed hTR interacts with a tetrameric complex composed of dyskerin, NOP10, NHP2 and the chaperone protein NAF1 (Egan E.D. and Collins K. 2010). In order to achieve the complete maturation of the 3' extended form, the cap binding complex (CBC) attracts the NEXT-exosome complex, forming a CBCN complex and implementing co-transcriptional 3'-processing or degradation of telomerase RNA in the nucleus (Ntini E. et al. 2013).

In particular, the NEXT-exosome complex shortens the long precursor in the nucleus, inducing further maturation of telomerase RNA instead of degradation. This step occurs only in a context where the assembly of an intact dyskerin complex occurs, otherwise hTR precursor is degraded in its entirety (Tseng C.K. et al. 2015). Telomerase RNA intermediates shortened by the activity of the NEXT complex are polyadenylated by the TRF4/5-AIR1/2-(TRAMP) complex and can be directly processed in the mature form of telomerase RNA by PARN, which removes the polyadenylation products (Tseng C.K. et al. 2015). This maturation step is favored if the 5' end is capped with a 7-monomethylguanosine and made available for binding by PARN (Balatsos N.A. et al. 2006). Therefore, an important regulatory mechanism is represented by the hypermethylation of the monomethylguanosine cap catalyzed by the trimethylguanosine synthase TGS1 (Zhu Y. et al. 2001).

Once telomerase RNA is processed and completely matured, hTR is routed to Cajal bodies. The accumulation of telomerase in Cajal bodies is mediated by a protein named

Telomere Cajal body protein 1/WD repeat-containing protein 79 (TCAB1/WDR79) which binds to the CAB-box within telomerase RNA. Depletion of TCAB1/WDR79 does not affect hTR accumulation, but leads to a cell cycle arrest and impedes the recruitment of telomerase to telomeres, leading to telomere shortening and premature aging, suggesting that this protein acts as a scaffold for the mature hTR-H/ACA RNP to localize to the CBs (Yuan P. et al. 2014). Cajal bodies are subnuclear sites where the methyltransferase TGS1 catalyzes the transfer of two methyl-groups on the 5'-monomethylguanosine cap of hTR, generating its 2,2,7-trimethylguanosine cap (TMG) (Venteicher A.S. and Artandi S.E. 2009; Tang W. et al. 2012).

Human TGS1 was first designated as PRIP-interacting protein with methyltransferase domain (PIMT) due to its capability to interact with PPAR-interacting protein (Zhu Y. et al. 2001). TGS1 is a highly conserved hypermethylase that can occur in two different isoforms, a full-length long cytoplasmic isoform (LF) and a shorter nuclear isoform (SF) of 65–70 kDa. The long isoform is predominantly associated with the maturation of snRNAs. On the other hand, the short isoform exhibits methyltransferase activity and is able to bind box C/D and H/ACA of snoRNPs and telomerase RNA, pointing to a role of this isoform in hypermethylation of snoRNAs and hTR (Verheggen C. and Bertrand E. 2012).

The methyltransferase domain of TGS1 is located in the C-terminus and is conserved among various species (Mouaikel J. et al. 2002). In particular, human TGS1 catalyzes two successive methyl group transfers, each from one *S*-adenosyl-l-methionine (AdoMet) to the exocyclic nitrogen N2 of the cap-guanine, generating two *S*-adenosyl-l-homocysteine molecules (AdoHcy) and the modified 2,2,7-trimethylguanosine ($m_3G$)-cap (Hausmann S. and Shuman S. 2008).

Mutational analysis indicates that TGS1 is required in pre-mRNA splicing, and this is dependent upon its function in cap trimethylation. In addition, cells lacking TGS1 showed a striking and unexpected loss of nucleolar structural organization (Colau G. et al. 2004).

#### 1.5.1.4 Telomerase action at telomeres

Telomere length in telomerase-positive cells is influenced by a plethora of variables: the absolute telomerase levels, the frequency of telomerase-telomere interactions and the number of telomeric repeats added to each telomere (Cifuentes-Rojas C. and Shippen D.E. 2012).

Telomerase-dependent telomere elongation is a three steps mechanism that normally occurs in S phase and includes: binding of telomerase to telomeric 3' ssDNA; addition of 50-60 nucleotides to the 3'-overhang of chromosomes and successive translocation and repositioning of the 3'-overhang of telomere with the 3' template boundary of hTR to start a new round of telomere elongation (Figure 1.10) (Schmidt J.C. and Cech T.R. 2015).

Shelterin proteins can play key roles during telomere elongation by mediating telomerase activity at telomeres. In particular, telomerase is able to physically interact with TPP1 through the TEN domain of hTERT (Zaug A.J. et al. 2010). TPP1/telomerase RNP interaction might lead to telomerase recruitment at telomeres (Abreu E. et al. 2010). On the other hand, the shelterin proteins TRF2 and POT1 are negative regulators of telomere length. POT1 binding to a single-stranded G-overhang restricts telomerase access to telomeres and TRF2-dependent t-loop formation can prevent telomerase recruitment at telomeres leading to a critical loss of telomeric DNA (Hockemeyer D. and Collins K. 2015). Moreover, the Shelterin protein TRF1 acts in *cis* as a negative length regulator at each individual telomere. In particular, an inappropriately long telomere can recruit a large amount of TRF1, blocking telomerase-mediated elongation of that particular chromosome end (Smogorzewska A. et al. 2002). Another negative regulator of telomere length in human cells is TERRA RNA, which directly binds telomerase complex inhibiting telomerase activity at telomeres (Schoeftner S. and Blasco M.A. 2008).

The catalytic subunit of telomerase hTERT binds telomeres upstream of the hTR template/DNA interaction. The hTR template is reverse transcribed into DNA by the activity of hTERT, which synthesizes a short telomeric repeat (TTAGGG). The new strand can now be translocated in a 5′ direction for the processive synthesis of additional telomeric repeats on the same telomeric end. The ability of telomerase to mediate a single round of synthesis is described as nucleotide addition processivity, whereas realignment of the enzyme for a second round of addition is described as repeat addition processivity (RAP). RAP is the ability of hTERT to add various telomeric sequence without dissociating from the same chromosome terminus. After telomerase-mediated extension of the 3′-end, the lagging-strand synthesis machinery fills in the opposite strand (MacNeil D.E. et al. 2016).

Telomerase action is under a strict cell cycle control. Pieces of evidence have demonstrated that telomerase recruitment and the association of hTR with telomeres occur only in S phase (Nandakumar J. and Cech T. R. 2013).

Cell cycle regulation of telomerase action at telomeres might derive from regulation of telomerase holoenzyme. Indeed, it has been shown that hTERT and hTR complex can be assembled irreversibly, with consequent transcription of new hTR and assembly of active RNP in $G_1$ phase. Furthermore, TCAB1 association with hTR undergoes cell cycle regulation as well, controlling hTR translocation to Cajal bodies and impinging on telomerase processivity (Vogan J.M. and Collins K. 2015).

Telomerase processivity can be impinged by a plethora of factors including temperature, substrate concentration, G-quadruplex interacting-agents or proteins that interact with telomerase or telomeric DNA (Morin G.B. 1989; Bosoy D. and Lue N.F. 2004; Maine I.P. et al. 1999; Hardy C.D. et al. 2001).

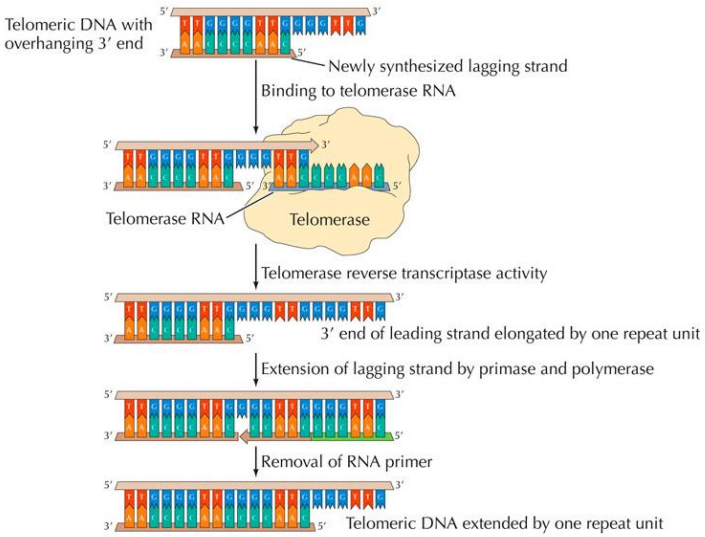


**Figure 1.10. Telomerase activity at telomeres:** the enzyme recognizes telomeric ssDNA, adds telomeric repeats to the 3' overhang using its own complementary RNA strand. When sufficient telomeres have been added, an RNA primer is attached, and DNA polymerase transcribes the existing DNA strand. The fragments are joined by Ligase (The Cell. Fourth edition).

### 1.5.1.5 Cajal Bodies and telomere homeostasis

The subnuclear organelles known as Cajal bodies (CB) are highly conserved organelles present in most eukaryotic cells with high transcriptional demands. CBs are dynamic structures, responding to the cellular environment and to changes in levels of RNA synthesis and RNP assembly. They are frequently detected at the nucleolar periphery and contain locally high concentrations of transcription factors, survival motor neuron

(SMN) protein complex and an 80- kilodalton (kDa) structural protein, coilin (Ogg S.C. and Lamond A.I. 2017). Moreover, CBs are enriched in a broad range of nuclear factors, including snRNPs and snoRNPs as well as polymerase II transcription factors.

Coilin is the main marker of CBs and it functions as a scaffold protein for their assembly (Machyna M. et al. 2015). It promotes RNP biogenesis by concentrating snRNPs and their assembly intermediates in CBs, acting as a chaperone of nuclear small non-coding RNAs. Zebrafish embryos depleted for coilin are unable to complete embryogenesis and display splicing defects and reduced numbers of mature snRNPs (Strzelecka M. et al. 2010). Moreover, coilin could be also involved in higher order chromatin organization (Machyna M. et al 2015). Genes encoding snRNAs, snoRNAs and histone mRNAs were found closely associated with CBs in cytological assays (Machyna M. et al. 2015).

Another key protein is the WD40 encoding RNA antisense to p53 gene, WRAP53 (also known as TCAB1), crucial for its role as a scaffold protein involved in telomerase localization, telomere and Cajal body assembly, and DNA double strand break repair (Stern J.L. et al. 2012; Henriksson S. et al. 2014; Vogan J.M. et al. 2015). TCAB1 controls the proper ubiquitylation at DNA damage sites and the downstream assembly of 53BP1, BRCA1, and RAD51 modulating DSB repair by both HDR and NHEJ (Henriksson S. et al. 2014).

Cajal bodies are organeless highly involved in ribonucleoprotein (RNP) biogenesis. Specifically, Cajal bodies are important maturation point for RNPs involved in splicing, histone mRNA processing and telomere formation. In particular, spliceosomal small nuclear RNPs (snRNPs), small nuclear RNA (snRNA) component of the snRNP is modified in the CB (Machyna M. et al. 2013). Two modifications predominate in snRNAs and have been associated with CBs i) pseudouridylation and ii) 2'-O-methylation. Pseudouridylation is the isomerization of uridine to pseudouridine while 2'-O-methylation is the methylation of the 2'- hydroxyl group of the ribose of any ribonucleoside, an important feature of spliceosomal snRNAs (Meier U.T. 2016). Moreover, CBs play an important role in the regulation/control of telomerase activity, as already highlighted in section 1.5.1.3.

#### 1.5.1.6 Regulation of telomerase activity

In vertebrates, expression and activity of telomerase is detectable in germ and stem cells. In somatic cells telomerase activity and TERT levels decrease as cells

differentiate, and telomerase activity is not detectable in most cells in adult mammals (MacNeil D. et al. 2016). Moreover, more sensitive analysis unveiled that tissues with high proliferative potential (bone marrow, gastroinstestinal tract, testis, lymphocytes) exhibit telomerase activity (Teichroeb J.H. et al. 2016). The reactivation of telomerase is a crucial step in the onset of about 90% of human cancers (Prescott J. et al. 2012).

The major determinant of telomerase activity is is represented by the protein component hTERT. Of notice, telomerase RNA abundance is increased in various tumors when compared to normal cells, suggesting that hTR regulation can contribute to the strict control of telomerase activity (Cifuentes-Rojas C. and Shippen D.E. 2012).

The hTERT promoter is exposed to strict transcriptional regulation by a plethora of transcription factors, epigenetic and post-translational modifications.

hTERT transcription is directly controlled by oncogenes as c-Myc, transcription factors such as Sp1 as well as by tumor suppressors such as WT1 and p53 (Patel P.L. et al. 2016; Bisson F. et al. 2015; Sitaram R.T. et al. 2010). In fact, increased expression of c-Myc, common in cancer cells, results in increased telomerase activity (Khattar E. and Tergaonkar V. 2017). Conversely WT1 and p53 negatively regulate telomerase activity and inactivation or complete loss of these proteins result in telomerase activation during tumorigenesis.

In addition to transcriptional regulation, hTERT gene expression is strongly influenced by epigenetic gene regulation such as DNA methylation, histone acetylation, histone methylation but also non-coding RNA.

Recent studies demonstrated a particular situation related to DNA methylation in hTERT promoter. The degree to which the hTERT promoter is methylated plays a role in carcinogenesis of different types of cancer because of the major effect of methylation status on telomerase expression and activity (Castelo-Branco P. et al. 2016; Leao R.R. et al. 2015; Pettigrew K. et al. 2012). Treatment with the DNA methyltransferase inhibitor 5'-aza-2'-deoxycitidine caused an increase hTERT expression. Importantly, it has been shown that the hTERT CpG island is methylated in many telomerase-negative and telomerase-positive cultured cells and tumors. Demethylation of DNA with 5-azacytidine induced expression of hTERT, suggesting that DNA methylation can contribute to hTERT repression in some cells (Dessain S.K et al. 2000; Zinn R.L. et al 2007).

In addition to DNA methylation, histone acetylation controls hTERT mRNA expression. Experiments in human somatic cells treated with histone deacetylase inhibitor (HDACi) such as Trichostatin A (TSA) showed that enhanced acetylation of

histones impact on hTERT expression via its activity on DNMT1 promoter (Choi J.H. et al. 2010). Normal human cells show transcriptional reactivation of hTERT promoter after TSA treatment. Remarkably in cancerous cells TSA treatment can activate or represses hTERT expression depending on cell type and methylation status. This suggests that other regulatory mechanisms cooperate with histone acetylation to control hTERT mRNA expression (Suenaga M. et al. 2002).

The regulation of telomerase can occur at a post-translational level as well (MacNeil D.E. et al. 2016). It is well documented that, in vertebrates, telomerase activity is modulated by phosphorylation. hTERT can be phosphorylated by c-Abl leading to a three-fold reduction in telomerase activity and consequent telomere (Kharbanda S. et al. 2000). Telomerase enzymatic component can be phosphorylated by the kinase Akt, which induces translocation of hTERT from the cytoplasm to the nucleus and activates telomerase activity (Sasaki T. et al. 2014).

Ubiquitination may also influence telomerase activity. The activity of Makorin Ring Finger Protein 1 (MKRN1) mediates ubiquitination of hTERT. In fact, overexpression of MKRN1 leads to degradation of hTERT, causing a decrease in telomerase activity and telomere shortening (Kim J.H. et al. 2005).

Moreover, C-terminus of Hsc70-interacting protein (CHIP) is able to interact with hTERT in the cytoplasm, regulating its abundance through a ubiquitin-mediated degradation. Overexpression of CHIP blocks hTERT entry into the nucleus, inducing its degradation and consequently inhibiting telomerase activity (Lee J.H. et al. 2010).

hTR regulation contributes to telomerase activity control as well. In particular, transcription of telomerase RNA is activated by the transcription factors Sp1 and HIF-1 and conversely, repressed by Sp3, which integrates cues from the MAPK signaling cascade to silence the hTR promoter (Cairney C.J. & Keith W.N. 2008). hTR expression is tightly controlled by epigenetic mechanism since it has been shown that decreased levels of H3 and H4 acetylation is associated with an increase of telomerase RNA transcription (Atkinson S.P. et al. 2005). Finally, at least six sites in hTR are subjected to post-transcriptional modification by pseudouridylation. In vitro telomerase reconstitution experiments with pseudouridylated telomerase RNA result in a slight attenuation of telomerase activity though it causes an enhancement of the enzyme's processivity (Kim N.K. et al. 2010).

### 1.5.2 ALT : Alternative lengthening of telomeres

A significant number of tumors (~10%) utilizes homologous recombination (HR)-based TMM, known as ALT. It is frequently observed in tumors of mesenchymal origin as well as in a significant fraction of breast carcinomas and other epithelial malignancies (Subhawong A.P. et al. 2009; Henson J.D. and Reddel R.R. 2010)

The evidence for recombination based mechanism for telomere maintenance came from a study showing that a DNA tag inserted into one telomere was copied to other non-homologous telomeres and was also duplicated in its original location in human telomerase negative cells (Neumann A.A. et al. 2013; Cesare A.J. and Reddel R.R. 2010).

#### 1.5.2.1 Mechanisms of Alternative Lengthening of Telomeres

Alternative Lengthening of Telomeres mechanism includes synthesis of new telomeric DNA on the basis of a DNA template (Reddel R.R. et al. 1997). In particular, it has been proposed that a telomere can use itself or a telomere on a sister chromatid or other chromosome as a template to add new telomeric repeats. Moreover, it has been demonstrated in yeast that circles of extrachromosomal DNA can be used as a template (Natarajan S. and McEachern M.J. 2002). The hypothesis that ALT involves homologous recombination is supported by the fact that genes encoding HR proteins are essential for survival of telomerase negative cells (Lieberman R. and You M. 2017).

A putative four steps model has been proposed and includes strand invasion of the donor molecule, copying of the template, dissolution of the recombination intermediate and subsequent synthesis of the complementary strand (Figure 1.11, left panel) (Pickett H.A. and Reddel R.R. 2015).

The initiation of ALT mechanism necessitates the replacement of POT1 firstly with the replication protein A (RPA) and in a second moment with RAD51, a protein necessary for strand invasion and annealing to the complementary strand (Sung P. and Klein H. 2006) at the single-stranded overhang. The second step is presumably performed by DNA polymerase δ or ζ, given the supposed role of these two polymerases in homologous recombination (Maloisel L. et al. 2008; Sharma S. et al. 2012). The third step is the dissolution of the homologous recombination intermediates such as the Holliday junctions (HJ) before chromosome segregation. A plethora of proteins are involved in this crucial step, the RecQ-like BLM helicase provides the translocase function for Holliday junction migration, while the topoisomerase III alpha-RMI1

subcomplex works as a proficient DNA decatenase, together resulting in double-Holliday-junction unlinking (Swuec P. and Costa A. 2014). In particular, two mechanisms can occur in a competing manner: HJ dissolution and HJ resolution. During the resolution pathway, each HJ is cleaved by a resolvase, a specific endonuclease. The combination of cleavage orientations, which can be asymmetric or symmetric, can generate both crossover and noncrossover products. In contrast, during dissolution, each strand engaged in the HJ is reassociated with its original complementary strand, preventing exchange of genetic material between the two homologous sequences, generating only noncrossover products (Bizard A.H. and Hickson I.D. 2014). Indeed, SLX4 and BLM proteins, respectively components of the resolution and dissolution complex, seem to directly interact with TRF2 (Wilson J.S. et al. 2013; Opresko P.L. 2002) suggesting a competitive role for the aforementioned complexes in the processing of HR intermediates.

The template for telomere DNA synthesis in an ALT context might be a sister chromatid (Figure 1.11 a), alternatively telomeres are able to loop out or loop back in order to serve as a template for themselves (Figure 1.11 b-c). Recently, it has been shown that a long-range movement driven by homology-directed searching mechanism exists and is able to induce telomere clustering that indeed provides distant copy template (Figure 1.11 d) (Cho N.W. et al. 2014).

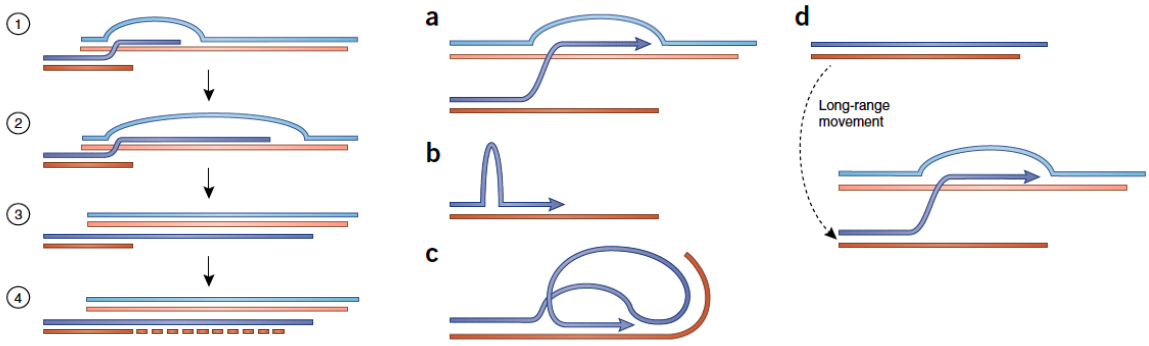


**Fig. 1.11. ALT mechanism**: Putative four steps model of ALT mechanism (left panel). Different possible DNA copy templates in alternatie lengthening of telomere mechanism (right panel). Use of a nearby copy template in the sister-chromatid telomere (**a**) or in the same telomere by looping out (**b**) or by t-loop formation (**c**) is depicted. (**d**) A distant telomere may be used as a copy template after long-range movement (adapted from Pickett H.A. and Reddel R.R. 2015).

In addition to canonical telomeric features, ALT cells are defined by special characteristics related to telomeres (Cesare A.J. and Reddel R.R. 2010). It is now widely accepted that ALT cells display highly heterogenous telomere length (O'Sullivan R.J. et al. 2014), high levels of telomere sister chromatid exchange (T-SCE), abundant extrachromosomal telomeric DNA that includes circular forms such as double-stranded telomeric circles (t-circles) and partially single-stranded circles (C-circles or G-circles), but also linear double-stranded DNA and very high molecular weight structure (t-complex DNA) (Nabetani A. and Ishikawa F. 2009; Henson J.D. et al. 2009). Finally, in ALT cells telomeric DNA and associated binding proteins are found in promyelocytic leukaemia nuclear bodies (PML bodies) defined as ALT-associated PML bodies (APBs) (Yeager T.R. et al. 1999) which are enriched in proteins involved in HR, suggesting that ALT activity may occur in these nuclear bodies (Cesare A.J. and Reddel R.R. 2010).

Several factors are essential for ALT telomere maintenance. For instance a striking correlation has been observed between ALT activity in human cancers and loss of the ATP-dependent helicase ATRX or its binding partner, the H3.3-specific histone chaperone DAXX, both of which are nuclear proteins, constituents of PML bodies (Pickett H.A. and Reddel R.R. 2015; Amorim J.P. et al. 2016). DAXX functions as a histone H3.3 chaperone and, together with ATRX facilitates the incorporation of the histone variant H3.3 into telomeric and pericentromeric chromatin in a replication-independent chromatin assembly pathway. Mutations in members of the ATRX/DAXX chromatin remodeling complex have been implicated in the activation of ALT mechanism. In particular, altered deposition of the histone variant H3.3 due to defects in the ATRX/DAXX complex compromise the maintenance of heterochromatin at the telomeres, significantly increasing the formation of G-quadruplex structures. The presence of G-quadruplexes leads to replication fork stalling and collapse, providing a substrate for MRN-dependent homologous recombination and maintenance of telomere length through ALT (Clynes D. et al. 2015).
Moreover, TERRA is an important factor highly associated to ALT activation. In fact, compared to telomerase-positive cancer cells ALT cells contain elevated levels of TERRA, which largely localizes to APBs (Arora L. and Azzalin C.M. 2015). TERRA can promote telomere length maintenance in ALT cells by converting telomeres into efficient substrates for HR due to the fact that TERRA can form recombinogenic RNA:DNA hybrid structures by base pairing with the C-rich strand of telomeres (Arora L. and Azzalin C.M. 2015).

#### 1.5.2.2 ALT-associated PML nuclear bodies

One of the most shared features of telomerase negative cells is the presence of promyelocytic nuclear bodies that frequently associate with telomeres. These complexes are called ALT-associated PML nuclear bodies (APBs) (Dilley R.L. et al. 2015).

PML nuclear bodies, also known as PML oncogenic domains (PODs), are dynamic structures often present in the cell nucleus that consist of two main proteins: PML and Sp100.

PML protein is the key organizer of these domains, that recruits an ever-growing number of proteins in order to form the functional complex.

PML bodies are interferons and oxidative stress-responsive protein, sequestration and SUMO-driven degradation centres. Depending on the cell type, stress signal and the repertoire of recruited proteins, PML bodies might mediate various downstream activities such as senescence and tumour suppression, sensing and repair of DNA damage (Chang H.R. et al. 2017). In particular, PML is an essential player for Ras-induced p53-mediated senescence. Importantly, p53 protein together with many of its regulatory enzymes can be detected in PML bodies, suggesting that nuclear bodies concentrate different factors involved in the post-translational modifications (phosphorylation, sumoylation, acetylation, etc.) of p53. The retinoblastoma (Rb) protein and the E2F transcription factor are recruited to PML nuclear bodies in order to respond to various stimuli, such as oncogenic signals (Sahin U. et al. 2014).

One of the important functions of PML-NBs is to sense and repair DNA damage thanks to their interaction with γH2AX and the MRN complex (Chang H.R. et al. 2017).

PML bodies are usually not associated with nucleic acids, but in ALT positive cells, a subset of PML often colocalize with telomeric chromatin and telomere-associated proteins, thus forming the APBs (Yeager T.R. et al. 1999). Moreover, these bodies contain proteins involved in DNA damage response and more importantly in homologous recombination such as Rad50/Mre11/NBS1 complex and Rad51/Rad52, together with the replication factor A (RPA), the helicase BLM and the telomeric repeat-binding factors TRF1 and TRF2.

Although the real function of APBs in ALT cells has not been fully elucidated yet, it is likely that APBs are involved in ALT-dependent telomere elongation (Chung I. et al. 2012).

## 1.6 MicroRNAs-dependent regulation of telomerase expression

The most studied class of small non-coding RNAs (ncRNA) are microRNAs (miRNAs) which appear as important cytoplasmic regulators of gene expression. miRNAs act as post-transcriptional repressors of their messenger RNA targets inducing mRNA degradation and/or translational repression, coordinating plenty of processes. miRNAs play a pivotal role in disease stases as a consequence of their deregulated expression or function.

### 1.6.1 MicroRNAs biogenesis

miRNAs are 19-25 nucleotides long single-stranded RNAs expressed in plants, animals and viruses. miRNAs biogenesis is a tightly regulated multistep process that occurs both in the nucleus and in the cytoplasm (Figure 1.12). microRNAs are transcribed by RNA polymerase II from independent genes or from RNAs of protein-coding or non-coding genes producing a primary miRNA (pri-miRNA). Pri-miRNAs are characterized by a hairpin structure and they are processed in the nucleus by the RNase III Drosha and the co-factor DGCR8, giving rise to ~70 nucleotides long precursor miRNA (pre-miRNA) (Hammond S.M. 2015).

An alternative miRNA biogenesis pathway, called miRtron pathway, is based on the processing of miRtrons, regulatory RNAs, which leads to the formation of pre-miRNAs without the Drosha-mediated cleavage.

pre-miRNAs are transferred by Exportin 5 to the cytoplasm and processed by the RNase III Dicer, generating a dsDNA, named miRNA/miRNA*, which includes the mature miRNA guide, and the complementary passenger strand, the miRNA* (Iorio M.V. and Croce C.M. 2012).

According to the thermodynamic features of the miRNA/miRNA* duplex, one of the two strands becomes the strand incorporated into the RISC (RNA-induced silencing complex) (guide strand or miRNA) and the other one gets degraded (the passenger strand or miRNA*). In particular, the strand with the weakest binding at its 5-end is

more likely to become the guide strand (Meijer H.A. et al. 2014). Moreover, strand selection relies on the ratios GC/AU content in 5′ of miRNA and miRNA* strand: a high content of AU in the 5′ of one strand is going to be selected over the complementary strand and vice versa (Granados-Lopez A.J. et al. 2017).

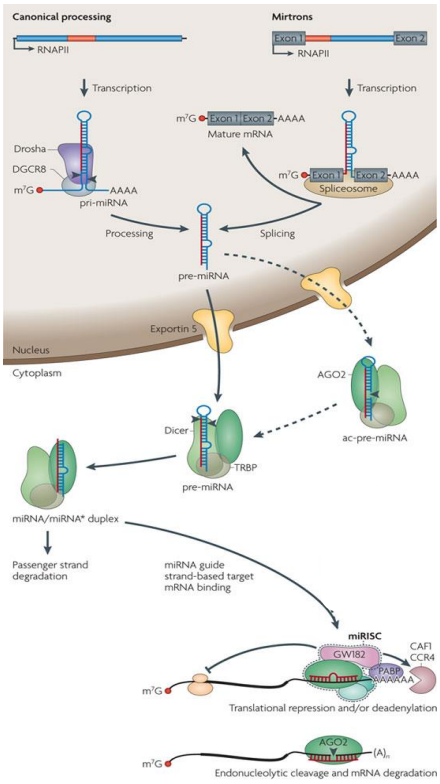


**Fig.1.12. Schematic model of microRNA biogenesis**: In the canonical pathway, RNA polymerase II transcribes pri-miRNAs, which are then processed by the Drosha–DGCR8 complex to generate pre-miRNAs. These double stranded hairpin structures are transported by exportin 5 into the cytoplasm, where they are further processed by Dicer–TRBP and loaded into Argonaute 2 (AGO2)-containing RNA-induced silencing complexes (RISCs) to suppress downstream target gene expression. miRNAs are also produced though non-canonical pathways, such as spliceosome-dependent mechanisms. The miRNA biogenesis pathway is a tightly regulated process. (Krol J. et al. 2010)

The mature miRNA is able to dinamically bind predominantely the 3' UTR of a mRNA using a particular sequence of 6-8 nucleotides at the 5' end of the miRNA known as "seed region". If the complementarity between the miRNA and mRNA is perfect, the effect on the binding target RNA is degradation; if the complementarity is only partial the consequence is the repression of translation (Iorio M.V. and Croce C.M. 2012).

The mature miRNAs prevalently binds the 3'-untranslated region (3' UTR) of target mRNA using its seed region even though various evidences have shown that the 5'-

UTR or the coding region can be target of mature miRNAs as well (Moretti F. et al. 2010).

### 1.6.2 miRNA deregulation in cancer

miRNAs have a crucial relevance for all the steps of tumorigenesis, indeed alterations in their expression and consequently in the expression of their target mRNAs can contribute to tumor formation and progression (Stahlhut C. and Slack F.J. 2013). It has become ever more apparent that miRNAs are dysregulated in most, if not all, cancers.

An individual miRNA has the ability to regulate a wide range of targets with opposing oncogenic or tumor suppressive functions, therefore miRNA function is context dependent. Indeed, certain miRNAs have been shown to be oncogenic in one scenario, but tumor suppressive in another. As an example, miR-29 can act as a tumour-suppressor miRNA in lung tumors whereas has oncogenic functions in breast cancer (Fabbri M. et al. 2007; Gebeshuber C.A. et al. 2009) or miR-125b acts as an oncomiR in the vast majority of haematological malignancies or as a tumor suppressor in solid tumors (Shaham L. et al. 2012; Sun Y.M. et al. 2013).

miRNA expression is strictly regulated and reduced or increased levels of mature miRNAs in tumors are often the result of deregulated transcription caused by epigenetic silencing, genetic loss, chromosomal amplification, deletion or defects in the miRNA biogenesis pathway (He X.X. et al. 2015; Parodi F. et al. 2016; Kan C.W. et al. 2015; Balatti V. et al. 2015). Indeed, Drosha or Dicer alterations can impinge on miRNA biogenesis in cancer (Merritt W.M. et al. 2008; Nakamura T. et al. 2007; Thomson J.M. et al. 2006).

In addition, tumor suppressors and oncoproteins are tightly linked with the control of miRNA expression. For instance, p53 can induce the transcription of several miRNAs such as the miR-34 family, which in turn can trigger apoptosis in colon cancer cell line (Feng Z. et al. 2011). Conversely, the oncoprotein MYC elicits the expression of the oncogenic miR-17-92 cluster and negatively regulates the transcription of tumor suppressor miRNAs, such as let-7 and miR-29 family members (Chang T.C. et al. 2009; Mott J.L. et al. 2010).

Aberrant microRNA expression in cancer has also been associated with epigenetic regulation such as DNA methylation and histone modifications. T24 bladder cancer cells or human fibroblasts treated with 5'-aza-2'-deoxycytidine, a DNA

methyltransferase inhibitor, and the histone deacetylase (HDAC) inhibitor 4-phenylbutyric acid (PBA), caused a strong modulation of various miRNAs including miR-127 (Saito Y. et al. 2009). Treatment with 5'-aza-2'-deoxycytidine of clear cell renal cell carcinoma (ccRCC) significantly promoted the expression of miR-200c. Accordingly, miR-200c gene transcription in ccRCC cells was mediated by the methylation status of the CpG island within the promoter region. Furthermore, hypermethylation of the miR-200c promoter may be a significant cause of downregulation of miR-200c in ccRCC tissues and cell lines (Jiang J. et al. 2016).

miRNA deregulation may be involved in tumor initiation and progression, thus providing the rationale for using miRNAs as potential therapeutic targets or tools in cancer. Indeed, miRNAs detection can provide important informations about the developmental lineage and differentiation stage of tumors (Lu J. et al. 2005). Importantly, miRNA can be used as prognostic markers to predict patients' outcome. Several studies have shown that miRNAs are differentially expressed in diseased tissues and differentially enriched in plasma, serum and other body fluids, potentially making them useful in the clinical practice as non-invasive biomarkers.

Lawrie C.H. et al. (2008) reported for the first time the presence of circulating microRNAs in serum samples of patients with diffuse large B-cell lymphoma (DLBCL). It was shown that higher levels of specific microRNAs are associated with diagnosis and prognostic outcome in DLBCL patients. This data suggests that microRNAs have a key potential as clinically useful non-invasive biomarkers in cancer.

Importantly, higher levels of miR-10b, miR-141, and miR-155 were found in the sera of lung cancer patients than in patients with benign disease pointing towards a key role of these miRNAs in a clinical context (Roth C. et al. 2011).

Urine miR-1 and miR-133b were identified as possible diagnostic and even prognostic biomarkers of kidney disease (Ben-Dov I.Z. et al. 2014; Trionfini P. et al. 2015).

### 1.6.3 Regulation of telomerase expression by miRNAs in human cancer

The enzymatic subunit of telomerase may be regulated at the post-transcriptional level via direct and indirect targeting by miRNAs. Given the importance of hTERT for immortalization of cancer cells, recent studies investigated the role of miRNAs in regulating hTERT expression in human cancer. Indeed, various evidences showed that miR-491-5p, miR-1182, miR-1207-5p, miR-1266, miR-138, let-7g, miR-133a, miR-342

and miR-541 are able to directly regulate hTERT mRNA levels in a wide range of tumors (Table 3).

| miRNA | Tissue type | Mode of action | Reference |
|---|---|---|---|
| miR-491-5p | Cervical cancer | Unknown, inhibits *hTERT* | Zhao et al., 2015 |
| miR-1182 | Gastric cancer | Binds the ORF of *hTERT* mRNA, preventing translation | Zhang et al., 2015 |
| miR-1207-5p | Gastric cancer | Represses *hTERT* in normal tissues | Chen et al., 2014 |
| miR-1266 | Gastric cancer | Represses *hTERT* in normal tissues | Chen et al., 2014 |
| miR-138 | Anaplastic thyroid carcinoma (ATC) | Interaction with 3′UTR of *hTERT* to reduce protein expression | Mitomo et al., 2008 |
| let-7g | Pulmonary fibrosis | Interaction with 3′UTR of *hTERT* to reduce expression | Singh et al., 2010 |
| miR-133a | Jurkat cells | Interaction with 3′UTR of *hTERT* to reduce expression | Hrdličková et al., 2014 |
| miR-342 | Jurkat cells | Interaction with the 3′UTR of *hTERT* to reduce expression | Hrdličková et al., 2014 |
| miR-541 | Jurkat cells | Interaction with the 3′UTR of *hTERT* to reduce expression | Hrdličková et al., 2014 |

**Table 3**. hTERT post-transcriptional regulation via miRNAs (Lewis K.A. and Tollefsbol1 T.O. 2016).

*Zhao Q. et al. (2015)* showed that hTERT is a specific target of miR-491-5p, which is able to suppress cervical cancer cell growth by targeting the enzymatic subunit of telomerase. In cervical cancer cells the overexpression of miR-491-5p causes a significant reduction of hTERT expression and inhibited the PI3K/AKT signaling pathways, finally leading to a significant decreased tumor growth.

miR-1182 was identified as a miRNA that specifically targets the open reading frame of hTERT in gastric cancer, thus attenuating gastric cancer proliferation and metastasis (Zhang D. et al 2015). Various evidences have shown that hTERT has a key role in the regulation of cell proliferation and metastasis control in an independent manner of its role on telomere homeostasis control. Zhang D. et al. demonstrated that the overexpression of miR-1182 inhibited the proliferation and migration of gastric cancer cells *in vitro* and *in vivo*.

miR-1207-5p and miR-1266 were shown to directly suppress hTERT expression in gastric cancer exerting their function without the direct binding to the 3' UTR of hTERT (Chen L. et al. 2014). Recent studies showed that miR-1207-5p and miR-1266 were significantly downregulated in cancer tissue, thus contributing to increased hTERT protein expression and leading to the development of gastric cancer. The ectopic expression of miR-1266 and miR-1207-5p inhibited growth and invasion of

gastric cancer cells, indicating that the delivery of miR-1207-5p and miR-1266 may be an effective treatment for gastric cancer (Chen L. et al. 2014).

miR-138 was demonstrated to directly bind the hTERT 3′UTR and modulate hTERT protein expression in anaplastic thyroid carcinoma and cervical cancer (Mitomo S. et al. 2008; Zhou N. et al. 2016). miR-138 expression determines a specific reduction in hTERT protein expression, suggesting that loss of miR-138 is involved in the gain of hTERT protein expression in human anaplastic thyroid carcinoma, sustaining the acquisition of malignant behavior in thyroid carcinomas (Mitomo S. et al. 2008). miR-138 acts as a tumor suppressor in cervical cancer by suppressing cancer growth, inhibiting cell migration, invasion and enhancing apoptosis. miR-138 was found to exert its function by directly targeting hTERT, acting as a novel potential therapeutic agent for the treatment of cervical cancer (Zhou N. et al. 2016).

Hrdličková R. et al. (2014) demonstrated that at least five different miRNAs (let-7g*, miR-133a, miR-342-5p, miR-491-5p, and miR-541-3p) directly regulate hTERT expression levels. The same set of miRNAs also participate in the regulation of TCF7, MSI1, and PAX5 which are strictly involved in the regulation of the Wnt pathway.

The interplay between the Wnt pathway and telomerase has functional consequences: a regulatory network could be established to control both telomerase activity and cell proliferation. This network may be important in cells where telomerase and Wnt pathways are both involved such as in stem cells or several tumor types. Even though let-7g*, miR-133a, miR-138 and miR-491 can inhibit hTERT expression, thus decreasing cell proliferation, the effect of these miRNAs on proliferation was pronounced only in cells with a highly activated Wnt pathway, suggesting that the inhibition of Wnt target genes by these miRNAs was responsible for most of this effect.

In conclusion, multiple miRNAs are able to regulate telomerase activity, proliferation rate, cell migration, invasion and apoptosis via the direct interaction with hTERT. miRNA-dependent regulation of the enzymatic subunit of telomerase might assume a key role in tumor progression because of the miRNA-dependent impairment of telomerase activity and function, which can result in telomere attrition as well as in the impairment of extra-telomeric functions of telomerase such as apoptosis regulation, epithelial to mesenchymal transition (EMT) and cancer invasiveness.

# 2. AIM OF THE THESIS

In this study we aimed to explore new non-coding RNA related pathways that regulate telomerase and telomere homeostasis in cancer cell models.

In particular, my PhD thesis aimed:

- To identify novel miRNAs that can regulate telomerase expression in breast cancer cells and to demonstrate clinical relevance for these miRNAs (**project 1**)

- To study the role of the trimethylation of hTR by the RNA methyltransferase TGS1 in telomere homeostasis (**project 2**)

# 3. MATERIALS AND METHODS

## 3.1 Cell lines and culture

Cell lines used were obtained from ATCC and have not been cultured for longer than 6 months. In this project MCF-7 (Michigan Cancer Foundation-7, breast adenocarcinoma), SK-BR-3 (breast adenocarcinoma derived), T-47D (ductal carcinoma), HCT-116 (colorectal carcinoma) and H1299 (non-small cell lung cancer) cells were cultured in RPMI-1640, with the addition of 10% FBS (Gibco). MDA-MB-231 (breast adenocarcinoma), MDA-MB-468 (breast adenocarcinoma), MDA-MB-157 (medulallary carcinoma), HeLa (cervix adenocarcinoma) and U-2 OS (osteosarcoma), cells were cultured in DMEM with the addition of 10% heat-inactivated FBS .

MDA-MB-231 stably overexpressing miR-296 and miR-512 were selected with blasticidin (8mg/mL) while MDA-MB-231 infected with retroviral vectors encoding shControl and shTERT were selected with puromycin (2ug/mL). MDA-MB-231 infected with pBabe empty were selected with puromycin (2ug/mL) while cells overexpressing pBabe-TERT were selected with hygromicin (100ug/mL)

H1299 cells stably overexpressing FLAG-TERT and hTR were generated through the transfection of the respective linearized vector and were selected using blasticidin (5 μg/mL) and puromicin (1μg/mL)

MDA-MB-231 cells were treated with 5'-Aza-2'-deoxycytidine (Sigma) at a concentration of 1, 3 o 10 μmol/L for 5 days and the compound was added fresh each day. Moreover, MDA-MB-231 was treated with Trichostatin A (Sigma) for 24h at a concentration of 1 μmol/L while Suberoylanilide hydroxamic acid (SAHA) (Sigma) was used for 48h at a concentration of 5 μmol/L.

H1299 cells were treated with Sinefungin (Santa Cruz) at a concentration of 100 μmol/mL for 3 or 10 days and the compound was added fresh every two days.

## 3.2 Cloning of specific 3'-UTR into psiCHECK-2 expression vector

The 3'-UTR of hTERT was amplified by PCR from genomic DNA of HeLa cells. The PCR reaction was performed in a total volume of 50 ul using:

2,5 μl of DMSO (Dimethyl sulfoxide),

1,75 μl dNTPs (10 nM),

5 μl of Buffer 1 (10X),

0.75 μl of Taq DNA polimerase (Expand long template PCR mix Roche),

1 μl (100 ng/μl) of genomic DNA

10 pmol of the following primers:

| Oligo name | Sequence |
|---|---|
| TERT FW | GCCGCGGCCGCTGGCCACCCGCCCACAGCCAG |
| TERT REV | GCCGCGGCCGCCAAAACTGAAAAAC |

The sequence of the restriction enzyme NotI was inserted at the end of the primers in order to allow cloning of PCR fragment in the luciferase reporter vector (psiCHECK-2). In the first step, the PCR product has been cloned into pCR2.1-TOPO vector using TOPO TA-cloning kit (Invitrogen). The 3'-UTR was sequenced to ensure the absence of any mutation, after this sequencing step the sequence and the psiCHECK-2 vector have been cut with NotI (New England BioLabs), the vector has been treated with phosphatase alkaline to avoid the re-ligation of the vector (1µl of AP for 30 minute - 37°C, New England BioLabs). The PCR product and psiCHECK-2 vector were legated using DNA ligase T4 (ROCHE) at 16°C over night. The ligation product was used to transform competent bacteria HIT DH5α (UBI).
The psiCHECK-2 vector with the specific 3'-UTR was sequenced in order to verify the correct orientation of the insert in to the vector.

## 3.3 Generation of mutant 3'-UTR of TERT

TERT-3'-UTR mutants have been generated using the QuikChange II XL Site-Directed Mutagenesis Kit (Agilent). The protocol was performed according to the manufacturer's suggestions and the specific primers are listed below:

| Oligo name | Sequence |
|---|---|
| TERT-Δ83-85 FW | AGGGAGGGAGGGGCAAACCACACCCAGGCCC |
| TERT-Δ83-85 REV | GGGCCTGGGTGTGGTTTGCCCCTCCCTCCCT |
| TERT-Δ479-481 FW | CCTGCACCTGGAGAAGGGTCCCTGTGGGTCAAATTG |
| TERT-Δ479-481 REV | CAATTTGACCCACAGGGACCCTTCTCCAGGTGCAGG |
| TERT-Δ164-166 FW | CCTGCATGTCCGGCTGAAGGCTTGTTGTCCGGCTGAG |
| TERT-Δ164-166 REV | CTCAGCCGGACAACAAGCCTTCAGCCGGACATGCAGG |

## 3.4 miRNA library vectors

The library contains 439 expression vectors which was kindly provided by the group of R. Agami (Division of Gene Regulation, The Netherlands Cancer Institute, Amsterdam). Each vector (derived from Mouse Embryonic Stem Cell Virus) (Voorhoeve P.M. et al 2007) contains the genomic sequence of ~500 nt that encoded a specific miRNAs, cloned downstream to the viral promoter CMV. The vectors contain the gene that allows the resistance to Blasticidin, used to select the positive clones in eukaryotic cells.

The DNA of all vectors of the library used in this study were transformed into bacterial cells HIT competent DH5α (UBI) and plasmid DNA was obtained using miniprep kit (Qiagen). The plasmid DNA obtained was sequence before using it in the screening.

## 3.5 Luciferase reporter screening

HeLa and MDA-MB-231 cells were cotransfected with 18 ng of 3'-UTR luciferase reporter plasmids (TERT) and 80 ng of mimic miRNA siRNAs.

Cells have been transiently transfected in a 48 well plate using Lipofectamine 2000 (Life Technologies). Seventy-two hours post-transfection cells were lysed in LBL lysis Buffer 5x and lysates were loaded in a GloMax Microplate Luminometer (Promega) to analyze the Renilla/Firefly luciferase reporter activity by the Dual Luciferase Reporter Assay System (Promega).

The reporter activity was expressed as Renilla/Firefly luciferase ratio. A Mann-Witney non parametric test was used to calculate the statistical significance.

## 3.6 Transfection of siRNA and RNA-oligonucleotides

siRNA or RNA-oligonucleotides used to transiently transfect cells are the following:

Human, ON-TARGETplus non-targeting siRNA#1 (Dharmacon)

ON-TARGETplus smartpool TRF1 siRNAs (Dharmacon)

ON-TARGETplus smartpool TGS1 siRNAs (Dharmacon)

ON-TARGETplus smartpool RAD51 siRNAs (Dharmacon)

miRIDIAN microRNA mimic negative control siRNA (Dharmacon)

hsamiR-296-5p mimic siRNAs (Dharmacon)

miRIDIAN microRNA hsa-miR-296-5p hairpin inhibitor (Dharmacon)

hsa-miR-512-5p mimic siRNAs (Dharmacon)

miRIDIAN microRNA hsa-miR-512-5p hairpin inhibitor (Dharmacon)

Cells were seeded the day before transfection, the following day, cells were transfected using RNAiMAX Lipofectamine (Invitrogen) and siRNA or RNA-oligonucleotides at a final concentration of 30nM according to the manufacturer's instructions.

## 3.7 Protein extracts and Western blotting

The whole-cell lysates were prepared using a modified RIPA buffer (20 mmol/L Tris-HCl (pH 7.5) 350 mmol/L NaCl, 1 mmol/L $Na_2EDTA$, 1 mmol/L EGTA, 1% NP-40, 1% sodium deoxycholate, 2.5 mmol/L sodium pyrophosphate, 1 mmol/L b-glycerophosphate, 1 mmol/L $Na_3VO_4$, 1 mg/mL leupeptin).

In order to prepare nuclear extracts, cells were resuspended in Buffer 1 (20 mmol/L Hepes-KOH (pH 7.9), 10 mmol/L KCl, 1.5 mmol/L $MgCl_2$, 1 mmol/L EDTA, 1 mmol/L EGTA, 0.2% NP40) and incubated for 10 minutes on ice. Nuclei were pelleted and lysed in Buffer 2 (20 mmol/L Hepes-KOH (pH7.9), 350 mmol/L NaCl, 1.5 mmol/L $MgCl_2$, 10 mmol/L KCl, 10% glycerol, 1 mmol/L dithiothreitol).

Both whole cell lysates and nuclear extracts have been additioned with complete protease inhibitor (Roche) and sonicated. After centrifugation, supernatants have been recovered and used for Western blotting according to standard procedures.

The primary antibodies used are listed in the antibodies table 3.24.

Membranes were incubated with the specific secondary antibodies bound to the HRP enzyme (horseradish peroxidase-conjugated antibody) (GE Healthcare) and the levels of protein expression were detected by chemiluminescence using the ECL system (GE Healthcare) with subsequent exposure on autoradiography film (GE Healthcare).

## 3.8 Vectors and vector construct

p-Babe-hygro-hTERT, pMKO.1-puro hTERT shRNA,pLPC-NFLAG-TERT vectors have been purchased by Addgene. miR-296 vector was included in the miRNA library kindly provided by the group of R. Agami while miR-512 vector was cloned in our laboratory using the following primers:

(BamHI) GC-GGATCC- CCAAAGTGCTGGGATTACAG ;

(ECORI) GC-GAATTC- AAGAGGCAACCAATCCAGAC .

## 3.9 RNA extraction and RT-PCR

Total RNA was prepared using QIAzol Lysis Reagent (Qiagen) and reverse transcribed with QuantiTect Reverse Transcription Kit (Qiagen) according to the manufacturer's instructions.

For miRNA analysis 10 ng of RNA were reverse transcribed using the hsa-miR-296-5p, hsa-miR-512-5p and RNU49 TaqMan™ MicroRNA Assay systems (Applied Biosystems).

The stem loop real-time PCR was performed by using Taqman Fast PCR Master mix (Life Technologies), according to manufacturer's suggestions. Quantitative miRNA expression data was analyzed using a Bio-Rad CFX96 C1000 Touch Real-time PCR Detection System.

For quantitative mRNA expression analysis 500 ng of total RNA were reverse transcribed using the QuantiTect Reverse Transcription kit (Qiagen) according to the manufacturer's instructions. Quantitative PCR was performed using the SYBR Green Master Mix (Applied Biosystem) and analyzed with a StepOnePlus real time PCR machine (Applied Biosystem). mRNA levels were normalized to actin.

PCR primers used for quantitative real-time PCR:

| Oligo name | Sequence |
|---|---|
| hTERT FW | AACAAGCTGTTTGCGGGGAT |
| hTERT REV | CCAGGGTCCTGAGGAAGGTTT |
| ß-ACTIN FW | AGCACTGTGTTGGCGTACAG |
| ß-ACTIN REV | TCCCTGGAGAAGAGCTACGA |
| hTGS1 FW | AGGAGCGGAGGATTGTAAG |
| hTGS1 REV | TCCTCTTCTTCTGTCGCCTG |
| hTR FW | CCTAACTGAGAAGGGCGTAGG |
| hTR REV | GAATGAACGGTGGAAGGCG |
| hTRF1 FW | GCTGTTTGTATGGAAAATGGC |
| hTRF1 REV | CCGCTGCCTTCATTAGAAAG |
| hTRF2 FW | CATGCAGGCTTTGCTTGTCA |
| hTRF2 REV | CTGCATAACCCGGAGCAATA |

## 3.10 Immunofluorescence

Cells were washed with 1x PBS and fixed in 4% paraformaldehyde (PFA) for 15 minutes.

Subsequently cells were washed with 1x PBS, treated with citrate buffer (0.1% sodium citrate, 0.05% Triton X-100) for 10 minutes at room temperature and washed with 1x PBS, 0,1% Tween-20. Cells were blocked for 1 hour in 3% BSA (1X PBS, 0.1% Tween-20) and incubated with primary antibodies (check 2.23 antibodies table) diluted in blocking solution for 2h at room temperature in a wet chamber. Cells were washed three times in 0.3% BSA (1X PBS, 0.1% Tween-20) for 5 minutes and incubated with Alexa-fluor secondary antibodies (Invitrogen) (1:500) diluted in washing solution for 1h in a wet chamber. After incubation, slides were washed three times in 0.3% BSA (1X PBS, 0.1% Tween-20) for 10 minutes. Afterwards, DAPI (Vector Laboratories) was added in order to stain the nuclei and slides were incubated for 5 minutes. Slides were mounted with Vectashield.

Images were captured using classic immunofluorescence (Leica DM4000B) microscope. For classic immunofluorescence analysis, the number of co-localizations per focal plane was counted. Quantitative immunofluorescence analysis were performed using ImageJ. The Student t test was used to calculate the statistical significance.

## 3.11 Interphase Telomere Q-FISH

Cells were briefly washed in 1X PBS, fixed with 4% formaldehyde (PFA) for 2 minutes at RT and washed three times for 5 minutes with 1X PBS. Slides were dehydrated with three successive washes in 70%, 90%, and 100% ethanol for 5 minutes each and let to airdry for 20 minutes at RT. Afterwards, PNA-telomere probe (Table 1) were added to each slide and cover with a coverslip, the slides were denaturated at 80 °C for 3 minutes exactly.

The slides were incubated for 2 hours at RT in the dark in a wet chamber. After the incubation, slides were washed in mild agitation twice for 15 minutes with FISH solution (Formamide 70%, Tris pH 7.2 10mM, BSA 0.1%, H2O) at RT, followed by three washes of 5 minutes in 1X TBS with 0,01% of Tween-20 at RT. Nuclei were stained with DAPI included in a fourth wash.

The slides were then dehydrated with 3 washes in 70%, 90%, 100% of ethanol, left to airdry for 20 minutes and mounted with Vectashield. Images were captured using Leica DM4000B microscope.

Telomere signals intensity of interphase nuclei was analyzed using TFL-TELO software. The Student t test was used to calculate the statistical significance.

| Stock | PNA-Telomere Probe (1 slide) | Final Concentration |
|---|---|---|
| 1M Tris pH 7.2 | 0.25 µl | 10 mM |
| Buffer MgCl pH 7.0 (25 mM MgCl, 9 mM citric acid, 82 mM Na2HPO4) | 2.14 µl | |
| Deionized Formamide | 17.5 µl | 70% |
| probe 25 µg/ml | 0.5 µl | 0.5 µg /ml |
| Blocking Reagent 10% | 1.25 µl | 0.5% |
| $H_2O$ | 3.36 µl | |

**Table 1.** PNA-telomere probe solution

## 3.12 Retroviral transduction of human cells

HEK 293GP (Gag and Pol) were used as packaging cell line. The solution containing DNA and $CaCl_2$ (2,5 M $CaCl_2$ sterilized by filtration) for a 10cm dish was prepared adding sequentially:

$H_2O$ up to 450 ul

50ul $CaCl_2$

5-10 g of specific plasmid DNA.

In a different tube 500 µl of 2X Hepes Buffer Saline were added and the DNA solution was transferred drop by drop to the 2X HBS tube and mixed by introducing air bubbles and incubated for 20-30 minutes in order to allow the efficient formation of DNA-CaPO4 precipitates. After the incubation, this solution was added to cells and incubated at 37 °C. for 6 hours, after which the medium was changed and cells were incubated for additionally 48 hours. Subsequently, the supernatant containing the virus was collected, filtered and mixed with 1ml of fetal bovine serum (FBS) and 8 µg/ml of polybrene. This solution was used to infect selected cells. The day after, medium was changed. After 24 hours the specific antibiotic to select transfected cells was added.

## 3.13 TRAP assay

Telomerase activity was measured using TRAPeze Telomerase Detection Kit (Millipore S7700). Cells were transiently transfected with specific siRNA or RNA-oligonucleotides or treated with the RNA-methyltransferase inhibitor sinefungin and three or 10 days days after were washed with ice cold 1X PBS and lysed with 1X CHAPS buffer for 30 minutes on ice. Samples were centrifuged at 12,000 g for 20 minute at 4 °C and the supernatants were transferred into a fresh tube and the protein concentration was determined using Bradford reagent (Sigma).

100, 50 or 25 ng of the supernatant fraction was incubated at 30 °C for 30 minutes and subjected to a PCR, using DreamTaq DNA Polymerase (Thermo Scientific). Heat-inactivated lysates and TSR8 were used as control. Samples were then loaded in a 10% non-denaturing polyacrylamide gel in 0,5 X TBE buffer and run for 1,5 hours at 400 volts. Subsequently, the gel was stained with SYBR Gold nucleic acid gel (Life Technologies) according to the manufacturer's instructions; the acquisition of images was performed with a gel DOC XR system (BIO-RAD).

ImageJ Software was used to determine the intensity of the TRAP products.

Non-heat-treated samples, (x) and heat-treated samples, (x0); primer-dimer/PCR contamination control, (r0), positive PCR control - TSR8 (r). The signal from S-IC (Standard internal PCR control) in non-heat-treated samples (c) and TSR8 control (cr) was measured. The following formula was used to calculate TRAP activity:

$$\frac{(x-x0)/c}{(r-r0)/cr} \text{x}100.$$

## 3.14 Bisulfite assay

MDA-MB-231 cells were treated with 5'-Azacytidine at a concentration of 3 μM for 5 days, after which genomic DNA was isolated.

Cells were resuspended in protein K buffer (Ambion) and then genomic DNA was extracted using phenol/Chloroform/isoamyl alcohol (Fischer scientific). A total of 500 ng of genomic DNA was converted with Qiagen EpiTect Bisulphite kit following the manufacturer's instructions and amplified by PCR with the following primer sets designed using MethPrimer software (Li L.C. and Dahiya R. 2002).

| Oligo name | Sequence | Position |
|---|---|---|
| miR-296 CpG-1 island FW | GTGAAAGTAAGTTTTATTGATGGT | 1751bp upstream miR-296 |
| miR-296 CpG-1 island REV | CAAAAAATTCCAAAAACCCTTAAA | |
| miR-296 CpG-2 island FW | GTGTTAGGAGTGGAGATAGGATAGT | 88bp downstream miR-296 |
| miR-296 CpG-2 island REV | TCAATAAAAATAAAAAAAACCTCC | |
| miR-512 CpG-1 island FW | TTGTAATTTTAGTATTTTGGGAGGT | 2806bp upstream of miR-512-1 |
| miR-512 CpG-1 island REV | AAAACAATCTCACTCTATTACCCAAAC | |
| miR-512 CpG-2 island FW | TTTTTTTTGAGGGATTAGAATTTGTT | 17692 bp upstream of miR-512-1 |
| miR-512 CpG-2 island REV | CCCTAAACTTCCTAATTAAATAAAAAACTA | |

The obtained PCR products were gel purified and cloned into pCR2.1 using the TA cloning kit (Invitrogen). Individual clones were sequenced with M13 Fw and M13 Rev primers. Obtained sequences were analyzed using QUMA software.

## 3.15 FACS analysis

MCF-7 and MDA-MB-231 cells were transiently transfected with specific mimic-miRNA siRNAs oligonucleotides and three days post-transfection the medium and the cells were recovered and centrifuged for 5 minutes at 1000 rpm. The supernatant was removed, cells were washed with 500 μl of 1X PBS and centrifuged for 5 minutes at 1000 rpm. Afterwards, 1X PBS was removed and 300 μl of 1X PBS with 700 μl of 100% ice-cold ethanol were added, cells were incubated for 30 minutes at -20 °C.

Subsequently, samples were centrifuged for 5 minutes at 4000 rpm, the supernatant was

eliminated and cells were washed with 1X PBS. The samples were centrifuged again and additioned with:

100 μl of 1X PBS / 0,1% NP40

2 μl of RNase A (10mg/ml).

Then the samples was carefully mixed and left to incubate for 10 minutes at RT.

300 μl of Propidium Iodide (50 μg/ml) (Sigma)solution was added in order to reach a final volume of 400 μl for sample.

Apoptosis rate was measured using Dead Cell Apoptosis Kit with Annexin V Alexa Fluor488 & Propidium Iodide (PI) (Invitrogen V13241), according to the manufacturer's suggestions. For flow cytometry, a FACSCalibur flow cytometer (BD Biosciences) operated by CellQuest software was used; at least 30,000 events were collected per sample. Results were analyzed using the FlowJo software (Tree Star, Ashland, OR, USA).

## 3.16 Growth curve

MDA-MB-231 and MCF-7 cells were transfected twice by a distance of 3 days with the specific mimic-miRNA siRNA. Cells were counted at day 0, 1, 3 and 6 for MDA-MB-231 and at day 6 only for MCF-7. Stable MDA-231 cells overexpressing hTERT were transiently transfected with the specific RNA-oligonucleotides at day 0 and 3, then the cells were counted at day 6.

The non-parametric Mann-Whitney test was used to calculate the statistical significance.

## 3.17 Bioinformatics on clinical data from breast cancer patients

miRNA expression values in breast cancer samples were obtained from EMBL-EBI EGAS00000000122. Gene expression values, clinical data and survival data were obtained using KM plotter and GOBO. In order to evaluate the impact of gene signatures on breast cancer survival, the patient samples were split into two groups according to various quantile expressions (median for GOBO and using the best cut-off algorithm or KM plotter) of the proposed signatures, a Mantel-Haenszel test was applied and was obtained a Kaplan–Meier survival curve. Statistical analysis has been performed using R software environment for statistical computing (R Core Team (2015). R: A language and environment for statistical computing. R Foundation for Statistical Computing, Vienna, Austria. http://www.R-project.org/) and Bioconductor.

## 3.18 ChIP assay and telomere dot-blots

Cells were fixed adding formaldehyde to culture medium to a final concentration of 1% and incubated for 15 min at RT in mild agitation. The addition of glycine to a final concentration of 0.125 M stopped the cross-linking. Crosslinked cells were washed

twice with cold 1X PBS, scraped and lysed for 10 minutes at 4 °C in a lysis buffer containing 1% SDS, 50 mM Tris-HCl (pH 8.0), 10 mM EDTA and supplemented with protease inhibitors.

Lysates were sonicated to obtain chromatin fragments >1 kb and centrifuged for 15 min in a microcentrifuge at room temperature. Chromatin was diluted 1:10 with 1.1% Triton X-100, 0.01% SDS, 1.2 mM EDTA, 167 mM NaCl and 16.7 mM Tris-HCl (pH 8.0) containing protease inhibitors and precleared with Protein A or Protein G agarose beads

(Santa Cruz). Chromatin was incubated with 3,5 µg of specific antibodies (check 3.23 antibodies table) or rabbit/mouse IgG as negative control rocking overnight at 4°C. Protein A or Protein G agarose beads were then added and the incubation continued for 1 h. Immunoprecipitated pellets were washed with 0.1% SDS, 1% Triton X-100, 2 mM EDTA, 20 mM Tris-HCl (pH 8.0) and 150 mM NaCl (one wash); 0.1% SDS, 1% Triton X-100, 2 mM EDTA, 20 mM Tris-HCl (pH 8.0) and 500 mM NaCl (one wash); 0.25 M LiCl, 1% NP-40, 1% sodium deoxycholate, 1 mM EDTA and 10 mM Tris-HCl, pH 8.0 (one wash); and 10 mM Tris-HCl (pH 8.0) and 1 mM EDTA (two washes). Chromatin was eluted from the beads twice by incubation with 250 µl of 1% SDS/ 50mM $NaHCO_3$ for 15 min rocking at room temperature. After adding 20 µl of 5 M NaCl, crosslinks were reversed by incubation for 4 h at 65 °C. Samples were supplemented with 20 µl of 1 M Tris-HCl (pH 6.5), 10 µl of 0.5 M EDTA, 20 µg of RNase A and 40 µg of proteinase K and incubated for 1 h at 45°C. DNA was recovered by phenol-chloroform extraction, ethanol precipitation and spotted into a dot-blot with a Hybond N+ membrane which was hybridized with a telomeric probe obtained from a plasmid containing 1.6 kb of TTAGGG repeats. For total DNA samples, aliquots corresponding to a 1:10 dilution of the amount of lysate used in the immunoprecipitations were processed along with the rest of the samples during the crosslink reversal step.

## 3.19 RNA immunoprecipitation

Total RNA extracted from transiently transfected with specific siRNAs or treated cells was resuspended in RIPA buffer containing RNase inhibitors (RNase OUT - Life Technologies). 100 µg of total RNA was incubated with mouse anti-2,2,7-trimethylguanosine rocking for 4 hours at 4 °C. Protein G agarose beads were then added and the incubation continued for 3 hours. After three washes with RIPA supplemented with RNase Inhibitors, the pelleted resin was centrifuged and the

bounded RNA was extracted using QIAzol Lysis Reagent (Qiagen) as manufacturer's instructions.

The purified RNA was reverse transcribed using QuantiTect Reverse Transcription Kit (Qiagen) and quantitative PCR was performed using the SYBR Green Master Mix (Applied Biosystem) and analyzed with a StepOnePlus real time PCR machine (Applied Biosystem). mRNA levels were normalized to actin.

## 3.20 Northern blot

To perform Northern blot analysis total RNA (10 µg) was loaded onto 1.2% formaldehyde

agarose gels and separated by electrophoresis. RNA was then transferred to Nylon membranes overnight and blots were incubated overnight rocking at 65°C with a probe of 450 bp labelled with $^{32}P$ using the Amersham Rediprime II DNA Labeling System (GE Healthcare) that specifically hybridizes to telomerase RNA component, obtained from a vector containing the gene encoding for hTR. Afterwards membranes were washed twice with Wash Buffer (20 mM $NaPO_4$ pH 7.2, 1% SDS) rocking for 20 minutes at 65°C.

Subsequently, the levels of hTR expression were detected by exposure on autoradiography film (GE Healthcare). GAPDH was used as a loading control.

## 3.21 Antibodies table

| Antibody | Company | WB | IF | ChIP |
|---|---|---|---|---|
| Mouse anti-2,2,7-trimethylguanosine (clone K121) | Millipore MABE302 | ✓ | | |
| Mouse anti-actin | Sigma A2228 | ✓ | | |
| Rabbit anti-caspase 3 | Cell Signalling 9662 | ✓ | | |
| Rabbit anti-cleaved caspase-3 (Asp175) | Cell Signalling 9661 | ✓ | | |
| Rabbit anti-coilin (H-300) | Santa Cruz sc-32860 | | ✓ | |
| Mouse anti-FLAG M2 (clone M2) | Sigma F3165 | ✓ | ✓ | ✓ |
| Mouse anti-PARP 1 | Calbiochem AM30 | ✓ | | |
| Rabbit anti-PIMT | Bethyl A300-814A | ✓ | | |

| | | | | |
|---|---|---|---|---|
| Rabbit anti-PML (H-238) | Santa Cruz sc-5621 | | ✓ | |
| Rabbit anti-TRF1 (N19)-R | Santa Cruz sc-6165-R | | ✓ | |
| Mouse anti-TRF2 (clone 4A794) | Millipore 05-521 | | ✓ | ✓ |
| Mouse anti- γH2AX (ser139) (clone JBW301) | Millipore 06-570 | ✓ | | |

# 4. RESULTS

## 4.1 Project 1: Silencing of miR-296 and miR-512 ensures hTERT dependent apoptosis protection and telomere maintenance in basal-type breast cancer cells

### 4.1.1 miR-296-5p and miR-512-5p target the 3'UTR of hTERT and are down-regulated in breast cancer

In order to establish a list of miRNA candidates with a high specificity for the 3'UTR of hTERT, an *in silico* analysis was performed using PITA (Kertesz M. et al. 2007), TargetScan (Lewis B.P et al. 2005; Friedman R.C. et al. 2009; Grimson A. et al. 2007; García D.M. et al. 2011) and micro-RNA.org (Betel D. et al. 2008) that use different algorithm. After candidate identification, a high-throughput luciferase screening for candidate validation was performed.

In particular, Hela cells were transiently co-transfected with i) candidate mimic-miRNA siRNAs and ii) a luciferase reporter vector containing the Renilla luciferase cDNA fused to the full length 3'UTR of hTERT as well as a Firefly luciferase expression cassette, necessary to correct for transfection efficiency. Three days post transfection, Renilla to Firefly luciferase luminescence ratio was determined by dual-luminometry. Seventysix% of candidate miRNAs showed reduced Renilla to Firefly luminescence values (<1) when compared to non-specific control mimic-miRNA siRNAs (Figure 4.1.1 A; B).

We selected miRNAs for further validation that i) mediate at least 50% reduction of luciferase reporter activity and ii) show altered expression in a miRNA expression dataset containing 1,302 breast tumors with detailed clinical annotation (Dvinge H. et al. 2013). Given that hTERT re-expression is critical for cellular immortalization, we hypothesized that functionally relevant miRNAs are down-regulated in breast cancer, thus facilitating improved telomere maintenance and protection from apoptosis.

Among candidate miRNAs that mediate at least 50% reduction of hTERT 3'UTR reporter activity, only miR-296-5p, miR-512-5p and miR- 1207-5p showed significant down-regulation in breast cancer when compared to healthy tissue (Figure 4.4.1 C). Expression levels of miR- 16-1*, miR-541, miR-637, miR-661 or miR-608 are not altered in breast cancer tissue.

miR-296-5p has a tumor suppressive role in breast, prostate, non-small cell lung cancer and glioblastoma (Vaira V. et al. 2012; Wei J.J. et al. 2011; Xu C. et al. 2016; Savi F. et al. 2014; Lee K.H. et al. 2014). miR-512-5p can activate apoptosis in lung and gastric cancer and target hTERT in head and neck squamous cell carcinoma (Li J. et al. 2015; Chu K. et al. 2016; Adi Harel S. et al. 2015; Saito Y. et al. 2009).

Given the downregulation of miR-296-5p and miR-512-5p in breast cancer, we decided to focus our functional analysis on these candidates.

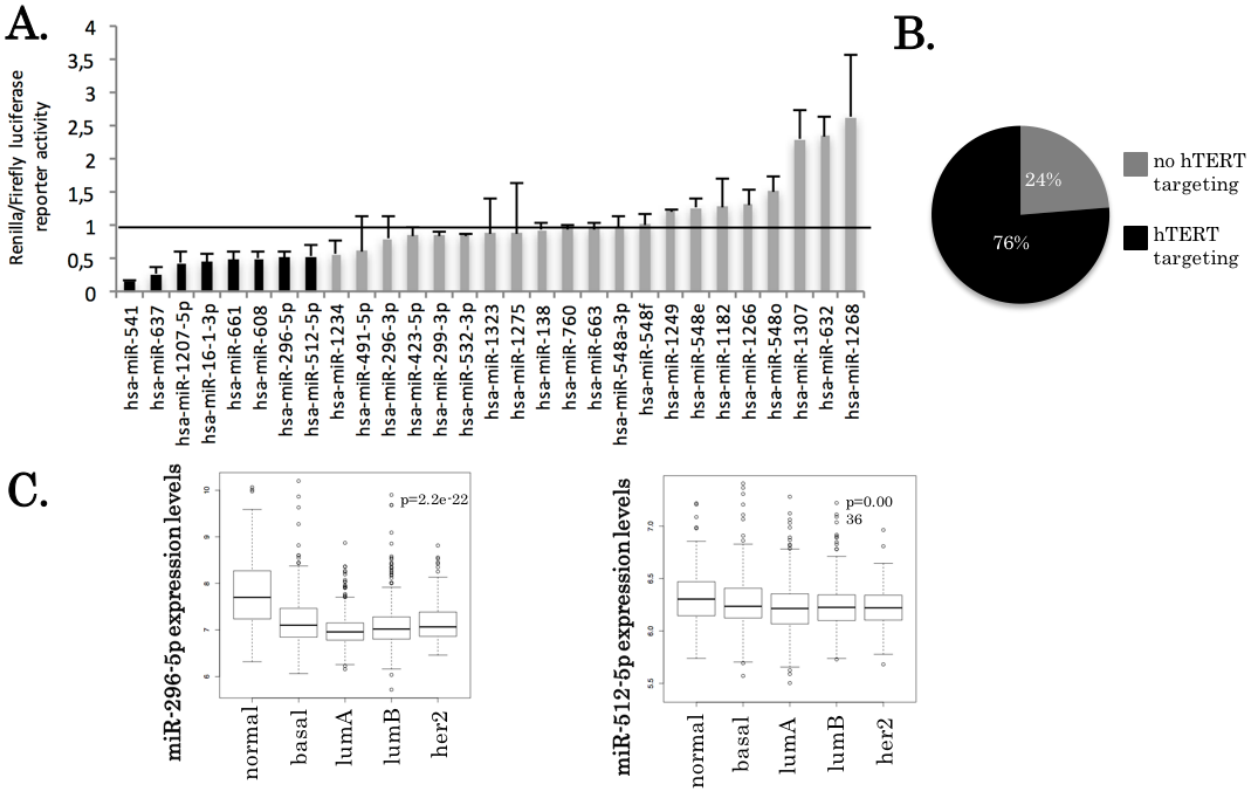


**Figure 4.1.1. A.** Results of the high throughput luciferase screen. Renilla:Firefly luciferase ratios of individual candidate are shown. Ratios Renilla:Firefly <1 indicate miRNA-dependent targeting of the TERT 3'UTR. Candidate miRNAs with Renilla:Firefly ratio <0,5 are indicated with black bars and were considered for further analysis. 3 independent experiments was performed and a Student t test was used to calculate standard deviation, shown by error bars. **B.** Proportion of candidate miRNAs that reduced hTERT-3'UTR luciferase reporter activity. **C.** miR-296-5p and miR-512-5p expression levels in normal breast tissue and human breast cancer subtypes. Expression values are shown in box blots at a log2 scale; a Wilcox test was used to calculate the indicated p-values.

### 4.1.2 miR-296-5p and miR-512-5p regulate telomere homeostasis by targeting the 3' UTR of hTERT

The 3' UTR of TERT contains three different predicted target sites for miR-296-5p (nucleotides 59-94, 457-495, 456-494) and one target site for miR-512-5p (nucleotides 141-177) (Figure 4.1.2 A; B). All target sites are exclusively found in primates (data not shown).

In order to directly validate the specificity of miR-296-5p and miR-512-5p for the 3' UTR of hTERT, different luciferase reporter constructs carrying deletions of the individual miR-296-5p and miR-512-5p target sites were generated. To validate the specificity of miR-296-5p three mutants have been generated: the first lacks the nucleotides 83-85 (Δ83-85), the second lacks the remaining two target sites (Δ479-481) and the Δ83-85, Δ479-481 construct that lacks all miR-296 target sites. In analogy, a construct with a deletion in the hTERT 3'UTR covering the miR-512-5p target site at position 168-170 (Δ168-170) was generated.

MDA-MB-231 and Hela cells have been transiently co-transfected with wild type or individual 3'UTR TERT mutants in combination with either mimic negative control or mimic-miRNA siRNAs. Three days post-transfection Renilla to Firefly luciferase luminescence ratio was determined by dual-luminometry. Ectopic introduction of mimic miR-296-5p and miR-512-5p significantly reduced luciferase activity in both MDA-MB-231 (Figure 4.1.2 C; H) and Hela (data not shown) cells when compared to mimic negative control. Importantly, ectopic expression of the deletion mutants of miR-296-5p and miR-512 target sites (Δ83-85- Δ479-481- Δ83-85, Δ479-481-Δ168-170) renders the 3'UTR of hTERT resistant to miR-296-5p and miR-512-5p dependent regulation (Figure 4.1.2 D-F; H,I).

Importantly, MDA-MB-231 cells, co-transfected with mimic miR-296-5p and miR-512-5p and mutant constructs, showed a significant increase in the luciferase activity when compared to cells co-transfected with the respective wild-type 3' UTR construct (Figure 4.1.2 G, J). All these effects were recapitulated in Hela cells (data not shown).

Together, these data demonstrate target specificity of miR-296-5p and miR-512-5p for the 3'UTR of human TERT.

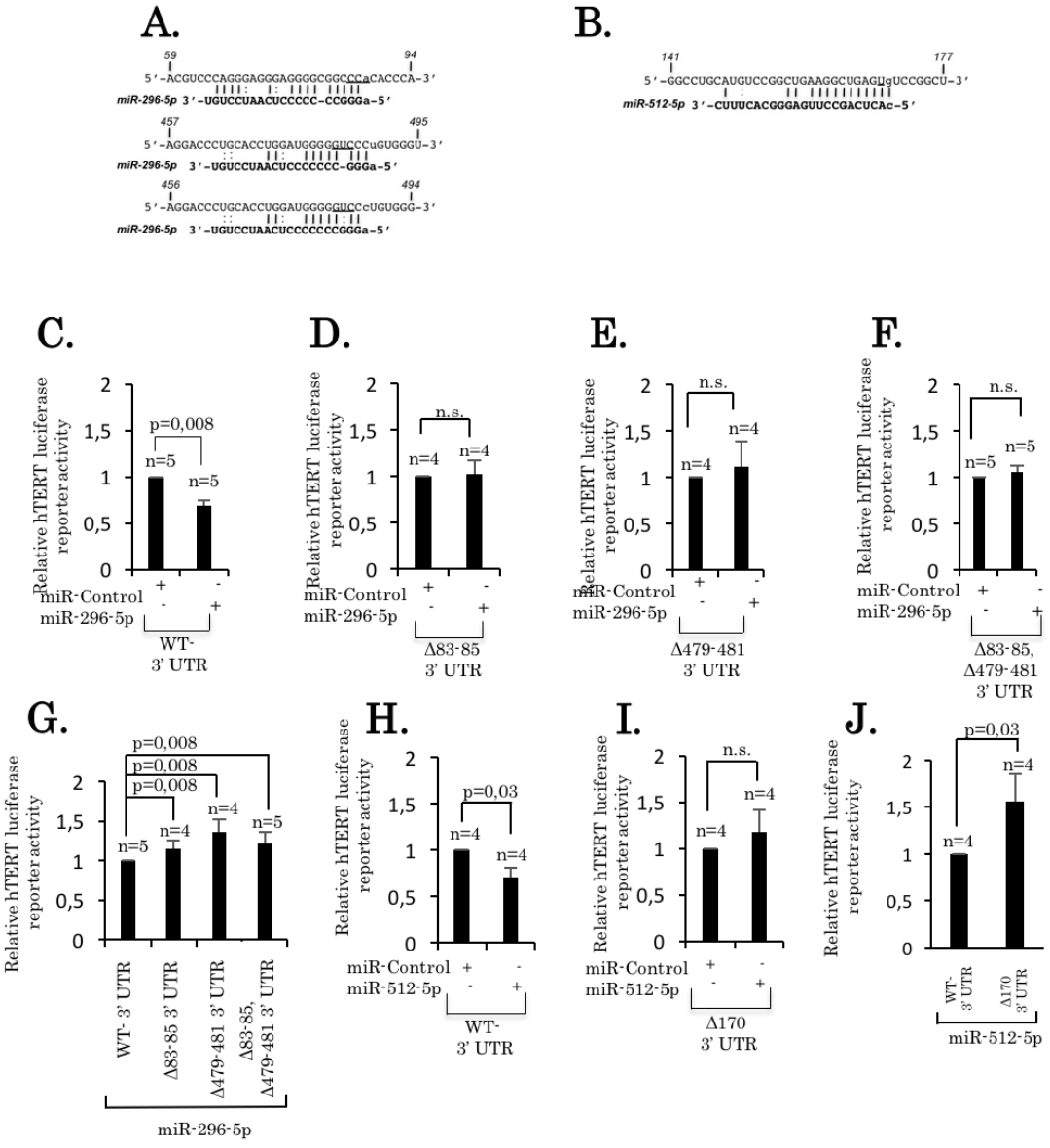


**Figure 4.1.2. A,B.** Schematic representation of miR-296-5p and miR-512-5p target sites in the 3'UTR of hTERT; the underlined nucleotides indicate the position of deletions in mutant hTERT 3'UTR constructs generated. **C-F.** Luciferase reporter assays in MDA-MB-231 breast cancer cells co-transfected with mimic-miR-296-5p and wild type hTERT 3'UTR constructs (C) or constructs that contain mutations of the respective miR-296-5p target sites (D-F). Mutations of miR-296-5p target sites result in increased luciferase reporter activity, when compared to the hTERT wild-type 3'UTR reporter constructs. **G**. Luciferase reporter assays using MDA-MB-231 cells co-transfected with mimic-miR-296-5p siRNAs and the indicated hTERT 3'UTR luciferase reporters. Mutations in the hTERT 3'UTR increase luciferase reporter activity when compared with the wild type construct. **H,I**. Luciferase reporter assays in MDA-MB-231 cells co-transfected with mimic-miR-512-5p and wild type hTERT 3'UTR constructs (H) or a construct that contains a mutations of the predicted miR-512-5p target sites (I). **J.** Luciferase reporter assays using MDA-MB-231 cells co-transfected with mimic-miR-512-5p siRNAs and the indicated hTERT 3'UTR luciferase reporters. Mutations in the hTERT 3'UTR increase luciferase reporter activity. n, number of independent experiments; error bars show standard deviation, C-M: p values were calculated using a Mann Whitney test; n.s., non significant - p-value >0,05.

### 4.1.3 miR-296-5p and miR-512-5p negatively regulate telomerase activity

We next wished to better evaluate the role of miR-296-5p and miR-512-5p in regulating telomerase expression and telomerase activity.

Ectopic transfection of mimic miR-296-5p and miR-512-5p in two different telomerase positive breast cancer cell lines, MCF7 and MDA-MB-231, resulted in a significant reduction of endogenous hTERT mRNA expression levels (Figure 4.1.3 A, C). As control, MCF7 cells were transiently transfected with a specific siRNA that targets hTERT. In contrast, the introduction of antago-miRNAs that directly target endogenous miR-296-5p or miR-512-5p resulted in a significant increase of hTERT mRNA expression levels, both in MCF7 and MDA-MB-231 cells (Figure 4.1.3 B, D). Together, this indicates that hTERT levels are miR-296-5p and miR-512-5p dosage sensitive in breast cancer cells.

To test whether the reduction of hTERT mRNA levels, caused by ectopic miR-296-5p and miR-512-5p, leads to the inhibition of telomerase activity, telomerase repeat amplification protocol (TRAP) was performed. TRAP is a method to determine telomerase activity *in vitro* and includes three steps: extension of a telomere repeat containing oligonucleotide, PCR amplification, and detection of telomerase products by electrophoresis.

MCF7 cells were transiently transfected with miR-296-5p or miR-512-5p mimics and protein extracts were subjected to TRAP in order to measure telomerase activity in vitro. As expected, ectopic introduction of miR-296-5p and miR-512-5p resulted in a significant reduction of telomerase activity in MCF7 cells (Figure 4.1.3 E-H). Next MDA-MB-231 cells have been transduced with a retroviral vector containing a miR-296 or miR-512 mini-gene cassette in order to understand the long-term effect of the mimic-miRNAs overexpression and telomerase activity have been measured.

MDA-MB-231 cells overexpressing miR-296-5p or miR-512-5p showed a decrease of telomerase activity and a concomitant significant telomere shortening after approximately 18 population doublings (Figure 4.1.3 I-J).

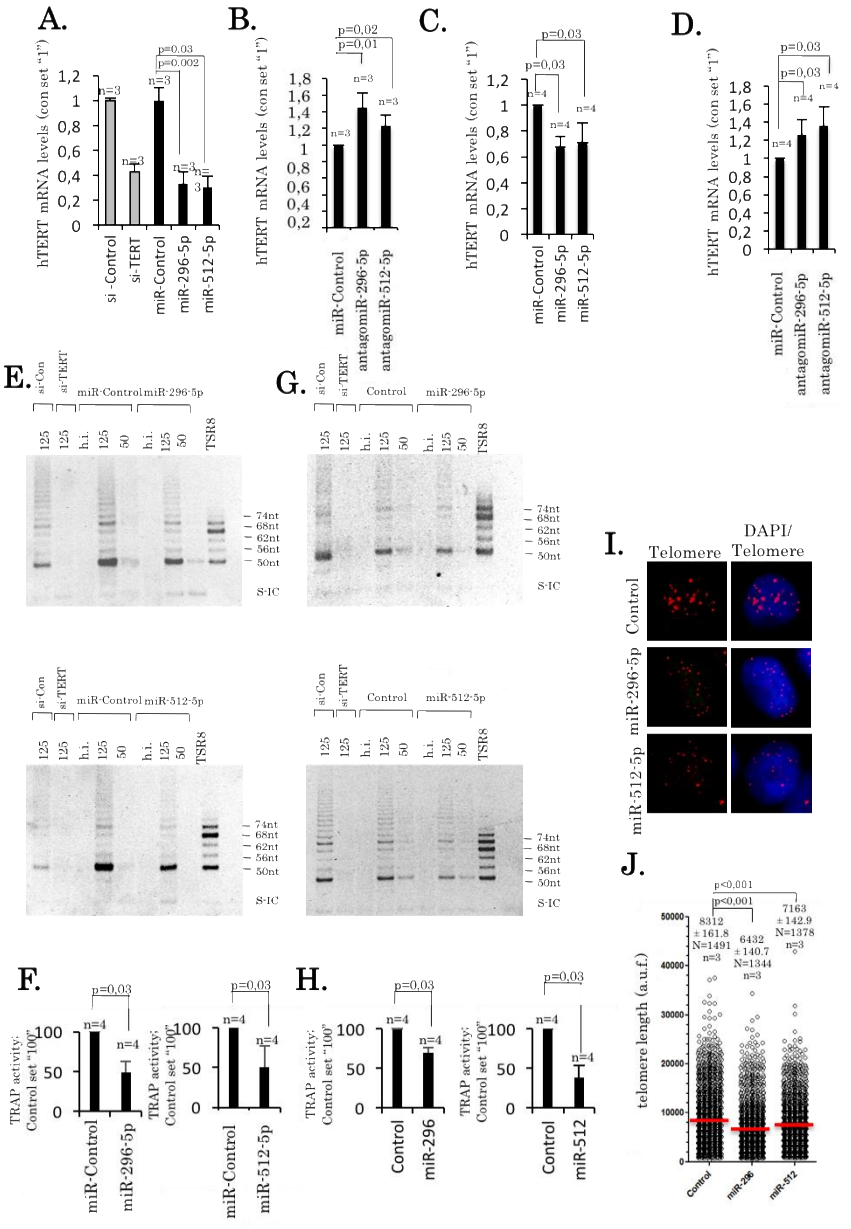


**Figure 4.1.3. A.** MCF7 cells were transiently transfected with hTERT specific siRNAs or miR-296-5p or miR-512-5p mimic-miRNA causing a reduction of hTERT mRNA expression as determined by quantitative RT-PCR. Actin was used as reference. **B**. Transient transfection of MCF-7 cells with antago-miR-296-5p or antago-miR-512-5p causes an increase of hTERT mRNA expression as determined by quantitative RT-PCR. Actin was used as reference. **C.** MDA-MB-231cells were transiently transfected with miR-296-5p or miR-512-5p mimic-miRNA causing a reduction of hTERT mRNA expression as determined by quantitative RT-PCR. Actin was used as reference. **D**. Transient transfection of MDA-MB-231 cells with antago-miR-296-5p or antago-miR-512-5p causes an increase of hTERT mRNA expression as determined by quantitative RT-PCR. Actin was used as reference. **E.** Telomerase activity in lysates of MCF-7 transiently transfected with the indicated siRNAs or mimic-miRNA-siRNAs, determined by the TRAP assay. 125 and 50 (ng) indicate the quantity of lysates used for the assay. **F.** Quantification of TRAP assay in MCF-7 cells: ectopic miR-295-5p and miR-512-5p significantly reduce telomerase activity. **G**. Telomerase activity in lysates of MDA-MB-231 transduced with a retroviral vector containing a miR-296 or miR-512 mini-gene cassette, determined by the TRAP assay. 125 and 50 (ng) indicate the quantity of lysates used for the assay **H**. Quantification of TRAP assay in MDA-MB-231 cells: ectopic miR-295-5p and miR-512-5p significantly reduce telomerase activity. **I, J**. Quantitative telomere DNA FISH of MDA-MD-231 cells overexpressing miR-296 or miR-512 minigenes, respectively. N, number of telomeres analyzed in DNA-FISH experiments. n, number of independent experiments; error bars show standard deviation, a.u.f., arbitrary fluorescence units; red line shows average telomere length; h.i., heat inactivated; S-IC, standard internal control;TSR8 control

template for PCR. A-G, p values were calculated using a Mann Whitney test; n.s., non significant - p-value >0,05. I-J, an unpaired students t-test was used to calculate statistical significance.

### 4.1.4 hTERT and miR-296-5p/miR-512-5p target genes and their expression relevance in breast cancer

In order to find evidence for a clinical relevance of miRNA dependent regulation of hTERT, we next set out to test whether hTERT expression or miR-296-5p or miR-512-5p target gene expression signatures impact on clinical parameters in human breast cancer.

#### 4.1.4.1 Impact of hTERT expression on clinical parameters in human breast cancer

Kaplan-Meier survival curves analysing two independent datasets, which include 4142 or 1881 breast cancer samples, revealed that increased hTERT expression is strictly linked with reduced distant metastasis free survival (DMFS) and relapse free survival (RFS) considering all breast cancer subtypes (Figure 4.1.4 A) (Györffy B. et al. 2009).
Importantly, hTERT expression does not impact on DMFS and RFS in breast cancer subtypes such as luminal A, luminal B, estrogen receptor positive, estrogen receptor negative, Erb2 positive or normal-like breast cancer (data not shown). Importantly, high expression is linked with poor survival in basal type breast cancer (Figure 4.1.4 B). In line with this, elevated hTERT expression is detectable in basal breast cancer (Figure 4.1.4 C).
Together these evidences suggest that mechanisms that regulate hTERT expression may have a special relevance in basal type breast cancer.

#### 4.1.4.2 Impact of miR-296-5p and miR-512-5p target genes signatures in human breast cancer

In order to better understand the clinical relevance of miR-296-5p and miR-512-5p in basal type breast cancer, we tested whether altered the expression of a set of miRNAs target genes can impact on clinical outcome in basal type breast cancer. Here, we focus on the reported miR-296-5p target genes HMGA1, MMP1, MAP2K3 and SCRIB that have been demonstrated to be implicated in human breast cancer (Vaira V. et al. 2012; Wei J.J. et al. 2011 as well as on IKBK and PUMA, that we previously validated by TaqMan RT-PCR in miR-296-5p transfected MDA-MB-231 cells (data not shown). In basal breast cancer, hTERT, HMGA1, MMP1, MAP2K3, SCRIB, PUMA and IKBKE

levels were found to be higher than in other breast cancer subtypes. Importantly, increased miR-296-5p target genes expression is tightly connected to a significant reduced DMFS and RFS in pooled breast cancer subtypes and basal type breast cancer (Figure 4.1.4 D-F).

Regarding miR-512-5p, we selected a panel of cancer relevant target genes, comprising the predicted targets CD44, COPZ1, LZTR1, MCL1 and MN1.
Our experiments revealed that out of this panel of miR-512-5p target genes only COPZ1, MN1 and LZTR1 were significantly down-regulated in MDA-MB-231 transiently transfected with mimic-miR-512-5p siRNAs (data not shown). The expression of these genes does not show strong variation between different breast cancer types and slightly improves distant metastasis free survival and relapse free survival in pooled breast cancer subtypes (Figure 4.1.4 G-I). Of note, in basal breast cancer DMFS and RFS were significantly reduced in the presence of increased miR-512-5p target gene expression (Figure 4.1.4 I).
In order to understand the basal expression of miR-296-5p and miR-512-5p in different breast cancer subtype, we evaluated endogenous miR-296-5p and miR-512-5p expression levels in a panel of breast cancer cell lines. We found that miR-296-5p levels are extremely low in basal type breast cancer cells including MDA-MB-231, MDA-MB-486 and MDA-MB-157 cell lines when compared to luminal type breast cell lines MCF-7, SK-BR3 or T-47D (Figure 4.1.4 J). miR-512-5p expression levels are low in luminal and basal type breast cancer cells (Figure 4.1.4 K). These data underline that down-regulation of miR-296-5p represents a general feature of basal-type breast cancer cells, while low miR-512-5p expression is a general feature of breast cancer cells. Altogether our data suggest that low miR-512-5p and miR-296-5p expression helps to establish an elevated miRNA target gene expression signature that promotes the aggressiveness of basal type breast cancer.

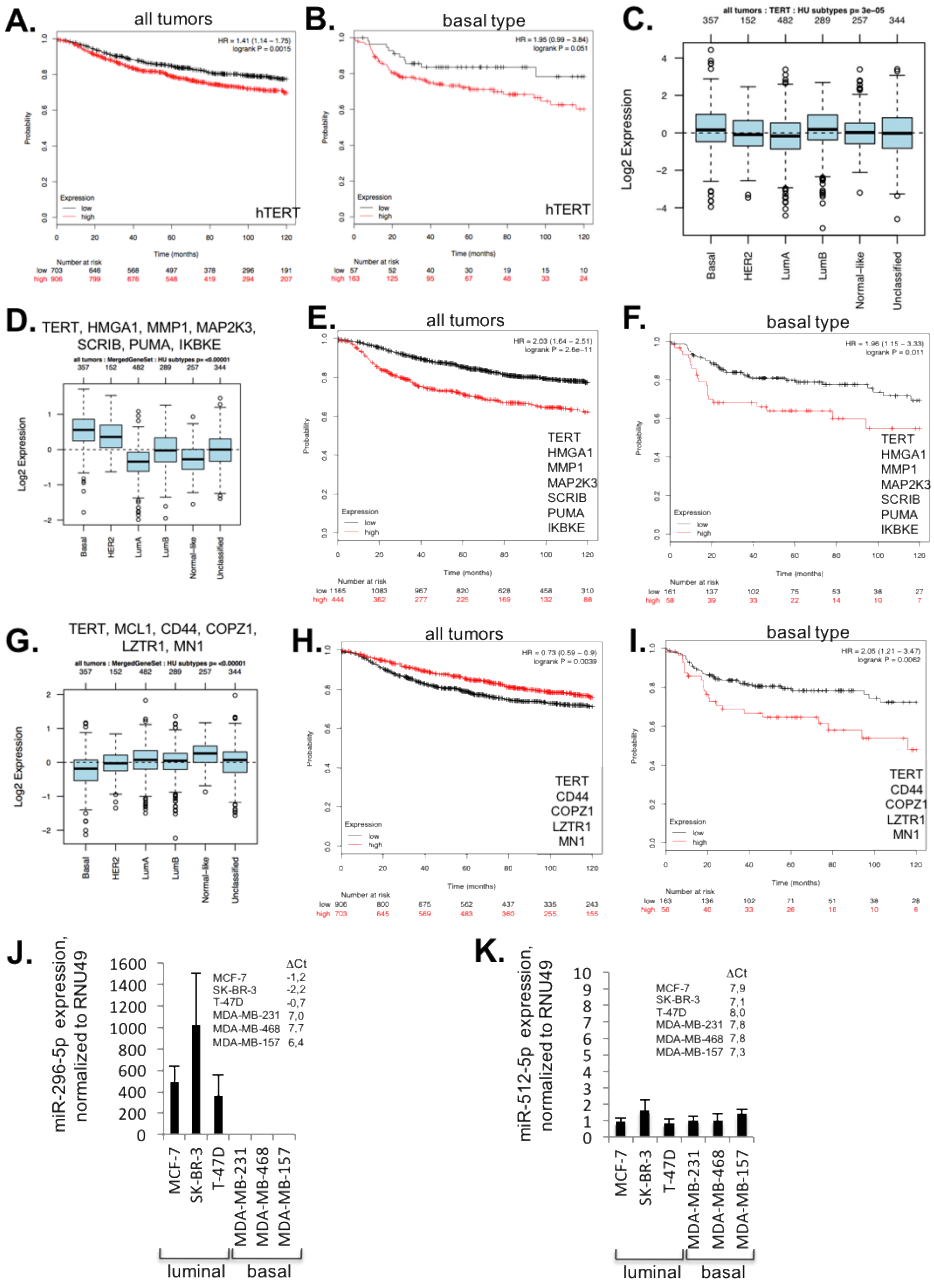


**Figure 4.1.4. A, B**. Kaplan–Meier survival curve considering distant metastasis free survival and relapse free survival (DMFS_mixed) across all types of breast cancer types (A) or basal type breast cancer (B). **C.** Box-plots showing hTERT expression in various breast cancer types; p indicates ANOVA test significance. **D.** Box-plots showing the expression of miR-296-5p target genes, previously validated in MDA-MB-231 cells. **E, F.** Kaplan–Meier survival curve including both distant metastasis free survival and relapse free survival in all subtypes of breast cancer (E) or basal type breast cancer (F). Cancer specimens with high expression of miR-296-5p target genes show poor prognosis. **G.** Box-plots showing the expression of miR-512-5p target genes validated in MDA-MB-231 cells. **H, I.** Kaplan–Meier survival curve considering both distant metastasis free survival and relapse free survival across all types of breast cancer (H) or basal type breast cancer (I). Basal type breast cancer patients with high expression of experimentally validated miR-512-5p target genes show poor survival. **J, K.** miR-296-5p and miR-512-5p expression in basal type and luminal type breast cancer cell lines, determined by quantitative TaqMan RT-PCR. RNU49 was used as reference. ΔCt values (Ct miR-296-5p – Ct RNU49) are indicated. J, K.: 3 independent experiments were carried out, error bars indicate statistical significance; to better visualize differences in miR-296-5p and miR-512-5p, respective expression levels were set "1" in MDA-MB-486 cells.

### 4.1.5 miR-296-5p and miR-512-5p impinge on cell proliferation of breast cancer cells

To assess the effects of both miRNAs on cell proliferation, MDA-MB-231 basal breast cancer cells were transiently transfected twice with mimic-miR-296-5p and mimic-miR-512-5p or the respective antagomiRNA siRNAs during a six day period.

Ectopic introduction of miR-296-5p and miR-512-5p mimics leads to a significant reduction of cell proliferation (Figure 4.1.5 A). In accordance, competing endogenous miR-296-5p and miR-512-5p by ectopic introduction of respective antagomiRNAs causes an increase of cell proliferation (Figure 4.1.5 A).

Cell cycle FACS analysis showed that ectopic expression of mimic miR-296-5p and miR-512-5p in MDA-MB-231 cells has a significant impact on cell cycle progression.

Ectopic introduction of miR-296-5p caused an increase in the number of G1 phase cells and a decreased number of cells in S and G2/M phase, indicating a block in G1/S phase (Figure 4.1.5 B). Conversely, miR-512-5p causes a significant increase of subG1 and G2/M phase cells and a decrease of cells in G1 and S phase, suggesting a role of miR-512-5p in the activation of cellular apoptosis (Figure 4.1.5 B). To better evaluate the molecular outcome of miR-296-5p/miR-512-5p dependent cell cycle alterations, western blotting analysis were performed. It was shown that ectopic expression of miR-296-5p causes a significant increase in p21 protein levels and a modest increase of PARP cleavage, suggesting a predominant role of miR-296-5p in senescence induction and a modest function in the activation of apoptosis program (Figure 4.1.5 C). Furthermore, miR-512-5p expression results in increased PARP and caspase 3 cleavage and in an increase of the DNA damage marker γH2AX, indicating a selective role for miR-512-5p in promoting apoptosis (Figure 4.1.5 C).

The crucial role of miR-512-5p in promoting apoptosis in MDA-MB-231 was confirmed by FACS analysis of Annexin V staining (Figure 4.1.5 D).

In order to validate that impaired proliferation is due to reduced hTERT expression, we transduced MDA-MB-231 with retroviruses encoding the human TERT cDNA. As expected, hTERT ectopic expression significantly rescued cell proliferation defects in miR-296-5p and miR-512-5p transiently transfected cells (Figure 4.1.5 E, F). Transfection of specific antago-miRNAs significantly improved cell proliferation defects (Figure 4.1.5 E, F).

In line with these evidences, by western blotting we assessed that ectopic hTERT determines a reduction of p21 in miR-296-5p transfected cells and an important

decrease of γH2AX protein levels as well as a reduction of PARP and caspase 3 cleavage both in miR-296-5p and miR-512-5p transfected cells (Figure 4.1.5 G).

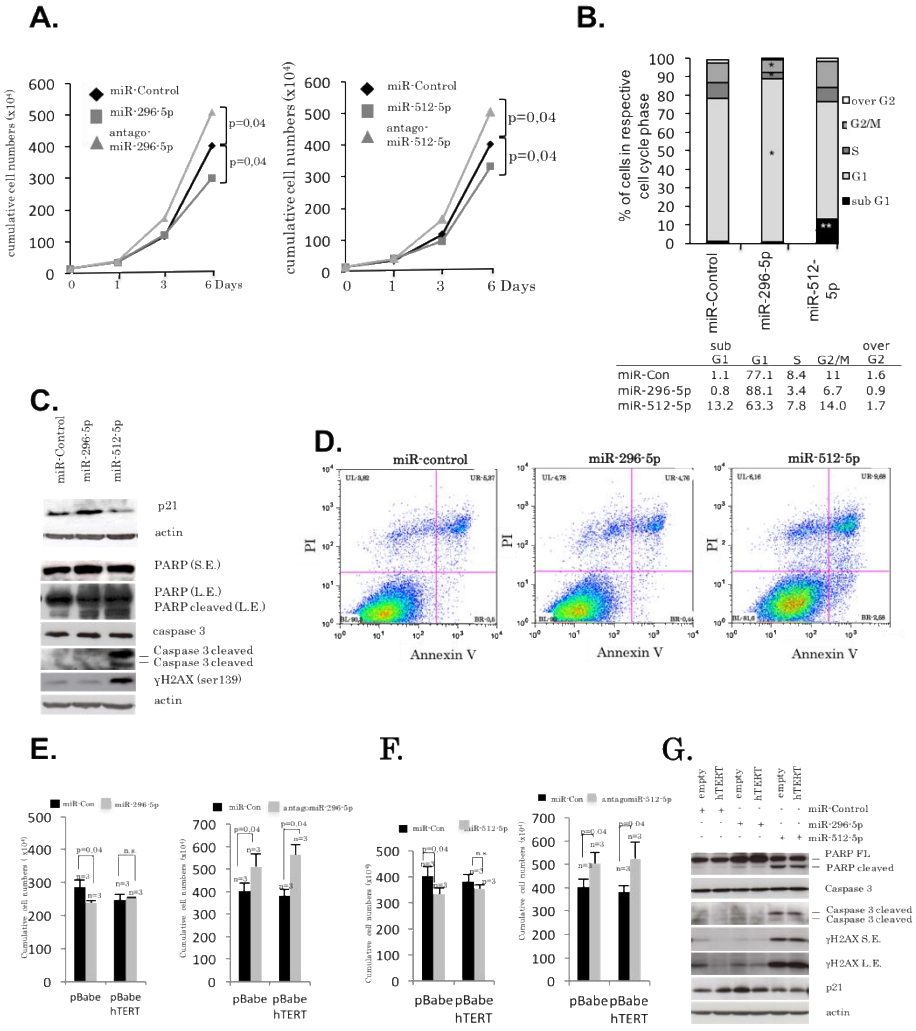


**Figure 4.1.5. A.** Cell numbers of MDA-MB-231 cells transiently transfected for two times with control miRNA, mimic-miR296-5p or mimic-miR-512-5p. miR-296-5p and miR-512-5p reduce cell proliferation. Antago-miRNAs improve MDA-MB-231 cell proliferation. Experiments were carried out at day 6 of transfection **B.** FACS cell cycle profile of MDA-MB-231 cells transiently transfected with the indicated mimic-miRNAs. Cells were treated as described in (A). Experiments were carried out in triplicate, average values are shown. **C.** Western blotting of apoptosis, DNA damage and proliferation markers. Actin was used as a loading control. **D.** FACS analysis of annexin V staining MDA-MB-231 cells transiently transfected with the indicated mimic-miRNA siRNAs. Cells were harvested for detection of externalised annexin V (apoptotic cells) and PI staining of DNA (necrotic cells). Undamaged live cells resulted as unstained (BL quadrant). Early apoptotic cells, positive to Annexin V only, are shown in the BR quadrant. Late apoptotic cells, positive for both Annexin and PI are shown in the UR quadrant. Necrotic cells, positive to PI only is shown in the UL quadrant. Ectopic miR-296-5p does not show a significant increase in apoptosis rate. **E.** Ectopic hTERT expression from a retroviral vector rescues proliferation defects of miR-296-5p transfected MDA-MB-231 cells. Transfection with antagomiR-296-5p siRNAs improves proliferation. Cumulative cell numbers were determined at day 6 of transfection. **F**. Ectopic hTERT expression from a retroviral vector rescues proliferation defects of miR-512-5p transfected MDA-MB-231 cells. Transfection with antago-miR-512-5p siRNAs improves proliferation. Cell numbers were determined at day 6. **G.** Western blotting of MDA-MB-231 cells, treated as described in (D) and (E). Ectopic hTERT rescues proliferation defects, DNA damage and apoptosis marker expression triggered by miR-296-5p or miR-512-5p. Actin was used as a loading control. n, number of independent experiments; error bars show standard deviation, p values were calculated using a Mann Whitney test; n.s., non significant - p-value >0,05. * indicates a p-value <0,05. FL, full length; S.E., short exposure; L.E., long exposure.

### 4.1.6 Epigenetic regulation of miR-296-5p and miR-512-5p

miR-296-5p and miR-512-5p expression levels are low in basal type breast cancer cell lines, thus suggesting that the respective gene loci might be subjected to a strict regulation via epigenetic silencing. To test this hypothesis, we measured miR-296-5p and miR-512-5p expression levels in MDA-MB-231 basal breast cancer cells after treatment with DNA methyltransferase (DNMT) or histone deacetylase (HDAC) inhibitors.

MDA-MB-231 cells treated with 5-aza-2'-deocycytidine (5-AZA), a specific inhibitor of DNA methyltransferases, showed a significant decrease of DNA methylation levels of CpG rich regions of interest and a dosage dependent increase of both of miR-296-5p and miR-512-5p (Figure 4.1.6 A, B).

MDA-MB-231 cells treated with the class I HDAC inhibitor trichostatin (TSA) or class I and II HDAC inhibitor Vorinostat (suberoylanilide hydroxamic acid or SAHA) showed a significant increase of miR-296-5p expression. Remarkably, miR-512-5p remained unchanged, suggesting that inhibition of HDAC is not sufficient to bypass methylation dependent silencing of the miR-512 locus (Figure 4.1.6 C, D). Importantly, the combined treatment of MDA-MB-231 with 5-AZA and SAHA determines a dramatic increase of miR-512-5p expression levels compared to cells treated with 5-AZA alone (90- vs. 25-fold increase, respectively) (Figure 4.1.6 E), whereas the combined treatment with TSA and 5-AZA did (Figure 4.1.6 E).

In contrast, miR-296-5p expression levels were significantly increased when 5-AZA-treated MDA-MB-231 cells were exposed to TSA or SAHA (Figure 4.1.6 F). Of note, under these experimental conditions, significant decrease of hTERT mRNA levels was also observeed (Figure 4.1.6 G).

We next wished to better understand whether release of silencing of miR-296-5p and miR-512-5p expression significantly contribute to reduced hTERT mRNA levels in cells treated with epigenetic inhibitors. For this reason, MDA-MB-231 cells were transiently transfected with antago-miR-296-5p and subjected to TSA treatment. We have found that, in this setup, the ectopic introduction of antago-miR-296-5p reduces hTERT mRNA levels, when compared to control miRNA transfected MDA-MB-231 treated with TSA (Figure 4.1.6 H top panel).

Accordingly, hTERT mRNA levels were measured in MDA-MB-231 cells transiently transfected with antago-miR-512-5p and treated with 5-AZA and SAHA. Again, hTERT

mRNA levels were significantly increased when miR-512-5p expression was antagonized by the introduction of specific antagomiRNAs (Figure 4.1.6 I top panel).
To test whether the observed alterations in hTERT expression are functionally relevant, we examined apoptosis markers and DNA damage markers expression in cells treated with epigenetic inhibitors and antagomiRs. We found that the levels of γH2AX, p21 and PARP in MDA-MB-231 cells treated with epigenetic inhibitors was reduced by transfection of antago-miR-296-5p or antago-miR-512-5p (Figure 4.1.6 H, I bottom panels).

Altogether these evidences suggest that DNA methylation and histone acetylation marks play a crucial role in controlling the silencing of miR-296-5p and miR-512-5p in basal type breast cancer cells to increase hTERT expression to protect cells from senescence and apoptosis.

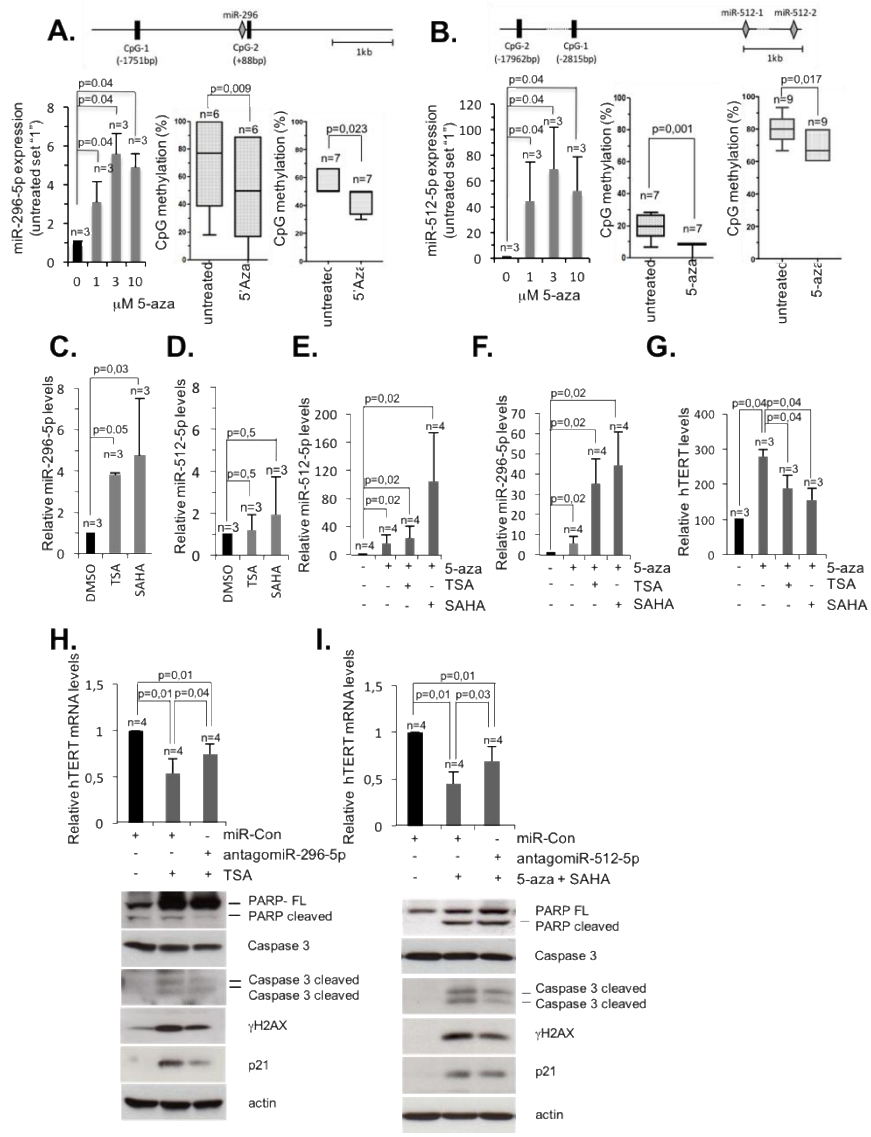


**Figure 4.1.6. A.** miR-296-5p expression upon inhibition of DNA methylation determined by quantitative TaqMan RT-PCR. RNU49 was used as reference. Top panel, Positions of CpG islands analyzed for the miR-296 locus. Numbers indicate distance from miR-296. Bottom left panel, miR-296-5p expression in MDA-MB-231 cells treated with 5-aza-2'-deoxycytidine (5-AZA). Bottom right panel, quantification of CpG island methylation in MDA-MB-231 cells treated with 5-AZA (3M). **B.** miR-512-5p expression upon inhibition of DNA methylation as determined by quantitative TaqMan RT-PCR. Expression levels were normalized against RNU49. Top panel, Position of CpG islands analyzed for the miR-512-1 and miR-512-2 genes. Numbers indicate distance from miR-512-1. Bottom left panel, miR-512-5p expression in MDA-MB-231 cells treated with 5-AZA. Bottom right panel, quantification of CpG island methylation in MDA-MB-231 cells treated with 5-AZA (3□M). **C.** miR-296-5p expression in TSA (1M) or SAHA (5M) treated MDA-MB-231 cells, determined by quantitative TaqMan RT-PCR. Expression levels were normalized against RNU49. **D.** miR-512-5p expression in TSA (1M) or SAHA (5M) treated MDA-MB-231 cells, as determined by quantitative TaqMan RT-PCR. **E.** miR-512-5p expression in MDA-MB-231 cells after treatment with the indicated chemical compounds, as determined by quantitative TaqMan RT-PCR. 5-AZA (1M) was added throughout the 5 days experimental period; TSA (1M) was added at day 4; SAHA (5M) was added at day 3. Expression levels were normalized against RNU49. **F.** miR-296-5p expression in MDA-MB-231 cells after 4 days of treatment with the indicated inhibitors (TSA, 1M; SAHA, 5M; 5-AZA, 1□M), as determined by quantitative TaqMan RT-PCR. **G.** hTERT expression in MDA-MB-231 cells after 4 days of treatment with the indicated inhibitors, as determined by quantitative RT-PCR. hTERT expression was normalized against actin. **H, I.** Top panels, hTERT expression in MDA-MB-231 cells after 4 days of treatment with the indicated inhibitors (TSA 1M; SAHA 5M; 5-AZA 0.15M), as determined by quantitative RT-PCR. hTERT expression was normalized against actin. Bottom panels, western blotting analysis of MDA-MB-231 cells after the indicated treatments. n, number of independent experiments; error bars show standard deviation. P values of bisulfite sequencing were calculated using an unpaired student's t-test; P values of RT-PCR experiments were calculated using a Mann Whitney test; n.s., non significant - p-value >0,05.

### 4.1.7 Model

Our work highlights an important miRNA dependent mechanism in telomere homeostasis and cancer biology. We propose that the imposition of repressive epigenetic marks such as DNA methylation and histone deacetylation cooperate in order to repress the expression of miR-296-5p and miR-512-5p in basal type breast cancer cells. This leads to increased expression of the enzymatic component of telomerase hTERT which, in turn, protects cells from senescence and apoptosis (Indran I.R. et al. 2011; Patel P.L. et al. 2016).

In line with this, we found that increased hTERT expression is linked with enhanced aggressiveness of basal type breast cancer. The fact that this result is also recapitulated by a miR-296-5p and mir-512-5p target gene expression signature underlines the relevance of miR-296-5p and miR-512-5p in basal type breast cancer.

## 4.2 Project 2: Telomere homeostasis regulation by the RNA methyltransferase TGS1

TGS1 is a dimethyltransferase that catalyzes two successive methyl group transfers, each from one S-AdoMet to the exocyclic nitrogen $N_2$ of the guanosine cap of snRNAs, snoRNAs and of hTR, generating a 2,2,7-trimethylguanosine cap (Hausmann S. and Shuman S. 2005; Mouaikel J. et al. 2002).

Evidence for a biological relevance of TGS1 in telomere biology comes from *Saccharomices cerevisiae*. In particular, lack of 2,2,7-trimethylguanosine cap on the telomerase RNA component TLC1 in strains that lack the enzyme tgs1 (Δtgs1) affects telomere length by impairing the coupling between telomerase and DNA polymerase activity and resulting in a premature aging phenotype (Franke J. et al. 2008; Tang W. et al. 2012).

The impact of TGS1 on hTR maturation and telomere homeostasis in vertebrate is poorly understood. We therefore performed loss of function experiments to examine the biological relevance of the 2,2,7-trimethylguanosine cap in telomere homeostasis in human cancer cells.

### 4.2.1 Knockdown and pharmacological inhibition of TGS1 results in reduced TGS1

In order to understand the role of TGS1 on telomerase homeostasis in cells that depend on telomerase for telomere maintenance, H1299 human non-small cell lung carcinoma cells were transiently transfected with TGS1 specific siRNA or treated with sinefungin, a reported inhibitor of TGS1 (Narayan A. et al. 2012). Sinefungin is a naturally occurring S-adenosylhomocysteine, a structural analogue of S-adenosyl-L-methionine (SAM), that inhibits transmethylation reactions related to DNA, RNA, proteins, and other molecules, by competing with SAM for occupancy of the methyl donor site on the enzyme (Zheng S. et al. 2006).

Transient knockdown of TGS1 resulted in a decrease in the expression of TGS1 mRNA and protein, whereas it did not significantly impinge on the expression levels of telomerase components hTERT and hTR and on TRF1 and TRF2 mRNAs (Figure 4.2.1 A-G).

To test the impact of TGS1 enzymatic activity inhibition on the expression of telomere regulators, H1299 cells were treated with sinefungin for 3 and 10 days. We found that the expression of key telomere regulators TRF1 and TRF2 were not altered by sinefungin (Figure 4.2.1 L, M). Remarkably, sinefungin caused a significant decrease of TGS1 protein amounts without altering the mRNA levels (Figure 4.2.1 H, I), suggesting that TGS1 inhibition might lead to TGS1 protein degradation.

We further found that a 3 days treatment of H1299 cells with sinefungin caused a significant increase of hTR expression without affecting hTERT expression (Figure 4.2.1 J-K). The positive impact on hTR expression is lost in prolonged treatment with sinefungin. This suggests that long-term inhibition of TGS1 does not significantly impact on hTR and hTERT expression.

Together, our data suggest that the impairment of TGS1 does not have a significant impact on the expression of key telomere regulators.

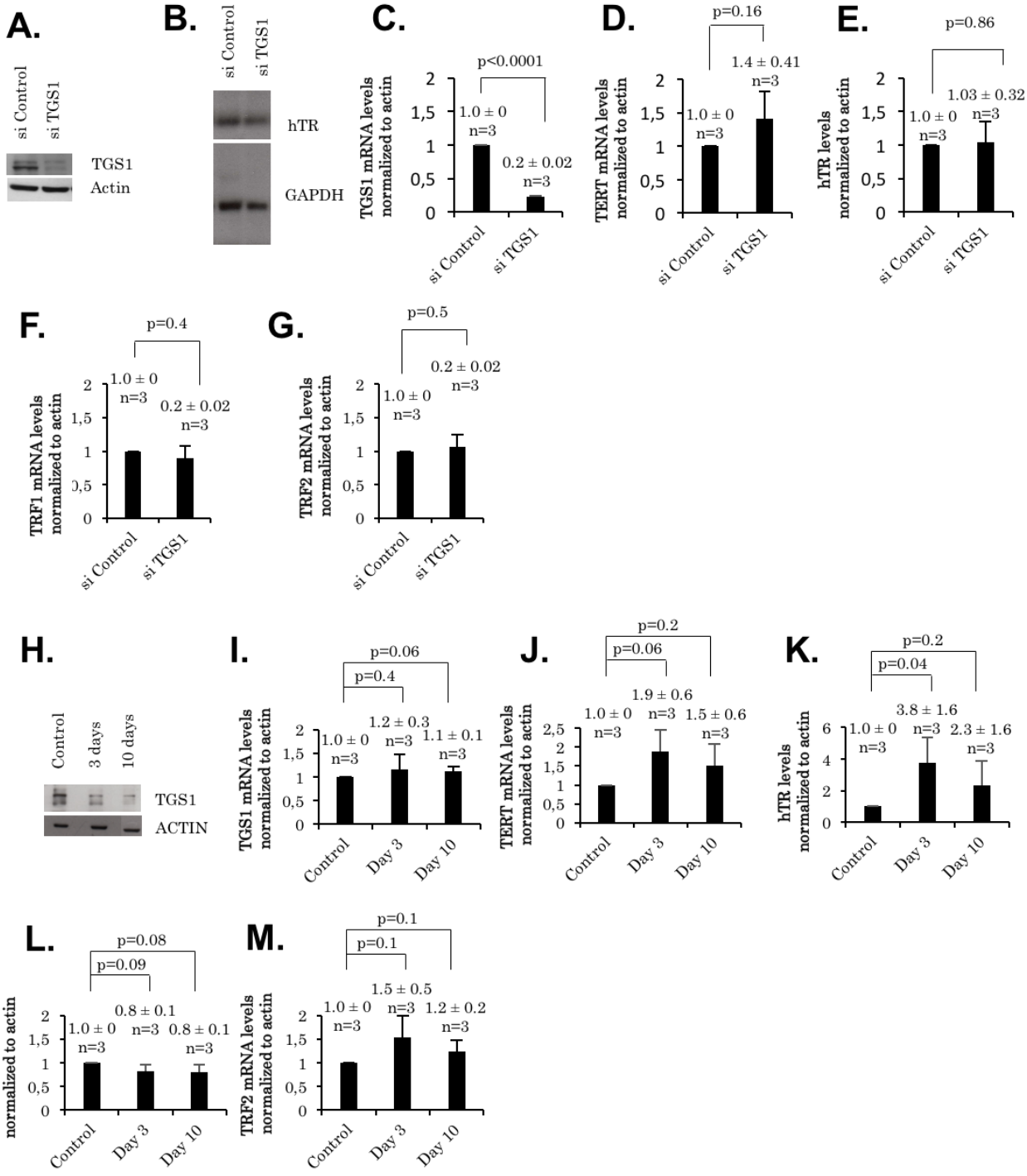


**Figure 4.2.1.** TGS1 expression levels. **A.** Western blotting performed in H1299 silenced for TGS1 for 72 hours to evaluate silencing efficiency. Actin was used as a loading control. **B**. Northern blot experiment performed in H1299 silenced for TGS1 for 72 hours to assess hTR expression changes in TGS1 loss condition. GAPDH was used as a loading control. TGS1 (**C**), hTERT (**D**) and hTR (**E**) RNA levels evaluated by qRT-PCR after 72 hours of TGS1 silencing. Actin was used as reference **F, G.** Shelterin components TRF1 and TRF2 mRNA expression levels evaluated by qRT-PCR after 72 hours of TGS1 silencing. **H**. Western blotting to assess TGS1 protein levels in sinefungin treated H1299 after 3 or 10 days. Actin was used as a loading control. TGS1 protein levels are decreased after sinefungin treatment **I**. TGS1 mRNA expression upon inhibition of RNA methyltransferase by sinefungin determined by quantitative RT-PCR. Actin was used as reference. hTERT (**J**) and hTR (**K**) RNA levels evaluated by qRT-PCR after 3 or 10 days of sinefungin treatment. **L, M**. Shelterin components TRF1 and TRF2 mRNA expression levels evaluated by qRT-PCR after sinefungin treatment for 3 and 10 days. n, number of independent experiments; error bars show standard deviation. P values were calculated using an unpaired student's t-test.

### 4.2.2 TGS1 mediates 2,2,7-trimethylation of hTR cap in vertebrate cells

To test whether the generation of the 2,2,7-trimethylguanosine cap of hTR depends on TGS1, we performed an RNA immunoprecipitation (RIP) analysis using a specific anti-2,2,7-trimethylguanosine antibody. RIP data showed an efficient enrichment of 2,2,7-trimethylguanosine hTR in H1299 cells transfected with the control siRNA, whereas such an enrichment was significantly reduced in cells depleted for TGS1 (Figure 4.2.2 A, B). To further control antibody specificity, we PCR amplified 7-monomethylguanosine capped TRF2 and actin mRNAs. As expected, actin and TRF2 mRNA levels were not particularly enriched in the anti-2,2,7-trimethylguanosine RIP (Figure 4.2.2 C, D).

Similarly, a significant reduction of hTR enrichement was observed in H1299 cells upon the exposure to sinefungin for 10 days (Figure 4.2.2 E, F). Again, anti-2,2,7-trimethylguanosine RIP did not enriche for TRF2 and actin (Figure 4.2.2 G, H).

Altogether, these data show that TGS1 drives the hypermethylation of the 5' cap of telomerase RNA component.

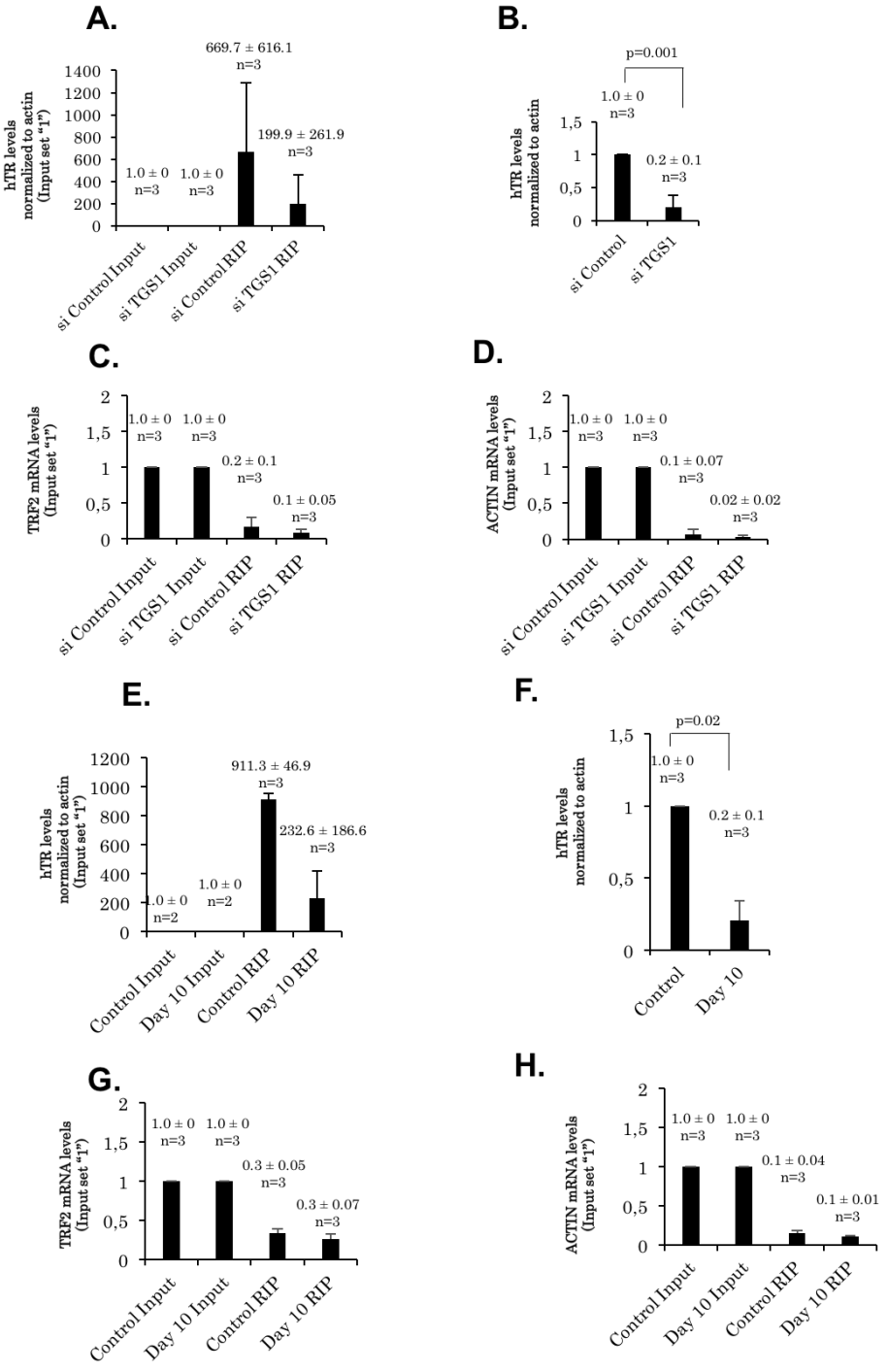


**Figure 4.2.2. A.** RNA immunoprecipitation experiment performed using a 2,2,7-trimethylguanosine specific antibody in TGS1 depletion condition. hTR levels are enriched in immunoprecipitated samples compared with the respective input. Actin was used as reference. **B.** hTR levels in immunoprecipitated samples decrease in TGS1 silencing condition. hTR expression levels were normalized against actin. **C.** TRF2 mRNA levels in immunoprecipitated samples decrease when compared with the respective input. **D.** Actin mRNA levels in immunoprecipitated samples decrease when compared with the respective input. **E.** RNA immunoprecipitation experiment performed in H1299 lung cancer cells treated with sinefungin for 10 days. hTR levels are enriched in immunoprecipitated samples compared with the respective input. Actin was used to normalize all samples. **F.** hTR levels in immunoprecipitated samples decrease in sinefungin treated samples when compared to untreated samples. hTR expression levels were normalized against actin. **G.** TRF2 mRNA levels in immunoprecipitated samples decrease when compared with the respective input. **H.** Actin mRNA levels in immunoprecipitated samples decrease when compared with the respective input. n, number of independent experiments; error bars show standard deviation. P values were calculated using an unpaired student's t-test.

### 4.2.3 TGS1 depletion increases telomerase activity and telomere length

The chemical modification of the 5' cap of hTR represents an important step in the maturation of hTR. We showed that TGS1 does not impact on hTR or hTERT expression.

However, the inhibition of 2,2,7-trimethylcapping of hTR might result in alterations in telomerase activity.

In order to understand whether loss of TGS1 impacts on telomerase activity, TRAP analysis has been performed. We found that telomerase activity was increased upon TGS1 depletion by RNAi, suggesting that telomerase activity *in vitro* is not impinged by the lack of the 2,2,7-trimethylguanosine cap of hTR (Figure 4.2.3 A).

We next wished to better evaluate the effect of TGS1 loss on telomere length homeostasis. H1299 cells were transfected with TGS1 specific siRNA during 9 days and DNA FISH using fluorescence labelled specific telomere probes was performed on interphase cells. We found that knockdown of TGS1 for 9 days resulted in a significant 21% telomere elongation (Figure 4.2.3 B). In line with this, average telomere length was increased in H1299 cells treated with sinefungin for 3 and 10 days. In particular, an increased number of telomere signals per cell as well as intensity representing telomeres have been detected after both 3 and 10 days of treatment. In particular, telomere length gradually increases by 14% after 3 days and 18 % after 10 days of sinefungin treatment (Figure 4.2.3 C).

In order to understand whether TGS1 transient loss of function or sinefungin treatment cause a persistent telomere elongation, reversibility experiments have been performed.

H1299 cells were transfected with TGS1 specific siRNA for 10 days and subsequently allowed to grow for 10 more days without any treatment. Telomere length and TGS1 protein levels were measured at day 10 and day 20 of the experiment. As expected, telomeres appeared elongated after 10 days of TGS1 knockdown and telomere length was maintained in the absence of TGS1 knockdown even though TGS1 protein levels were reconstituted (Figure 4.2.3 D, E). Same results were obtained using sinefungin in reversibility experiment (Figure 4.2.3 F, G)

Altogether these results identify TGS1 as a regulator of telomere length in human cells. The maintenance of telomere elongation phenotype upon the re-gain of TGS1 function suggests that TGS1 may have an important role in controlling the overall telomere length setting in cancer cells.

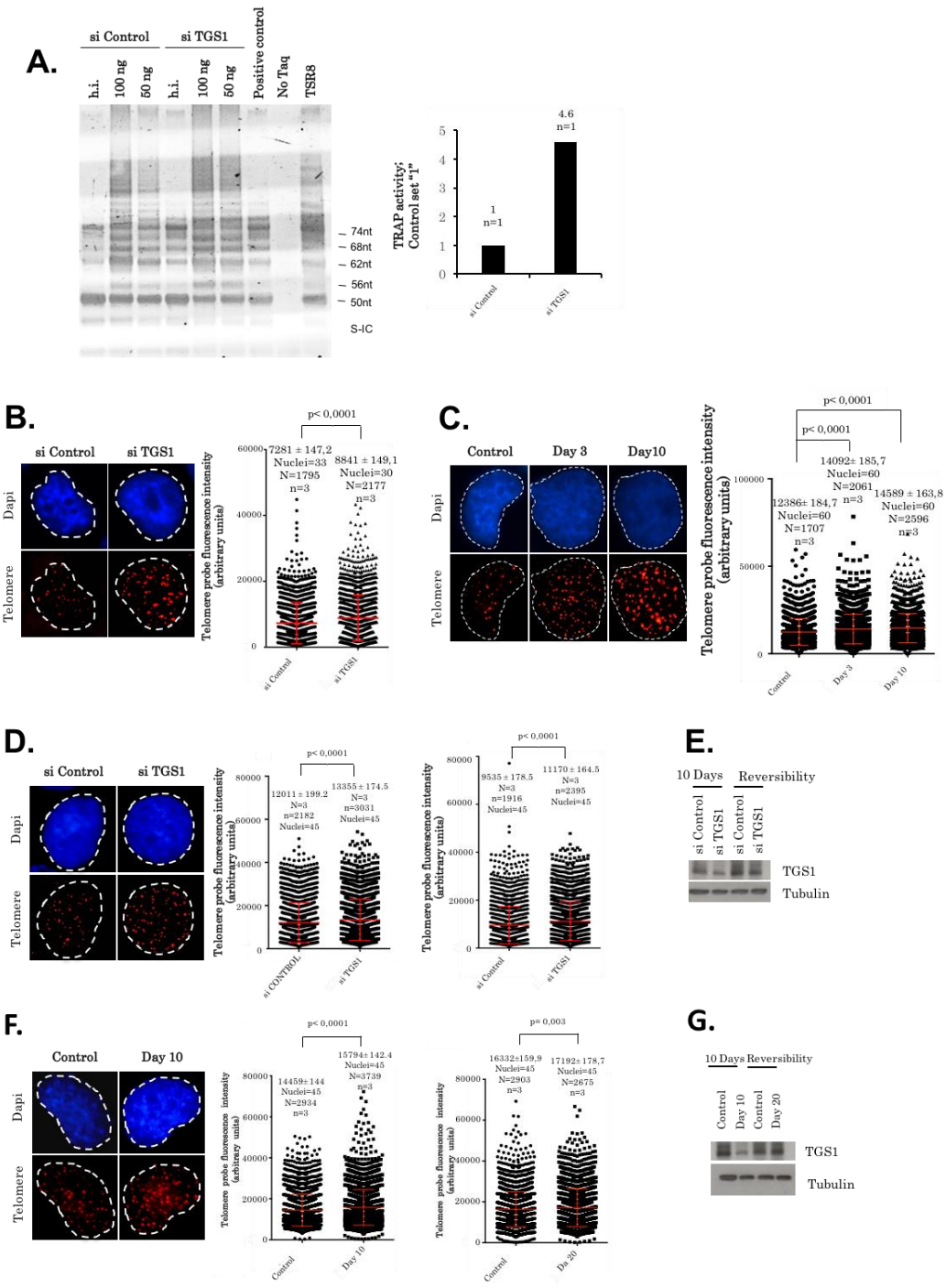


**Figure 4.2.3. A.** Telomerase activity in lysates of H1299 transiently transfected with the indicated siRNAs determined by the TRAP assay. Quantification of TRAP assay in H1299 cells: TGS1 silencing significantly increases telomerase activity. **B.** Quantitative telomere DNA FISH of H1299 cells depleted for TGS1. Telomere length is significantly increased upon TGS1 silencing. **C.** Telomere DNA FISH performed in H1299 lung cancer cells treated with sinefungin for 3 or 10 days. Telomere length is significantly increased. **D, E.** Telomere length assessed in H1299 cells by DNA FISH in TGS1 depleted cells and after 10 days without silencing and in H1299 cells treated with sinefungin and after 10 days without treatment. Telomere length remains significantly increased. N, number of telomeres analyzed in DNA-FISH experiments. n, number of independent experiments; error bars show standard deviation; red line shows average telomere length; h.i., heat inactivated; S-IC, standard internal control; TSR8 control template for PCR. P values were calculated using an unpaired student's t-test.

### 4.2.4 Lack of TGS1 impairs recruitment of telomerase to telomeres in "super-telomerase" H1299 cells

In vivo efficient elongation of telomeres requires the recruitment of the telomerase complex to chromosome ends via specific interactions with a variety of telomere binding proteins. Improved recruitment is linked with improved telomere maintenance and telomere elongation.

Importantly, in human cancer cells and embryonic stem cells, telomerase was detected in Cajal bodies (Hebert M.D. and Poole A.R. 2017; Hyjek M. et al. 2015). In line with this, Cajal bodies play an important role in telomere homeostasis. Remarkably, TCAB1 controls telomerase trafficking to Cajal bodies and colocalizes with telomeres during S-phase when telomerase catalyzes the addition of telomeric repeats to chromosome ends. Further, Cajal bodies are essential for telomerase maturation, assembly and recruitment to telomeres (Stern J.L. et al. 2012).

Given the unavailability of specific hTERT antibodies to our laboratory, we studied telomerase recruitment at telomeres in a "super-telomerase" H1299 cell line. In analogy to past studies (Cristofari G. et al. 2007; Abreu E. et al. 2010), we transduced H1299 cells with a retroviral vector encoding a FLAG epitope tagged hTERT and subsequently selected a single clone with high FLAG-hTERT expression levels (Clone 9). Subsequently, clone 9 cells were stably transfected with vector encoding for the RNA component of telomerase hTR. A single clone with high hTR expression was selected (Clone 22). The overexpression of the two core components of telomerase was validated by Western blotting and Northern blotting experiments (Figure 4.2.4 A-B). Association of telomerase with telomeres in clone 22 was demonstrated by TRF1/FLAG co-immunostaining and telomere ChIP (Figure 4.2.4 C-D).

In addition, the overexpression of the core components of telomerase causes an increase of telomere length (Figure 4.2.4 E) as well as a significant increase of the colocalization between Cajal bodies and telomeres (Figure 4.2.4 F).

In order to evaluate the effect of TGS1 depletion on telomerase localization, clone 22 cells were transiently transfected with a TGS1 specific siRNA and the colocalization of telomerase to telomeres was evaluated. We found that TGS1 depletion causes a significant reduction of the colocalization event between FLAG-hTERT and TRF1, indicating that telomerase recruitment to telomeres is impaired in this setup (Figure 4.2.4 G).

Altogether, these data suggest that TGS1 has a significant role in controlling telomerase recruitment to telomeres, but also for the correct localization of telomeres to Cajal bodies. In future experiments, these data will be validated by telomere ChIP.

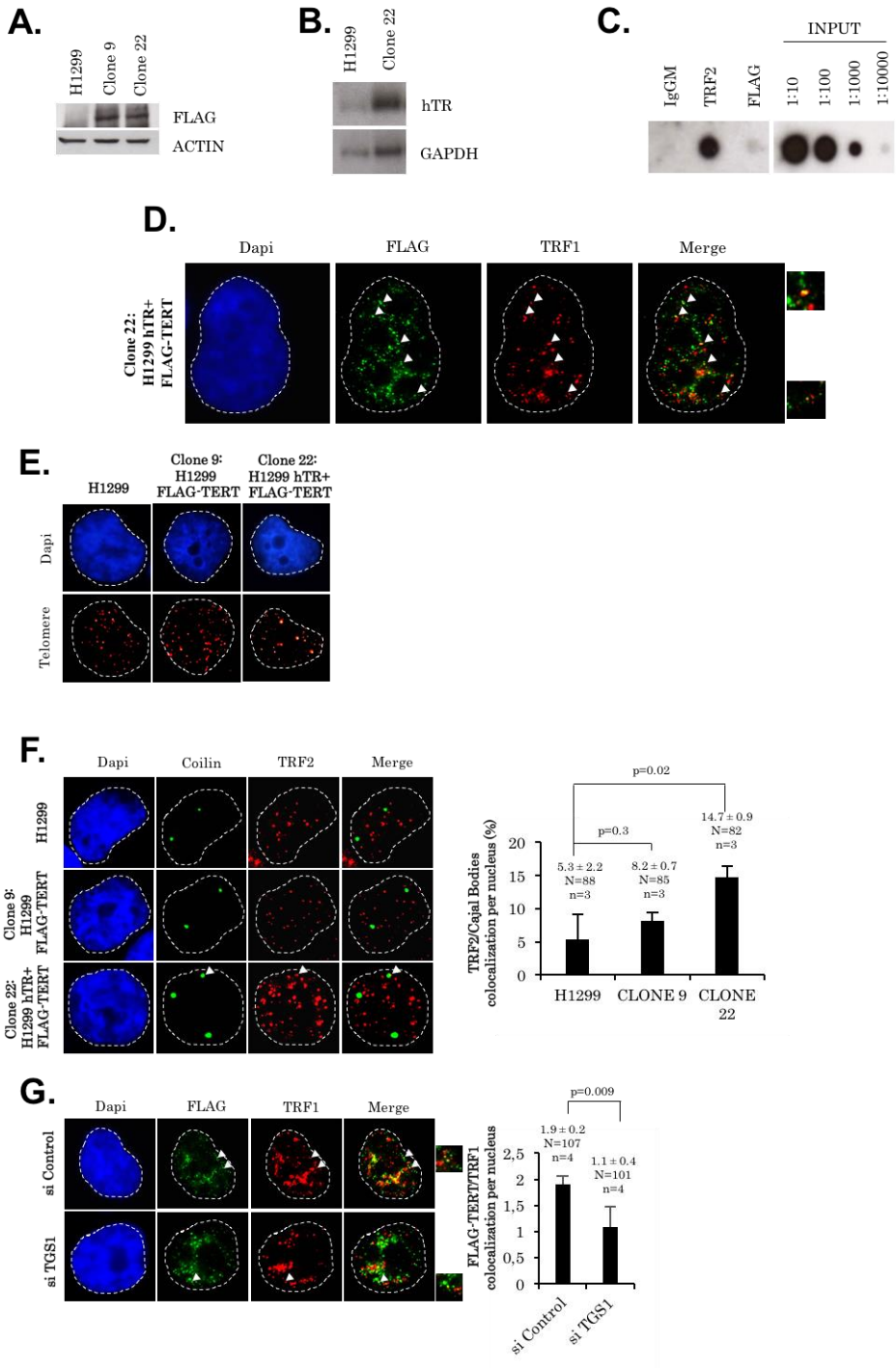


**Figure 4.2.4. A.** Western blot experiment showing overexpression efficiency of FLAG-TERT in H1299 cells. Actin was used as loading control. **B.** Northern blot experiment showing overexpression of hTR in H1299 cells. GAPDH was used as loading control. **C.** Telomeric ChIP performed to evaluate the interaction of FLAG-TERT with telomeric chromatin. Telomeric repeats binding of TRF2 was used as positive control. Control immunoglobulins mouse (IgG M) were used. Serial dilutions of chromatin extract (input) prepared from H1299 cells were loaded. Representative image is shown. **D.** Representative images of FLAG-TRF1 costaining in H1299 lung cancer cells overexpressing FLAG-hTERT and hTR

(clone 22). **E.** Representative images of telomere DNA FISH of interphase cells in H1299 lung cancer cells overexpressing FLAG-hTERT (clone 9) and FLAG-hTERT/hTR (clone 22). **F.** Representative images of COILIN-TRF2 costaining in H1299 lung cancer cells overexpressing FLAG-TERT (clone 9) and FLAG-TERT/hTR (clone 22). Right panel: quantification of TRF2/COILIN percentage colocalization. FLAG-TERT/hTR overexpression increases colocalization percentage between TRF2 and COILIN. **G.** Representative images of FLAG-TRF1 costaining in clone 22 depleted for TGS1. Right panel: quantification of FLAG-TRF1 colocalization number. Loss of TGS1 significantly decreases the number of colocalization between FLAG-TERT and TRF1. n, number of independent experiments; N, number of analysed nuclei; error bars show standard deviation. P values were calculated using an unpaired student's t-test.

### 4.2.5 TGS1 has a role in localizing telomeres to Cajal bodies in telomerase positive H1299 cells

Telomerase is targeted to Cajal bodies due to its crucial interaction with the Cajal body protein TCAB1, which associates with the CAB box domain within hTR (Venteicher et al. 2009; Schmidt J.C. and Cech T.R. 2015). Different studies showed that Cajal bodies play a crucial role in the assembly, function and trafficking of telomerase. In fact, telomerase RNA accumulates in Cajal bodies where the active telomerase is assembled and acts at telomeres in order to elongate them, showing that Cajal bodies and their components are essential for telomerase homeostasis and telomere maintenance (Stern J.L. et al. 2012; Zhong F. et al. 2011).

Our results using "super-telomerase" H1299 suggested a role for TGS1 in modulating the recruitment of telomerase to telomeres and Cajal Bodies.

We next asked whether loss of TGS1 impinges on telomere localization to Cajal bodies in unmodified telomerase positive H1299 cells. Specifically, a significant decrease of colocalization events between TRF2 and Cajal bodies was observed in H1299 cells transiently transfected with TGS1 siRNA. Interestingly, in this experimental setup a significant reduction of Cajal bodies number has been detected (Figure 4.2.5 A).

In line with these data, TGS1 inhibition by sinefungin treatment for 3 and 10 days caused a significant decrease of the percentage of colocalization events between TRF2 and Cajal bodies. Furthermore, after 10 days treatment with sinefungin H1299 cells were characterized by a significant decrease of Cajal bodies number (Figure 4.2.5 B). A role for TGS1 dependent recruitment of telomeres to Cajal bodies was validated in TGS1 knocked down clone 22 cells. In this setup, loss of TGS1 function caused a significant decrease in Cajal bodies number and in the percentage of colocalization events between TRF2 and coilin (Figure 4.2.5 C). Altogether, these data suggest that

TGS1 supports Cajal bodies formation and controls the proper localization of telomeres to Cajal bodies in telomerase positive cells.

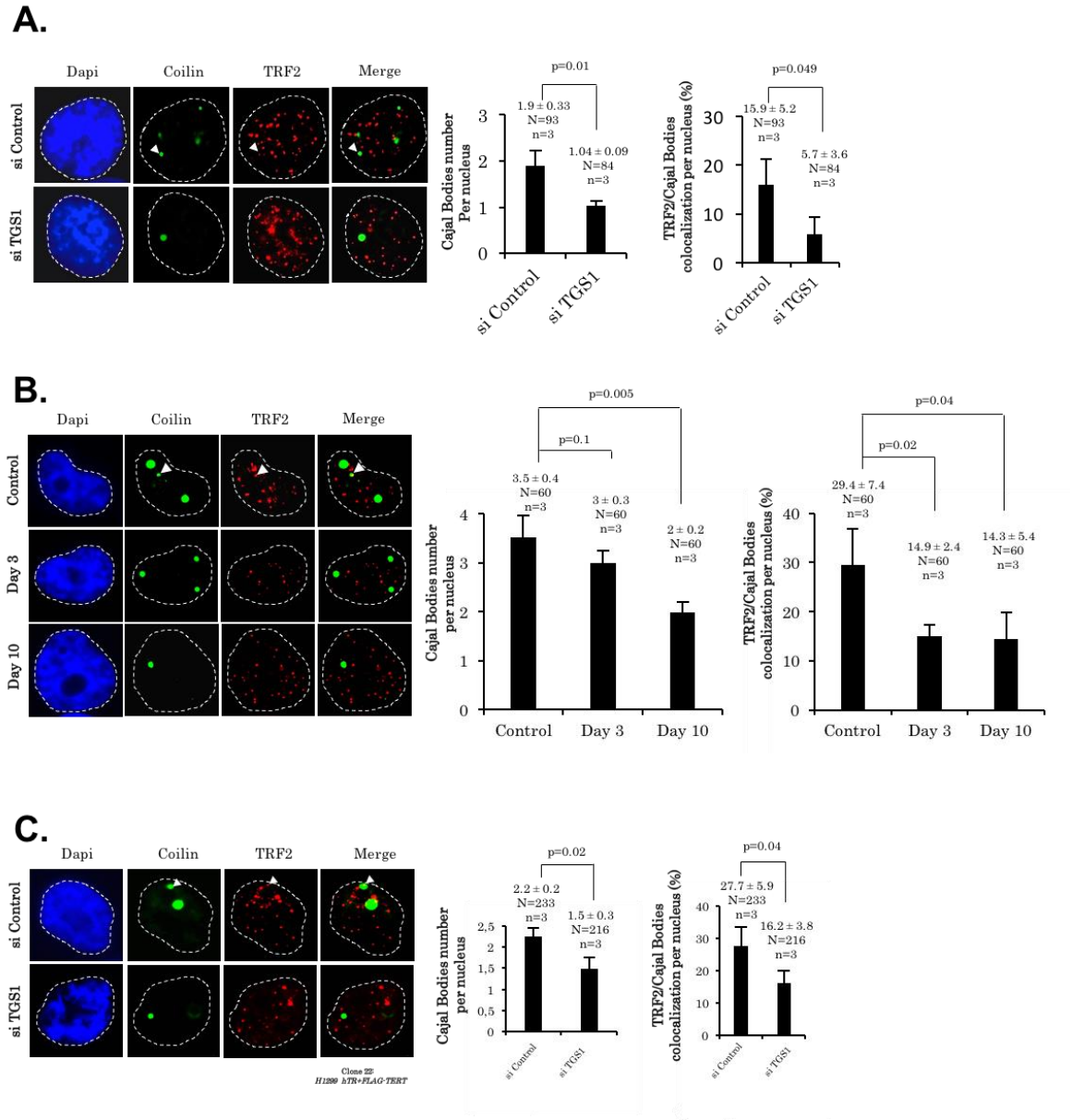


**Figure 4.2.5. A.** Representative images of COILIN/TRF2 costaining in H1299 lung cancer cells depleted for TGS1. Right panel: quantification of total number of Cajal Bodies and quantification of TRF2/COILIN percentage colocalization. TGS1 depletion reduces the total number of Cajal Bodies and the colocalization percentage of TRF2 and COILIN. **B.** Representative images of COILIN/TRF2 costaining in H1299 lung cancer cells treated with sinefungin for 3 and 10 days. Right panel: quantification of total number of Cajal Bodies and quantification of TRF2/COILIN percentage colocalization. Sinefungin treatment reduces the total number of Cajal Bodies after 10 days and the colocalization percentage of TRF2 and COILIN both after 3 and 10 days. **C.** Representative images of COILIN-TRF2 costaining in clone 22 depleted for TGS1. Right panel: quantification of total number of Cajal Bodies and quantification of TRF2/COILIN percentage colocalization. Loss of TGS1 significantly decreases the total number of Cajal bodies and the colocalization percentage of Cajal bodies and telomeres. n, number of independent experiments; N, number of analysed nuclei; error bars show standard deviation. P values were calculated using an unpaired student's t-test.

### 4.2.6 TGS1 loss determines a switch from telomerase-dependent to recombination-dependent telomere maintenance mechanism

The majority of human cancers maintains telomere length via the reactivation of telomerase, thus allowing indefinite cell proliferation. Thus, targeting telomerase represents a highly attractive anti-cancer therapy. However, one of the most relevant concern of anti-telomerase therapy is that telomerase positive cancer cells exposed to telomerase inhibitor may activate alternative pathway of telomere elongation, involving homologous recombination. However, mechanisms that impact on the choice between telomerase and telomerase independent telomere maintenance are poorly understood.

Our data show that loss of TGS1 function increases telomerase activity in an *in vitro* assay but at the same time impairs telomere localization to Cajal bodies and telomerase recruitment to telomeres. Nevertheless, loss of TGS1 function causes telomere elongation. We thus hypothesize that loss of TGS1 might drive telomere elongation via activation of ALT mechanisms.

A key feature of ALT cells is the appearance of ALT associated PML bodies (APBs) which are special promyelocytic leukemia (PML) bodies, enriched in telomeric DNA, shelterin proteins, DDR and HR factors (RAD51, RAD52, BLM, WRN and MRN complex) (Claussin C. and Chang M. 2015; Chung I. et al. 2012).

In order to test whether loss of TGS1 might release homologous recombination, we used H1299 cancer cells transiently depleted for TGS1 and determined the colocalization of TRF2 with PML. Remarkably, we found that loss of TGS1 correlates with an increased percentage of colocalizations of TRF2 with PML (Figure 4.2.6 A), indicating that depletion of TGS1 promotes the formation of APBs.

To validate TGS1 knockdown experiment, H1299 lung cancer cells have been treated with sinefungin for 3 and 10 days and the effect of sinefungin on APBs formation has been assessed. We again noticed a significant increase of PML bodies in cells treated for 10 days compared to untreated cells and of the percentage of colocalization events between TRF2 and PML was detected in cells treated with sinefungin for 10 days (Figure 4.2.6 B).

Together these data suggest that loss of TGS1 dependent maturation of telomerase RNA in telomerase positive cells promotes APBs formation in telomerase positive H1299 cells.

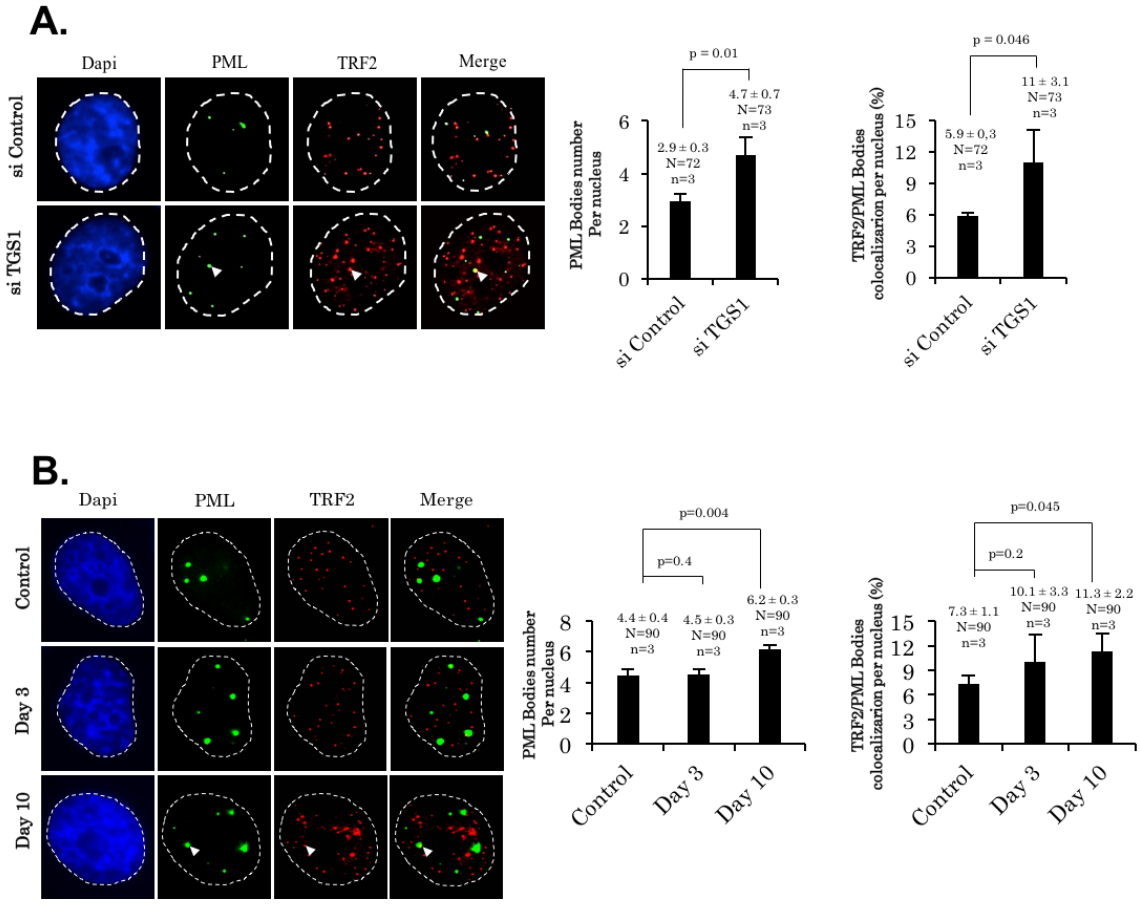


**Figure 4.2.6. A.** Representative images of PML/TRF2 costaining in H1299 lung cancer cells depleted for TGS1. Right panel: quantification of total number of PML Bodies and quantification of TRF2/PML percentage colocalization (APBs). Tgs1 depletion increases the total number of PML Bodies and the colocalization percentage of TRF2 and PML. **B.** Representative images of PML-TRF2 (APBs) costaining in H1299 cells treated with sinefungin for 3 and 10 days. Right panel: quantification of total number of PML Bodies and quantification of TRF2/PML percentage colocalization. Inhibition of TGS1 by sinefungin treatment significantly increases the total number of PML bodies and the colocalization percentage of PML Bodies and telomeres after 10 days of treatment. n, number of independent experiments; N, number of analysed nuclei; error bars show standard deviation. P values were calculated using an unpaired student's t-test.

### 4.2.7 Loss of TGS1 leads to increased recruitment of RAD51 to telomeres and PML bodies

The finding that loss of TGS1 function leads to increased APBs number points towards a recombination dependent telomere elongation in this context.

We thus wished to understand whether loss of TGS1 dependent maturation of telomerase RNA is paralleled by an increased recruitment of RAD51 to telomeres. We thus quantified colocalization events between TRF2 and RAD51 in H1299 cells transiently depleted for TGS1. We found that loss of TGS1 results in increased RAD51 loading at telomeres, indicative for increased abundance of recombinogenic telomeric DNA substrates (Figure 4.2.7 A).

APBs are hypothesized to form structural platforms that mediate telomere recombination, thus are characterized by the enrichment of proteins involved in homologous recombination such as the endonuclease MUS81, replication protein A, RAD51.

In line with this increased APBs numbers, we found a significant increase in the percentage of colocalization events between RAD51 and PML in H1299 lung cancer cells transiently depleted for TGS1 (Figure 4.2.7 B).

We next asked whether telomere elongation in TGS1 loss of function cells depends on RAD51. We performed interphase telomere DNA FISH in H1299 cells depleted for TGS1 or TGS1/RAD51 and quantified fluorescence intensity to obtain a quantitative measure for telomere length. As expected, telomere length is increased in a TGS1 loss of function condition. In contrast, the depletion of RAD51 significantly impairs telomere elongation in TGS1 loss of function cells (Figure 4.2.7 C).

Finally, combined TRF2/PML costaining revealed that abundance of APBs is significantly reduced upon TGS1 and RAD51 co-depletion when compared to cells depleted for TGS1 (Figure 4.2.7 D).

These data suggest that in the context of improper telomerase metabolism due to TGS1 loss of function some features commonly shared by cells that maintain telomeres via ALT are activated.

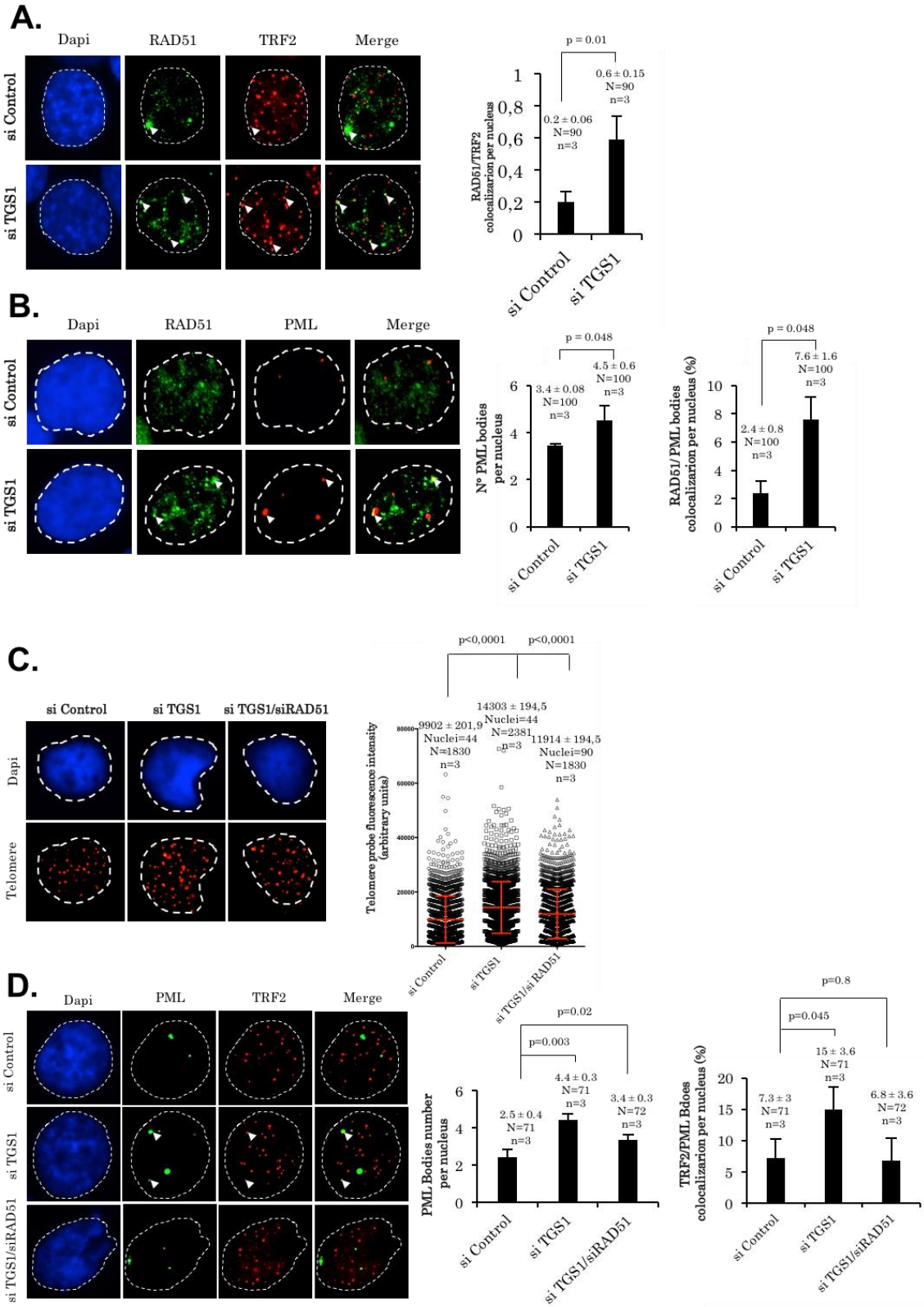


**Figure 4.2.7. A.** Representative images of RAD51/TRF2 costaining in H1299 lung cancer cells depleted for TGS1. TGS1 depletion significantly increases the colocalization percentage of RAD51 foci and telomeres. **B.** Representative images of RAD51/PML costaining in H1299 lung cancer cells depleted for Tgs1. Right panel: quantification of total number of PML Bodies and quantification of RAD51/PML percentage colocalization. Tgs1 depletion significantly increases both the total number of PML Bodies and the colocalization percentage of RAD51 foci and PML. **C.** Representative images of telomere DNA FISH in H1299 lung cancer cells depleted for TGS or for TGS1/ RAD51. Right panel: quantification of telomere

length. TGS1 depletion significantly increases telomere length compared to the control condition, while the combined silencing of TGS1/ RAD51 reduces telomere length when compared with the silencing of TGS1 alone. **D.** Representative images of PML-TRF2 (APBs) costaining in H1299 cancer cells depleted for TGS1 or TGS1/RAD51 in combination. Right panel: quantification of total number of PML Bodies and quantification of TRF2/PML percentage colocalization. TGS1 loss significantly increase the total number of PML bodies, the combined silencing of TGS1/RAD51 partially rescues the effect of TGS1 silencing on PML bodies number. TGS1 silencing increases the colocalization percentage of telomere and PML bodies, while the combined silencing of TGS1/RAD51 completely reverts the effect to the control condition. n, number of independent experiments; N, number of analysed nuclei; error bars show standard deviation. P values were calculated using an unpaired student's t-test.

# 5. DISCUSSION

The reverse transcriptase telomerase adds TTAGGG repeats onto mammalian telomeres, preventing their shortening. The activation of telomerase in malignant cancers is a crucial step in tumorigenesis, allowing cells to gain indefinite proliferative potential and immortality. Telomerase is ordinarily inactive in most somatic cells but can be detected in almost 85-90% of tumor cells (Shay J.W. and Bacchetti S. 1997; Hackett J.A. and Greider C.W. 2002).

In alternative, cancer cells of mesenchymal origin can use recombination based alternative lengthening of telomeres (ALT) to ensure infinite replicative potential.

My work aimed to unveil mechanisms that finely regulate telomerase in human cancer cells. In particular, we wanted i) to identify novel microRNAs that can regulate telomere homeostasis by the modulation of telomerase activity and to demonstrate clinical relevance for these microRNAs (**project 1**) and ii) to better understand the precise role of the trimethylguanosine synthase TGS1 on telomere homeostasis (**project 2**).

## 5.1 Project 1: Silencing of miR-296 and miR-512 ensures hTERT dependent apoptosis protection and telomere maintenance in basal-type breast cancer cells

The reactivation of telomerase allows the escape from replicative senescence and represents a pivotal step during cancer formation. In addition to its role on telomere maintenance by its enzymatic activity, hTERT was demonstrated to promote cancer progression by suppressing apoptosis (Singhapol C. et al. 2013). miR-1207-5p and miR-1266 target the 3'-UTR of hTERT in gastric cancer (Chen L. et al. 2014). miR-299-3p inhibits laryngeal cancer cell proliferation by targeting human telomerase reverse transcriptase mRNA (Li M. et al. 2015).

miRNAs that control hTERT expression in breast cancer have not been discovered yet. Performing a high-throughput luciferase screening, we have identified candidate miRNAs that specifically target the 3'UTR of hTERT. Among these, miR-296-5p and miR-512-5p are efficient regulators of hTERT expression and are significantly down-regulated in human breast cancer specimen, suggesting a crucial clinical relevance for breast cancer.

miR-296-5p is encoded by the lincRNA Nespas that is transcribed from parental allele of the imprinted GNAS cluster located at chromosome 20q13.3 (Robson J.E. et al. 2012). miR-296-5p has been demonstrated to regulate cancer progression, metastasis, and neo-vascularization by targeting the expression of multiple genes including HMGA1, PUMA and SCRIB (Cazanave S.C. et al. 2011; Vaira V. et al. 2012; Lopez-Bertoni H. et al. 2016).

miR-512-5p is encoded by the miR-512-1 and miR-512-2 genes located on human chromosome 19 and was reported to suppress apoptosis by targeting MCL-1 in gastric cancer and hTERT in head and neck squamous cell carcinoma (Saito Y. et al. 2009; Li J. et al. 2015).

Since their significant downregulation in breast cancer cells and their specificity for the 3' UTR of hTERT, we thus hypothesized that downregulation of miR-296-5p and miR-512-5p might represent an important step for the reactivation of telomerase expression in human breast cancer.

Functional validation experiments showed that miR-296-5p and miR-512-5p target three sites in the 3'UTR of hTERT. Performing a series of gain and loss of function experiments, we show that miR-296-5p and miR-512-5p specifically control hTERT

expression in 2 different human breast cancer cell lines derived from luminal and basal breast cancer type.

Furthermore, we found that hTERT mRNA expression and telomerase enzymatic activity is regulated by miR-296-5p and miR-512-5p in both basal and luminal breast cancer cell lines. In line with these data, we observed a significant telomere shortening in basal type MDA-MB-231 cells overexpressing miR-296-5p or miR-512-5p.

Altogether these evidences demonstrate that miR-296-5p and miR-512-5p have a critical impact on the expression of the telomerase protein component and consequently on telomerase activity and telomere homeostasis.

Several studies demonstrated an association of high telomerase expression with poor prognosis in cancer patients (Fernández-Marcelo T. et al. 2015). In line with these studies we found that high hTERT expression is tightly linked with poor survival basal breast cancer patients. Poor survival of basal type breast cancer with high hTERT expression was recapitulated in specimen with enhanced miR-296-5p or miR-512-5p target gene expression signatures. These evidences indicate a particular relevance for miR-296-5p, miR-512-5p and hTERT in basal type breast cancer.

miR-512-5p expression is low across all breast cancer subtypes, while miR-296-5p expression was efficiently down-regulated in specimen and cell lines derived from basal-type breast cancer. Ectopic expression of miR-296-5p and miR-512-5p triggered significant telomere shortening, induction of senescence and the activation of the apoptosis pathway, with the consequent impairment of cell proliferation rate, confirming an anti-proliferative role of miR-296-5p and miR-512-5p in basal type breast cancer.

Breast cancer cells ectopically expressing hTERT that lacks the 3'UTR and consequently the target sites for miR-296-5p and miR-512-5p showed that all the proliferation defects attributed to miR-296-5p and miR-512-5p dependent regulation of endogenous hTERT were rescued even though the anti-apoptotic and pro-survival functions of exogenous hTERT may prevail over those mediated by endogenous hTERT, which retain miRNAs target sites.

Thus, we propose that reduction of miR-296-5p and miR-512-5p expression in basal breast cancer subtype triggers a significant increase of hTERT, thereby enhancing resistance to apoptosis and improving telomere maintenance, promoting cancer cell aggressiveness.

Recent evidences have been shown that miR-512-5p is able to modulate the expression levels of the apoptosis regulator MCL-1, while miR-296-5p can reduce cell proliferation

rates in breast and prostate tumors by regulating the expression of SCRIB and HMGA1 (Vaira V. et al. 2012; Wei J.J. et al. 2011). These data suggest that miR-296-5p and miR-512-5p act as oncosuppressive miRNAs targeting different classical pathways of tumor aggressiveness, including the control of telomerase expression.

Low expression of miR-296-5p and miR-512-5p in breast cancer indicates that miR-296 and miR-512 hosting gene expression is strictly regulated. Interestingly, we have found that antagonizing DNA methylation by treating breast cancer cells with 5'-aza-2'-deoxycytidine (DNMTi) caused significantly increased miR-296-5p and miR-512-5p expression levels, paralleled by CpG demethylation in proximity of the miR-296 and miR-512 genes. When combining the DNMT inhibitor 5'-aza-2'-deoxycytidine and HDAC inibitors (TSA and SAHA) miR-296-5p and miR-512-5p expression levels were further increased.

In the majority of tumors, hTERT expression has been demonstrated to depend on the DNA methylation status at the hTERT promoter (Castelo-Branco P. et al. 2016). Indeed, a significant increase in hTERT expression levels due to the epigenetic modifications of the hTERT promoter after treating MDA-MB-231 cells with DNA methyltransferase (DNMTs) or histone deacetylases (HDACs) inhibitors such as 5'-aza-2' deoxycytidine and trichostatin A has been shown (Iliopoulos D. et al. 2009).

We have shown that loss of DNA methylation increases hTERT mRNA levels. Remarkably treatment of breast cancer cells with 5'-aza-2'-deoxycytidine and inhibition of HDACs using TSA or SAHA resulted in a remarkable reduction of hTERT mRNA levels when compared to cells only treated with 5'-aza-2'-deoxycytidine. In line with these evidences, hTERT expression levels were restored in TSA/SAHA treated cells upon transfection with antagomiR-296-5p or antagomiR-512-5p siRNAs. This suggests that treatment with HDAC inhibitors increases miR-296-5p and miR-512-5p levels, resulting in reduced hTERT expression. Consistent with elevated hTERT expression, cells displayed increased resistance to apoptotic stimuli induced by HDAC inhibitor treatment. This is in line with a role for hTERT in protecting from apoptosis. Together, this demonstrates that miR-296-5p and miR-512-5p play a pivotal role in controlling hTERT expression levels in cancer cells.

In conclusion with our work we identify miR-296-5p and miR-512-5p as miRNAs able to modulate the expression of the enzymatic component of telomerase hTERT. Various evidences demonstrated that decreased levels of miR-296-5p and miR-512-5p determine a concomitant increase of target genes strictly related to cancer transformation and

progression such as HMGA1 and MMP1 or MCL-1 and SCRIB that are involved in apoptosis protection and cell motility thereby promoting cancer progression, invasiveness and aggressiveness (Pegoraro S. et al. 2013; Liu H. et al. 2012; Savi F. et al. 2014; Saito Y. et al. 2009).

We propose a model where epigenetic mechanisms such as DNA methylation and histone deacetylation collaborate to silence miR-296-5p and miR-512-5p expression in basal type breast cancer cells, leading to a significant increase of hTERT levels. Increasing intracellular levels of mature miR-296-5p and miR-512-5p resulted in telomere shortening as well as induction of senescence and apoptosis, finally causing reduced cell proliferation. Thus we propose that hTERT increase improves telomere homeostasis by controlling telomere length in basal type breast cancer and increases resistance to apoptosis.

Altogether, the interplay between epigenetic gene regulation and miR-296 and miR-512 expression in controlling telomerase expression identifies basal type breast cancer as interesting cancer subtypes to exploit therapeutic strategies that aim to target human telomerase.

## 5.2 Project 2: Telomere homeostasis regulation by the RNA methyltransferase TGS1

The reactivation of telomerase-dependent telomere elongation mechanism is is mainly linked to the control of the enzymatic activity of hTERT.

In line with this, the reactivation of the reverse transcriptase also depends on the establishment of a precise maturation pathway of the RNA component hTR and on the assembly of hTR with the enzymatic component hTERT to properly form the core telomerase enzyme (Schmidt J.C. et al. 2015).

One key maturation step of the RNA component of telomerase involves the synthesis of a 2,2,7-trimethylguanosine cap at its 5' end executed by the RNA methyltransferase TGS1.

TGS1 is a specific enzyme that catalyses two serial methylation steps that are fundamental to convert the 7-monomethylguanosine ($m_7G$) caps initially present at snRNAs and snoRNAs to a 2,2,7-trimethylguanosine ($m_{2,2,7}G$) cap (Zhu Y. et al. 2001). The hypermethylation of the monomethylguanosine cap of snRNAs and snoRNAs occurs in specific nuclear foci, identified as Cajal bodies normally enriched in small nuclear and small nucleolar RNAs (Lemm I. et al. 2006; Hausmann S. et al. 2008).

Since hTR shows common features of snRNA and snoRNAs, the 7-monomethylguanosine cap of hTR is modified in Cajal Bodies such as the 7-monomethylguanosine cap of snRNAs and snoRNAs.

Cajal Bodies have a key role in completing biogenesis of telomerase holoenzyme, assisting in the transport of telomerase to telomeres and consequently impinging on telomere lengthen maintenance in telomerase positive cells (Stern J.L. et al. 2012). Due to the key relevance of TGS1 enzymatic activity on the maturation of telomerase RNA, we hypothesized that loss of TGS1 or inhibition of its enzymatic activity might represent an important step in the control of telomere homeostasis in cancer cells.

In line with previous evidences showing that hypermethylation of telomerase RNA occurs via the enzymatic activity of Tgs1 in *Saccharomyces cerevisiae*, we found that loss of TGS1 or inhibition of its methyltransferase activity by the use of sinefungin significantly impairs hypermethylation of the 5' cap of telomerase RNA in human telomerase positive cancer cells.

hTR mutations and alterations in hTR maturation have been linked to aberrant telomerase function (Chen Y.N. et al. 2016)

We thus hypothesized that a missing trimethylguanosine 5' cap of hTR caused by loss or inhibition of TGS1 might alter telomerase activity and telomere homeostasis. We found that decreased levels of TGS1 as well as enzymatic inhibition of TGS1 by sinefungin significantly increase telomerase activity *in vitro* in human cancer cells, confirming a role for the hypermethylation of the 5' cap of hTR for telomerase activity. In line with previous evidences which demonstrate that the absence of Tgs1 in *Saccharomyces cerevisiae* caused a significant telomere elongation, improved telomeric silencing and stabilized telomeric recombination (Franke J. et al. 2008), we observed a significant telomere lengthening in human cancer cells that lack TGS1 enzymatic activity. Furthermore, we found that this telomere elongation phenotype is maintained after reconstitution of cells with TGS1 expression or TGS1 enzymatic activity, suggesting that newly telomere length is maintained by endogenous mechanism of telomere maintenance.

Even though we observed increased *in vitro* global telomerase activity in H1299 cancer cells, we observed that TGS1 depletion or inhibition caused a significant impairment of telomerase recruitment to telomeres in human cancer cells. This evidence suggests that the intrinsic enzymatic activity of telomerase might be increased, however the lack of the trimethylguanosine cap might alter the the recruitment of telomerase to telomere. This impaired recruitment of telomerase at telomeres suggests that telomere elongation might occur in a telomerase independent manner.

Several studies demonstrate that telomerase inhibition can induce an important switch from telomerase-dependent to telomere elongation mechanism by activating ALT mechanisms (Qin X. et al. 2013; Chen W. et al. 2017; Hu J. et al. 2012). In line with these previous evidences, we found that TGS1 loss or inhibition, impairing hTR proper maturation, trigger a significant change in the localization of telomeres: lowering TGS1 expression or activity promotes the relocation of telomeres from Cajal bodies towards PML bodies where alternative lengthening of telomeres mechanisms can occur.

In ALT cells telomeric DNA and associated binding proteins are found in a subset of promyelocytic leukaemia nuclear bodies (PML bodies) defined as ALT-associated PML bodies (Cesare A.J. and Reddel R.R. 2016). Additional proteins involved in recombination (RAD51, RAD52, RPA, NBS1, SLX4, BLM, MRN, BRCA1, BRIT1) are enriched in APBs and are involved in the recombination pathway fundamental for telomere maintenance in ALT cells. Consistent with these reports, we demonstrated that depletion of TGS1 or inhibition of its enzymatic activity by sinefungin determined

an increase of nuclear APBs in telomerase positive cancer cells, a significant increased enrichment of RAD51 in PML bodies and an increased RAD51 loading at telomeres. Together these data indicate that loss of TGS1 activity impacts on important features of ALT cells: APBs formation and recruitment of homologous recombination factors to telomeres. In line with these evidences, we found that the combined depletion of TGS1 and RAD51 rescues the effect of TGS1 loss in terms of telomere elongation and APBs formation, confirming our hypothesis regarding the activation of homologous recombination in cells depleted for TGS1.
Future experiments are necessary i) to clearly show the altered recruitment of telomerase at telomeres in TGS1 loss of function conditions or inhibition of its enzymatic activity due to sinefungin treatment by telomeric ChIP ii) to demonstrate the activation of recombination at telomeric sister chromatid by CO-FISH iii) to prove that telomere elongation phenotype detected in TGS1 loss of function condition or inhibition is telomerase independent iv) to evaluate the impact of telomerase dependent-to-telomerase independent telomere maintenance switch on cancer aggressiveness and v) to validate the aforementioned findings in additional models of human cancers. Previous experiments performed in hTERT depletion conditions did not show an efficient downregulation of hTERT mRNA, thus H1299 cells depleted for TGS1 will be treated with a telomerase inhibitor and telomere length will be evaluated in order to elucidate whether telomere elongation depends on telomerase activity.

In conclusion, our work demonstrates that the synthesis of a 2,2,7-trimethilguanosine 5' cap of telomerase RNA catalysed by the enzyme TGS1 represents an important step in the maturation of hTR in human cancer cells. We demonstrate that TGS1 dependent maturation of telomerase RNA is essential for the proper localization of telomerase holoenzyme. The altered maturation of telomerase RNA component causes the impairment of telomerase recruitment and activity at telomeres, eventually promoting a switch from telomerase dependent telomere lengthening to the activation of the ALT pathway. In conclusion, our work demonstrate that TGS1 activity has a strong impact on telomere length homeostasis.

Our data identify TGS1 as an interesting target to modulate telomerase activity, thereby probably reducing cancer aggressiveness by inducing a forced shift from telomerase dependent to telomerase independent telomere maintenance. Indeed, various evidences have shown that cells that maintain telomere length via ALT On the

other hand, inhibition of TGS1 might represent an interesting strategy to elongate telomeres in telomerase positive stem cells, thus increasing the replicative potential of adult or aged stem cells.

# REFERENCES


Abreu, E. *et al.* TIN2-Tethered TPP1 Recruits Human Telomerase to Telomeres In Vivo. *Molecular and Cellular Biology* **30,** 2971–2982 (2010).

Adi Harel, S. *et al.* Reactivation of epigenetically silenced miR-512 and miR-373 sensitizes lung cancer cells to cisplatin and restricts tumor growth. *Cell Death and Differentiation* **22,** 1328–1340 (2015).

Aguilera, A. & García-Muse, T. R Loops: From Transcription Byproducts to Threats to Genome Stability. *Mol. Cell* **46,** 115–124 (2012).

Akiyama, B. M., Parks, J. W. & Stone, M. D. The telomerase essential N-terminal domain promotes DNA synthesis by stabilizing short RNA-DNA hybrids. *Nucleic Acids Res.* **43,** 5537–5549 (2015).

Amorim, J., Santos, G., Vinagre, J. & Soares, P. The Role of ATRX in the Alternative Lengthening of Telomeres (ALT) Phenotype. *Genes (Basel).* **7,** 66 (2016).

Arora, R. & Azzalin, C. M. Telomere elongation chooses TERRA ALTernatives. *RNA Biol.* **12,** 938–941 (2015).

Artandi, S. E. & DePinho, R. A. Telomeres and telomerase in cancer. *Carcinogenesis* **31,** 9–18 (2010).

Atkinson, S. P., Hoare, S. F., Glasspool, R. M. & Keith, W. N. Lack of telomerase gene expression in alternative lengthening of telomere cells is associated with chromatin remodeling of the hTR and hTERT gene promoters. *Cancer Research* **65,** 7585–7590 (2005).

Autexier, C. & Lue, N. F. The Structure and Function of Telomerase Reverse Transcriptase. *Annu. Rev. Biochem.* **75,** 493–517 (2006).

Balatsos, N. A. A., Nilsson, P., Mazza, C., Cusack, S. & Virtanen, A. Inhibition of mRNA deadenylation by the nuclear cap binding complex (CBC). *J. Biol. Chem.* **281,** 4517–22 (2006).

Balatti, V., Pekarky, Y. & Croce, C. M. Role of microRNA in chronic lymphocytic leukemia onset and progression. *J. Hematol. Oncol.* **8,** 12 (2015).

Bandaria, J. N., Qin, P., Berk, V., Chu, S. & Yildiz, A. Shelterin Protects Chromosome Ends by Compacting Telomeric Chromatin. *Cell* **164,** 735–46 (2016).

Baumann, P. Pot1, the Putative Telomere End-Binding Protein in Fission Yeast and Humans. *Science* **292,** 1171–1175 (2001).

Ben-Dov, I. Z. *et al.* Urine MicroRNA as Potential Biomarkers of Autosomal Dominant Polycystic Kidney Disease Progression: Description of miRNA Profiles at Baseline. *PLoS One* **9,** e86856 (2014).

Betel, D., Wilson, M., Gabow, A., Marks, D. S. & Sander, C. The microRNA.org resource: Targets and expression. *Nucleic Acids Research* **36,** D149–D153 (2008).

Bilaud, T. *et al.* Telomeric localization of TRF2, a novel human telobox protein. *Nature Genetics* **17,** 236–239 (1997).

Bisson, F. *et al.* Contribution of Sp1 to Telomerase Expression and Activity in Skin Keratinocytes Cultured With a Feeder Layer. *J. Cell. Physiol.* **230,** 308–317 (2015).

Bizard, A. H. & Hickson, I. D. The dissolution of double Holliday junctions. *Cold Spring Harb. Perspect. Biol.* **6,** a016477 (2014).

Blackburn, E. H. & Collins, K. Telomerase: An RNP Enzyme Synthesizes DNA. *Cold Spring Harb. Perspect. Biol.* **3,** a003558–a003558 (2011).

Blackburn, E. H. & Gall, J. G. A tandemly repeated sequence at the termini of the extrachromosomal ribosomal RNA genes in Tetrahymena. *Journal of Molecular Biology* **120,** 33–53 (1978).

Bosoy, D. & Lue, N. F. Yeast telomerase is capable of limited repeat addition processivity. *Nucleic Acids Res.* **32,** 93–101 (2004).

Bryce, L. a, Morrison, N., Hoare, S. F., Muir, S. & Keith, W. N. Mapping of the gene for the human telomerase reverse transcriptase, hTERT, to chromosome 5p15.33 by fluorescence in situ hybridization. *Neoplasia (New York, N.Y.)* **2,** 197–201 (2000).

Cairney, C. J. & Keith, W. N. Telomerase redefined: Integrated regulation of hTR and hTERT for telomere maintenance and telomerase activity. *Biochimie* **90,** 13–23 (2008).

Calado, R. T. & Young, N. S. Telomere maintenance and human bone marrow failure. *Blood* **111,** 4446–4455 (2008).

Castelo-Branco, P. *et al.* A cancer specific hypermethylation signature of the TERT promoter predicts biochemical relapse in prostate cancer: A retrospective cohort study. *Oncotarget* **7,** 57726–57736 (2016).

Cazanave, S. C. *et al.* A role for miR-296 in the regulation of lipoapoptosis by targeting PUMA. *The Journal of Lipid Research* **52,** 1517–1525 (2011).

Celli, G. B. & de Lange, T. DNA processing is not required for ATM-mediated telomere damage response after TRF2 deletion. *Nature Cell Biology* **7,** 712–718 (2005).

Celli, G. B., Denchi, E. L. & de Lange, T. Ku70 stimulates fusion of dysfunctional telomeres yet protects chromosome ends from homologous recombination. *Nature Cell Biology* **8,** 855–890 (2006).

Cesare, A. J. & Reddel, R. R. Alternative lengthening of telomeres: models, mechanisms and implications. *Nat. Rev. Genet.* **11,** 319–330 (2010).

Chang, H. R. *et al.* The functional roles of PML nuclear bodies in genome maintenance. *Mutat. Res. Mol. Mech. Mutagen.* (2017). doi:10.1016/j.mrfmmm.2017.05.002

Chang, T.-C. *et al.* Lin-28B transactivation is necessary for Myc-mediated let-7 repression and proliferation. *Proc. Natl. Acad. Sci.* **106,** 3384–3389 (2009).

Chen, J. L., Blasco, M. A. & Greider, C. W. Secondary structure of vertebrate telomerase RNA. *Cell* **100,** 503–514 (2000).

Chen, L. *et al.* miR-1207-5p and miR-1266 suppress gastric cancer growth and invasion by targeting telomerase reverse transcriptase. *Cell Death and Disease* **5,** e1034 (2014).

Chen, L. *et al.* miR-1207-5p and miR-1266 suppress gastric cancer growth and invasion by targeting telomerase reverse transcriptase. *Cell Death Dis.* **5,** e1034 (2014).

Chen, W., Xiao, B.-K., Liu, J.-P., Chen, S.-M. & Tao, Z.-Z. Alternative lengthening of telomeres in hTERT- inhibited laryngeal cancer cells. doi:10.1111/j.1349-7006.2010.01611.x

Chen, Y.-N. & Zhang, Y.-M. Human telomerase disease mutants and its relation with hepatocarcinoma. *Hepatoma Res.* **2,** 109 (2016).

Cho, N. W., Dilley, R. L., Lampson, M. A. & Greenberg, R. A. Interchromosomal homology searches drive directional ALT telomere movement and synapsis. *Cell* **159,** 108–121 (2014).

Choi, J.-H. *et al.* TSA-induced DNMT1 down-regulation represses hTERT expression via recruiting CTCF into demethylated core promoter region of hTERT in HCT116. *Biochem. Biophys. Res. Commun.* **391,** 449–454 (2010).

Chong, L. *et al.* A human telomeric protein. *Science (New York, N.Y.)* **270,** 1663–7 (1995).

Chu, K. *et al.* MiR-512-5p induces apoptosis and inhibits glycolysis by targeting p21 in non-small cell lung cancer cells. *International Journal of Oncology* **48,** 577–586 (2016).

Chung, I., Osterwald, S., Deeg, K. I. & Rippe, K. PML body meets telomere: the beginning of an ALTernate ending? *Nucleus* **3,** 263–75 (2012).

Cifuentes-Rojas, C. & Shippen, D. E. Telomerase regulation. *Mutat. Res.* **730,** 20–7 (2012).

Claussin, C. & Chang, M. The many facets of homologous recombination at telomeres. *Microb. cell (Graz, Austria)* **2,** 308–321 (2015).

Clynes, D. *et al.* Suppression of the alternative lengthening of telomere pathway by the chromatin remodelling factor ATRX. *Nat. Commun.* **6,** 7538 (2015).

Colau, G., Thiry, M., Leduc, V., Bordonné, R. & Lafontaine, D. L. J. The small nucle(ol)ar RNA cap trimethyltransferase is required for ribosome synthesis and intact nucleolar morphology. *Molecular and cellular biology* **24,** 7976–86 (2004).

Cristofari, G. *et al.* Human Telomerase RNA Accumulation in Cajal Bodies Facilitates Telomerase Recruitment to Telomeres and Telomere Elongation. *Molecular Cell* **27,** 882–889 (2007).

Cristofari, G. & Lingner, J. Telomere length homeostasis requires that telomerase levels are limiting. *The EMBO Journal* **25,** 565–574 (2006).

De Lange, T. Shelterin: The protein complex that shapes and safeguards human telomeres. *Genes and Development* **19,** 2100–2110 (2005).

Denchi, E. L. & de Lange, T. Protection of telomeres through independent control of ATM and ATR by TRF2 and POT1. *Nature* **448,** 1068–1071 (2007).

Deng, Z., Norseen, J., Wiedmer, A., Riethman, H. & Lieberman, P. M. TERRA RNA Binding to TRF2 Facilitates Heterochromatin Formation and ORC Recruitment at Telomeres. *Mol. Cell* **35,** 403–413 (2009).

Deryusheva, S., Choleza, M., Barbarossa, A., Gall, J. G. & Bordonné, R. Post-transcriptional modification of spliceosomal RNAs is normal in SMN-deficient cells. *RNA* **18,** 31–6 (2012).

Dessain, S. K., Yu, H., Reddel, R. R., Beijersbergen, R. L. & Weinberg, R. A. Methylation of the human telomerase gene CpG island. *Cancer Res.* **60,** 537–41 (2000).

Dilley, R. L. & Greenberg, R. A. ALTernative Telomere Maintenance and Cancer. *Trends in Cancer* **1,** 145–156 (2015).

Dimitrova, N. & de Lange, T. Cell Cycle-Dependent Role of MRN at Dysfunctional Telomeres: ATM Signaling-Dependent Induction of Nonhomologous End Joining (NHEJ) in G1 and Resection-Mediated Inhibition of NHEJ in G2. *Molecular and Cellular Biology* **29,** 5552–5563 (2009).

Diotti, R. & Loayza, D. Shelterin complex and associated factors at human telomeres. *Nucleus* **2,** 119–135 (2011).

Doksani, Y. & de Lange, T. The role of double-strand break repair pathways at functional and dysfunctional telomeres. *Cold Spring Harbor Perspectives in Biology* **6,** a016576–a016576 (2014).

Doksani, Y., Wu, J. Y., De Lange, T. & Zhuang, X. XSuper-resolution fluorescence imaging of telomeres reveals TRF2-dependent T-loop formation. *Cell* **155,** 345–356 (2013).

Dvinge, H. *et al.* The shaping and functional consequences of the microRNA landscape in breast cancer. *Nature* **497,** 378–382 (2013).

Egan, E. D. & Collins, K. An Enhanced H/ACA RNP Assembly Mechanism for Human Telomerase RNA. *Molecular and Cellular Biology* **32,** 2428–2439 (2012).

Egan, E. D. & Collins, K. Specificity and Stoichiometry of Subunit Interactions in the Human Telomerase Holoenzyme Assembled *In Vivo*. *Mol. Cell. Biol.* **30,** 2775–2786 (2010).

Egan, E. D. & Collins, K. Specificity and Stoichiometry of Subunit Interactions in the Human Telomerase Holoenzyme Assembled *In Vivo*. *Mol. Cell. Biol.* **30,** 2775–2786 (2010).

Fabbri, M. *et al.* MicroRNA-29 family reverts aberrant methylation in lung cancer by targeting DNA methyltransferases 3A and 3B. *Proc. Natl. Acad. Sci.* **104,** 15805–15810 (2007).

Feng, Z., Zhang, C., Wu, R. & Hu, W. Tumor suppressor p53 meets microRNAs. *J. Mol. Cell Biol.* **3,** 44–50 (2011).

Franke, J., Gehlen, J. & Ehrenhofer-Murray, A. E. Hypermethylation of yeast telomerase RNA by the snRNA and snoRNA methyltransferase Tgs1. *Journal of Cell Science* **121,** 3553–3560 (2008).

Friedman, R. C., Farh, K. K. H., Burge, C. B. & Bartel, D. P. Most mammalian mRNAs are conserved targets of microRNAs. *Genome Research* **19,** 92–105 (2009).

Fu, D. & Collins, K. Distinct biogenesis pathways for human telomerase RNA and H/ACA small nucleolar RNAs. *Molecular Cell* **11,** 1361–1372 (2003).

Fu, D. & Collins, K. Purification of Human Telomerase Complexes Identifies Factors Involved in Telomerase Biogenesis and Telomere Length Regulation. *Mol. Cell* **28,** 773–785 (2007).

Fumagalli, M. *et al.* Telomeric DNA damage is irreparable and causes persistent DNA-damage-response activation. *Nature Cell Biology* **14,** 355–365 (2012).

Gebeshuber, C. A., Zatloukal, K. & Martinez, J. miR-29a suppresses tristetraprolin, which is a regulator of epithelial polarity and metastasis. *EMBO Rep.* **10,** 400–5 (2009).

Ghosh, A. *et al.* Telomerase directly regulates NF-κB-dependent transcription. *Nat. Cell Biol.* **14,** 1270–1281 (2012).

Gillis, A. J., Schuller, A. P. & Skordalakes, E. Structure of the Tribolium castaneum telomerase catalytic subunit TERT. *Nature* **455,** 633–637 (2008).

Gomez, D. E. *et al. International journal of oncology. International Journal of Oncology* **41,** (University of Crete, Faculty of Medicine, Laboratory of Clinical Virology, 2012).

Granados-López, A. J. *et al.* Use of Mature miRNA Strand Selection in miRNAs Families in Cervical Cancer Development. *Int. J. Mol. Sci.* **18,** (2017).

Greider, C. W. & Blackburn, E. H. A telomeric sequence in the RNA of Tetrahymena telomerase required for telomere repeat synthesis. *Nature* **337,** 331–337 (1989).

Greider, C. W. & Blackburn, E. H. The telomere terminal transferase of tetrahymena is a ribonucleoprotein enzyme with two kinds of primer specificity. *Cell* **51,** 887–898 (1987).

Greider, C. W. & Blackburn, E. H. Identification of a specific telomere terminal transferase activity in tetrahymena extracts. *Cell* **43,** 405–413 (1985).

Griffith, J. D. *et al.* Mammalian telomeres end in a large duplex loop. *Cell* **97,** 503–514 (1999).

Grimson, A. *et al.* MicroRNA Targeting Specificity in Mammals: Determinants beyond Seed Pairing. *Molecular Cell* **27,** 91–105 (2007).

Gu, P. *et al.* Pot1 OB-fold mutations unleash telomere instability to initiate tumorigenesis. *Oncogene* **36,** 1939–1951 (2017).

Hackett, J. A. & Greider, C. W. Balancing instability: dual roles for telomerase and telomere dysfunction in tumorigenesis. *Oncogene* **21,** 619–626 (2002).

Hagelstrom, R. T., Blagoev, K. B., Niedernhofer, L. J., Goodwin, E. H. & Bailey, S. M. Hyper telomere recombination accelerates replicative senescence and may promote premature aging. *Proc. Natl. Acad. Sci. U. S. A.* **107,** 15768–73 (2010).

Hammond, S. M. An overview of microRNAs. *Adv. Drug Deliv. Rev.* **87,** 3–14 (2015).

Hardy, C. D., Schultz, C. S. & Collins, K. Requirements for the dGTP-dependent repeat addition processivity of recombinant Tetrahymena telomerase. *J. Biol. Chem.* **276,** 4863–71 (2001).

Hausmann, S. & Shuman, S. Giardia lamblia RNA cap guanine-N2 methyltransferase (Tgs2). *Journal of Biological Chemistry* **280,** 32101–32106 (2005).

Hausmann, S. *et al.* Genetic and Biochemical Analysis of Yeast and Human Cap Trimethylguanosine Synthase. *J. Biol. Chem.* **283,** 31706–31718 (2008).

Hayflick, L. & Moorhead, P. S. the Serial Cultivation of Human Diploid Cell Strains. *Experimental cell research* **1,** 585–621 (1961).

Hayflick, L. The limited in vitro lifetime of human diploid cell strains. *Experimental Cell Research* **37,** 614–636 (1965).

He, H. *et al.* POT1b protects telomeres from end-to-end chromosomal fusions and aberrant homologous recombination. *The EMBO Journal* **25,** 5180–5190 (2006).

He, X.-X. *et al.* The regulation of microRNA expression by DNA methylation in hepatocellular carcinoma. *Mol. Biosyst.* **11,** 532–9 (2015).

Hebert, M. D. & Poole, A. R. Towards an understanding of regulating Cajal body activity by protein modification. *RNA Biol.* **14,** 761–778 (2017).

Henriksson, S. *et al.* The scaffold protein WRAP53β orchestrates the ubiquitin response critical for DNA double-strand break repair. *Genes Dev.* **28,** 2726–38 (2014).

Henson, J. D. *et al.* DNA C-circles are specific and quantifiable markers of alternative-lengthening-of-telomeres activity. *Nat. Biotechnol.* **27,** 1181–1185 (2009).

Henson, J. D., Neumann, A. A., Yeager, T. R. & Reddel, R. R. Alternative lengthening of telomeres in mammalian cells. *Oncogene* **21,** 598–610 (2002).

Ho, A. *et al.* TRF1 phosphorylation on T271 modulates telomerase-dependent telomere length maintenance as well as the formation of ALT-associated PML bodies. *Sci. Rep.* **6,** 36913 (2016).

Hockemeyer, D. & Collins, K. Control of telomerase action at human telomeres. *Nat. Struct. Mol. Biol.* **22,** 848–852 (2015).

Hockemeyer, D. *et al.* Telomere protection by mammalian Pot1 requires interaction with Tpp1. *Nature Structural & Molecular Biology* **14,** 754–761 (2007).

Holohan, B. *et al.* Cell biology of disease: Telomeropathies: an emerging spectrum disorder. *J. Cell Biol.* **205,** 289–99 (2014).

Houghtaling, B. R., Cuttonaro, L., Chang, W. & Smith, S. A dynamic molecular link between the telomere length regulator TRF1 and the chromosome end protector TRF2. *Current Biology* **14,** 1621–1631 (2004).

Hrdličková, R., Nehyba, J., Bargmann, W., Bose, H. R. & Jr. Multiple tumor suppressor microRNAs regulate telomerase and TCF7, an important transcriptional regulator of the Wnt pathway. *PLoS One* **9,** e86990 (2014).

Hsiao, S. J. & Smith, S. Sister telomeres rendered dysfunctional by persistent cohesion are fused by NHEJ. *Journal of Cell Biology* **184,** 515–526 (2009).

Hu, J. *et al.* Antitelomerase therapy provokes ALT and mitochondrial adaptive mechanisms in cancer. *Cell* **148,** 651–663 (2012).

Hyjek, M., Wojciechowska, N., Rudzka, M., Kołowerzo-Lubnau, A. & Smoliński, D. J. Spatial regulation of cytoplasmic snRNP assembly at the cellular level. *J. Exp. Bot.* **66,** 7019–7030 (2015).

Iliopoulos, D., Satra, M., Drakaki, A., Poultsides, G. A. & Tsezou, A. Epigenetic regulation of hTERT promoter in hepatocellular carcinomas. *International Journal of Oncology* **34,** 391–399 (2009).

Indran, I. R., Hande, M. P. & Pervaiz, S. hTERT Overexpression Alleviates Intracellular ROS Production, Improves Mitochondrial Function, and Inhibits ROS-Mediated Apoptosis in Cancer Cells. *Cancer Res.* **71,** 266–276 (2011).

Iorio, M. V. & Croce, C. M. microRNA involvement in human cancer. *Carcinogenesis* **33,** 1126–1133 (2012).

Iorio, M. V & Croce, C. M. MicroRNA dysregulation in cancer: diagnostics, monitoring and therapeutics. A comprehensive review. *EMBO Mol. Med.* **4,** 143–59 (2012).

Jaskelioff, M. *et al.* Telomerase reactivation reverses tissue degeneration in aged telomerase-deficient mice. *Nature* **469,** 102–106 (2011).

Jiang, J. *et al.* Demethylation drug 5-Aza-2'-deoxycytidine-induced upregulation of miR-200c inhibits the migration, invasion and epithelial-mesenchymal transition of clear cell renal cell carcinoma in vitro. *Oncol. Lett.* **11,** 3167–3172 (2016).

Kan, C. W. S., Howell, V. M., Hahn, M. A. & Marsh, D. J. Genomic alterations as mediators of miRNA dysregulation in ovarian cancer. *Genes, Chromosom. Cancer* **54,** 1–19 (2015).

Kertesz, M., Iovino, N., Unnerstall, U., Gaul, U. & Segal, E. The role of site accessibility in microRNA target recognition. *Nat. Genet.* **39,** 1278–1284 (2007).

Kharbanda, S. *et al.* Regulation of the hTERT telomerase catalytic subunit by the c-Abl tyrosine kinase. *Curr. Biol.* **10,** 568–75 (2000).

Khattar, E. & Tergaonkar, V. Transcriptional Regulation of Telomerase Reverse Transcriptase (TERT) by MYC. *Front. Cell Dev. Biol.* **5,** 1 (2017).

Kibe, T., Osawa, G. A., Keegan, C. E. & de Lange, T. Telomere Protection by TPP1 Is Mediated by POT1a and POT1b. *Molecular and Cellular Biology* **30,** 1059–1066 (2010).

Kim, J. H. *et al.* Ubiquitin ligase MKRN1 modulates telomere length homeostasis through a proteolysis of hTERT. *Genes Dev.* **19,** 776–781 (2005).

Kim, N.-K., Theimer, C. A., Mitchell, J. R., Collins, K. & Feigon, J. Effect of pseudouridylation on the structure and activity of the catalytically essential P6.1 hairpin in human telomerase RNA. *Nucleic Acids Res.* **38,** 6746–56 (2010).

Kim, S. H. *et al.* TIN2, a new regulator of telomere length in human cells. *Nature genetics* **23,** 405–412 (1999).

Koh, C. M. *et al.* Telomerase regulates MYC-driven oncogenesis independent of its reverse transcriptase activity. *J. Clin. Invest.* **125,** 2109–2122 (2015).

Krol, J., Loedige, I. & Filipowicz, W. The widespread regulation of microRNA biogenesis, function and decay. *Nature Reviews Genetics* (2010). doi:10.1038/nrg2843

Lai, A. G. *et al.* The protein subunit of telomerase displays patterns of dynamic evolution and conservation across different metazoan taxa. *BMC Evol. Biol.* **17,** 107 (2017).

Laud, P. R. *et al.* Elevated telomere-telomere recombination in WRN-deficient, telomere dysfunctional cells promotes escape from senescence and engagement of the ALT pathway. *Genes and Development* **19,** 2560–2570 (2005).

Lavin, M. F. Ataxia-telangiectasia: from a rare disorder to a paradigm for cell signalling and cancer. *Nature Reviews Molecular Cell Biology* **9,** 759–769 (2008).

Leão, R. R. *et al.* 422 TERT promoter methylation is a pan-cancer biomarker with prognostic significance in prostate cancer patients. *Eur. Urol. Suppl.* **14,** e422–e422a (2015).

Lee, J. H., Khadka, P., Baek, S. H. & Chung, I. K. CHIP Promotes Human Telomerase Reverse Transcriptase Degradation and Negatively Regulates Telomerase Activity. *J. Biol. Chem.* **285,** 42033–42045 (2010).

Lee, K. H. *et al.* MicroRNA-296-5p (miR-296-5p) functions as a tumor suppressor in prostate cancer by directly targeting Pin1. *Biochimica et Biophysica Acta - Molecular Cell Research* **1843,** 2055–2066 (2014).

Lemm, I. *et al.* Ongoing U snRNP biogenesis is required for the integrity of Cajal bodies. *Mol. Biol. Cell* **17,** 3221–31 (2006).

Lewis, B. P., Burge, C. B. & Bartel, D. P. Conserved seed pairing, often flanked by adenosines, indicates that thousands of human genes are microRNA targets. *Cell* **120,** 15–20 (2005).

Lewis, K. A. & Tollefsbol, T. O. Regulation of the telomerase reverse transcriptase subunit through epigenetic mechanisms. *Frontiers in Genetics* **7,** (2016).

Li, B., Oestreich, S. & De Lange, T. Identification of human Rap1: Implications for telomere evolution. *Cell* **101,** 471–483 (2000).

Li, J., Lei, H., Xu, Y. & Tao, Z. Z. MiR-512-5p suppresses tumor growth by targeting hTERT in telomerase positive head and neck squamous cell carcinoma in vitro and in vivo. *PLoS ONE* **10,** e0135265 (2015).

Li, L.-C. & Dahiya, R. MethPrimer: designing primers for methylation PCRs. *Bioinformatics* **18,** 1427–1431 (2002).

Li, M. *et al.* microRNA-299-3p inhibits laryngeal cancer cell growth by targeting human telomerase reverse transcriptase mRNA. *Mol. Med. Rep.* **11,** 4645–9 (2015).

Lieberman, R. & You, M. Corrupting the DNA damage response: a critical role for Rad52 in tumor cell survival. *Aging (Albany. NY).* (2017). doi:10.18632/aging.101263

Lin, J. *et al.* Functional interplay between SA1 and TRF1 in telomeric DNA binding and DNA-DNA pairing. *Nucleic Acids Res.* **44,** 6363–76 (2016).

Liu, H. *et al.* hTERT promotes cell adhesion and migration independent of telomerase activity. *Sci. Rep.* **6,** 22886 (2016).

Liu, H. *et al.* The role of MMP-1 in breast cancer growth and metastasis to the brain in a xenograft model. *BMC Cancer* **12,** 583 (2012).

Liu, Z. *et al.* Telomerase reverse transcriptase promotes epithelial–mesenchymal transition and stem cell-like traits in cancer cells. *Oncogene* **32,** 4203–4213 (2013).

Lopez-Bertoni, H. *et al.* Epigenetic modulation of a miR-296-5p:HMGA1 axis regulates Sox2 expression and glioblastoma stem cells. *Oncogene* **35,** 4903–4913 (2016).

Low, K. C. & Tergaonkar, V. Telomerase: central regulator of all of the hallmarks of cancer. *Trends Biochem. Sci.* **38,** 426–434 (2013).

Lu, J. *et al.* MicroRNA expression profiles classify human cancers. *Nature* **435,** 834–838 (2005).

Machyna, M., Heyn, P. & Neugebauer, K. M. Cajal bodies: where form meets function. *Wiley Interdiscip. Rev. RNA* **4,** 17–34 (2013).

Machyna, M., Neugebauer, K. M. & Staněk, D. Coilin: The first 25 years. *RNA Biol.* **12,** 590–6 (2015).

Maciejowski, J., Li, Y., Bosco, N., Campbell, P. J. & de Lange, T. Chromothripsis and Kataegis Induced by Telomere Crisis. *Cell* **163,** 1641–1654 (2015).

MacNeil, D. E., Bensoussan, H. J. & Autexier, C. Telomerase Regulation from Beginning to the End. *Genes (Basel).* **7,** (2016).

Maine, I. P., Chen, S.-F. & Windle, B. Effect of dGTP Concentration on Human and CHO Telomerase †. *Biochemistry* **38,** 15325–15332 (1999).

Maloisel, L., Fabre, F. & Gangloff, S. DNA Polymerase  Is Preferentially Recruited during Homologous Recombination To Promote Heteroduplex DNA Extension. *Molecular and Cellular Biology* **28,** 1373–1382 (2008).

Maréchal, A. & Zou, L. RPA-coated single-stranded DNA as a platform for post-translational modifications in the DNA damage response. *Cell Res.* **25,** 9–23 (2015).

Maréchal, A. & Zou, L. RPA-coated single-stranded DNA as a platform for post-translational modifications in the DNA damage response. *Cell Res.* **25,** 9–23 (2015).

Martinez, P. *et al.* Increased telomere fragility and fusions resulting from TRF1 deficiency lead to degenerative pathologies and increased cancer in mice. *Genes Dev.* **23,** 2060–2075 (2009).

Martínez, P. & Blasco, M. A. Telomere-driven diseases and telomere-targeting therapies. *The Journal of Cell Biology* **216,** 875–887 (2017).

Martínez, P. & Blasco, M. A. Telomeric and extra-telomeric roles for telomerase and the telomere-binding proteins. *Nature Reviews Cancer* **11,** 161–176 (2011).

Martinez, P. *et al.* Mammalian Rap1 controls telomere function and gene expression through binding to telomeric and extratelomeric sites. *Nature Cell Biology* **12,** 768–780 (2010).

McClintock, B. The Behavior in Successive Nuclear Divisions of a Chromosome Broken at Meiosis. *Proceedings of the National Academy of Sciences of the United States of America* **25,** 405–16 (1939).

McKerlie, M., Walker, J. R., Mitchell, T. R. H., Wilson, F. R. & Zhu, X.-D. Phosphorylated (pT371)TRF1 is recruited to sites of DNA damage to facilitate homologous recombination and checkpoint activation. *Nucleic Acids Res.* **41,** 10268–10282 (2013).

Meijer, H. A., Smith, E. M. & Bushell, M. Regulation of miRNA strand selection: follow the leader? *Biochem. Soc. Trans.* **42,** 1135–1140 (2014).

Merritt, W. M. *et al.* Dicer, Drosha, and Outcomes in Patients with Ovarian Cancer. *N. Engl. J. Med.* **359,** 2641–2650 (2008).

Meyne, J., Ratliff, R. L. & Moyzis, R. K. Conservation of the human telomere sequence (TTAGGG). among vertebrates (vertebrate evolution/synthetic oligodeoxynucleotides/in situ hybridization/repetitive DNA). *Evolution* **86,** 7049–7053 (1989).

Mitchell, J. R. & Collins, K. Human Telomerase Activation Requires Two Independent Interactions between Telomerase RNA and Telomerase Reverse Transcriptase. *Molecular Cell* **6,** 361–371 (2000).

Mitomo, S. *et al.* Downregulation of miR-138 is associated with overexpression of human telomerase reverse transcriptase protein in human anaplastic thyroid carcinoma cell lines. *Cancer Sci.* **99,** 280–286 (2008).

Moretti, F., Thermann, R. & Hentze, M. W. Mechanism of translational regulation by miR-2 from sites in the 5' untranslated region or the open reading frame. *Rna* **16,** 2493–2502 (2010).

Morin, G. B. The human telomere terminal transferase enzyme is a ribonucleoprotein that synthesizes TTAGGG repeats. *Cell* **59,** 521–529 (1989).

Mott, J. L. *et al.* Transcriptional suppression of mir-29b-1/mir-29a promoter by c-Myc, hedgehog, and NF-kappaB. *J. Cell. Biochem.* **110,** 1155–1164 (2010).

Mouaikel, J., Verheggen, C., Bertrand, E., Tazi, J. & Bordonné, R. Hypermethylation of the cap structure of both yeast snRNAs and snoRNAs requires a conserved methyltransferase that is localized to the nucleolus. *Molecular Cell* **9,** 891–901 (2002).

Nabetani, A. & Ishikawa, F. Unusual Telomeric DNAs in Human Telomerase-Negative Immortalized Cells. *Mol. Cell. Biol.* **29,** 703–713 (2009).

Nakamura, T., Canaani, E. & Croce, C. M. Oncogenic All1 fusion proteins target Drosha-mediated microRNA processing. *Proc. Natl. Acad. Sci.* **104,** 10980–10985 (2007).

Nandakumar, J. & Cech, T. R. Finding the end: recruitment of telomerase to telomeres. *Nature reviews. Molecular cell biology* **14,** 69–82 (2013).

Narayan, A. *et al.* SPECIAL SECTION: MALARIA RESEARCH Regulation of gene expression in Plasmodium falciparum. *Curr. Sci.* **102,** (2012).

Natarajan, S. & McEachern, M. J. Recombinational Telomere Elongation Promoted by DNA Circles. *Molecular and Cellular Biology* **22,** 4512–4521 (2002).

Neumann, A. A. *et al.* Alternative lengthening of telomeres in normal mammalian somatic cells. *Genes Dev.* **27,** 18–23 (2013).

Nicholls, C., Li, H., Wang, J. Q. & Liu, J. P. Molecular regulation of telomerase activity in aging. *Protein and Cell* **2,** 726–738 (2011).

Niederer, R. O. & Zappulla, D. C. Refined secondary-structure models of the core of yeast and human telomerase RNAs directed by SHAPE. *Rna* **21,** 254–261 (2015).

Nikitina, T. & Woodcock, C. L. Closed chromatin loops at the ends of chromosomes. *Journal of Cell Biology* **166,** 161–165 (2004).

Nora, G. J., Buncher, N. A. & Opresko, P. L. Telomeric protein TRF2 protects Holliday junctions with telomeric arms from displacement by the Werner syndrome helicase. *Nucleic Acids Res.* **38,** 3984–98 (2010).

Ntini, E. *et al.* Polyadenylation site-induced decay of upstream transcripts enforces promoter directionality. *Nat. Struct. Mol. Biol.* **20,** 923–8 (2013).

Nunes, V. S. & Moretti, N. S. Nuclear subcompartments: an overview. *Cell Biol. Int.* **41,** 2–7 (2017).

O'Connor, M. S., Safari, A., Xin, H., Liu, D. & Songyang, Z. A critical role for TPP1 and TIN2 interaction in high-order telomeric complex assembly. *Proceedings of the National Academy of Sciences* **103,** 11874–11879 (2006).

O'Sullivan, R. J. *et al.* Rapid induction of alternative lengthening of telomeres by depletion of the histone chaperone ASF1. *Nature Structural & Molecular Biology* **21,** 167–174 (2014).

Oeseburg, H., De Boer, R. A., Van Gilst, W. H. & Van Der Harst, P. Telomere biology in healthy aging and disease. *Pflugers Archiv European Journal of Physiology* **459,** 259–268 (2010).

Oeseburg, H., de Boer, R. A., van Gilst, W. H. & van der Harst, P. Telomere biology in healthy aging and disease. *Pflügers Arch. - Eur. J. Physiol.* **459,** 259–268 (2010).

Ogg, S. C. & Lamond, A. I. Cajal bodies and coilin—moving towards function. *J. Cell Biol.* **159,** 17–21 (2002).

Okamoto, K. *et al.* A two-step mechanism for TRF2-mediated chromosome-end protection. *Nature* **494,** 502–505 (2013).

Olovnikov, A. M. A theory of marginotomy. The incomplete copying of template margin in enzymic synthesis of polynucleotides and biological significance of the phenomenon. *Journal of Theoretical Biology* **41,** 181–190 (1973).

Opresko, P. L. *et al.* Telomere-binding Protein TRF2 Binds to and Stimulates the Werner and Bloom Syndrome Helicases. *J. Biol. Chem.* **277,** 41110–41119 (2002).

Palm, W. & de Lange, T. How Shelterin Protects Mammalian Telomeres. *Annual Review of Genetics* **42,** 301–334 (2008).

Parodi, F. *et al.* Epigenetic dysregulation in neuroblastoma: A tale of miRNAs and DNA methylation. *Biochim. Biophys. Acta* **1859,** 1502–1514 (2016).

Patel, P. L., Suram, A., Mirani, N., Bischof, O. & Herbig, U. Derepression of hTERT gene expression promotes escape from oncogene-induced cellular senescence. *Proc. Natl. Acad. Sci. U. S. A.* **113,** E5024-33 (2016).

Pegoraro, S. *et al.* HMGA1 promotes metastatic processes in basal-like breast cancer regulating EMT and stemness. *Oncotarget* **4,** 1293–308 (2013).

Pettigrew, K. A. *et al.* Differential TERT promoter methylation and response to 5-aza-2′-deoxycytidine in acute myeloid leukemia cell lines: TERT expression, telomerase activity, telomere length, and cell death. *Genes, Chromosom. Cancer* **51,** 768–780 (2012).

Pickett, H. A. & Reddel, R. R. Molecular mechanisms of activity and derepression of alternative lengthening of telomeres. *Nat. Struct. Mol. Biol.* **22,** 875–880 (2015).

Podlevsky, J. D., Bley, C. J., Omana, R. V, Qi, X. & Chen, J. J.-L. The telomerase database. *Nucleic Acids Res.* **36,** D339-43 (2008).

Poulet, A. *et al.* TRF2 promotes, remodels and protects telomeric Holliday junctions. *The EMBO Journal* **28,** 641–651 (2009).

Prescott, J., Wentzensen, I. M., Savage, S. A. & De Vivo, I. Epidemiologic evidence for a role of telomere dysfunction in cancer etiology. *Mutat. Res. Mol. Mech. Mutagen.* **730,** 75–84 (2012).

Qin, X., Qi, B. & Zhao, B. Alternative lengthening of telomeres is induced by telomerase inhibitors in Barrett's esophageal cells. *Oncology Reports* **29,** 1399–1404 (2013).

Renaud, S. *et al.* Dual role of DNA methylation inside and outside of CTCF-binding regions in the transcriptional regulation of the telomerase hTERT gene. *Nucleic Acids Research* **35,** 1245–1256 (2007).

Rippe, K. & Luke, B. TERRA and the state of the telomere. *Nat. Struct. Mol. Biol.* **22,** 853–858 (2015).

Robson, J. E., Eaton, S. A., Underhill, P., Williams, D. & Peters, J. MicroRNAs 296 and 298 are imprinted and part of the GNAS/Gnas cluster and miR-296 targets IKBKE and Tmed9. *RNA* **18,** 135–144 (2012).

Roth, C., Kasimir-Bauer, S., Pantel, K. & Schwarzenbach, H. Screening for circulating nucleic acids and caspase activity in the peripheral blood as potential diagnostic tools in lung cancer. *Mol. Oncol.* **5,** 281–291 (2011).

Rubis, B. *et al.* Telomerase downregulation induces proapoptotic genes expression and initializes breast cancer cells apoptosis followed by DNA fragmentation in a cell type dependent manner. *Molecular Biology Reports* **40,** 4995–5004 (2013).

Sagie, S. *et al.* Telomeres in ICF syndrome cells are vulnerable to DNA damage due to elevated DNA:RNA hybrids. *Nat. Commun.* **8,** 14015 (2017).

Sahin, E. & DePinho, R. A. Axis of ageing: telomeres, p53 and mitochondria. *Nat. Rev. Mol. Cell Biol.* **13,** 397–404 (2012).

Sahin, U., Lallemand-Breitenbach, V. & de Thé, H. PML nuclear bodies: regulation, function and therapeutic perspectives. *J. Pathol.* **234,** 289–291 (2014).

Saito, Y. *et al.* Chromatin remodeling at Alu repeats by epigenetic treatment activates silenced microRNA-512-5p with downregulation of Mcl-1 in human gastric cancer cells. *Oncogene* **28,** 2738–2744 (2009).

Sarek, G., Marzec, P., Margalef, P. & Boulton, S. J. Molecular basis of telomere dysfunction in human genetic diseases. *Nature Structural & Molecular Biology* **22,** 867–874 (2015).

Sasaki, T. *et al.* AKT activation and telomerase reverse transcriptase expression are concurrently associated with prognosis of gastric cancer. *Pathobiology* **81,** 36–41 (2014).

Sauerwald, A. *et al.* Structure of active dimeric human telomerase. *Nat. Struct. Mol. Biol.* **20,** 454–460 (2013).

Savi, F. *et al. miR-296* /Scribble axis is deregulated in human breast cancer and *miR-296* restoration reduces tumour growth *in vivo*. *Clin. Sci.* **127,** 233–242 (2014).

Savic, V. *et al.* Formation of Dynamic γ-H2AX Domains along Broken DNA Strands Is Distinctly Regulated by ATM and MDC1 and Dependent upon H2AX Densities in Chromatin. *Mol. Cell* **34,** 298–310 (2009).

Schmidt, J. C. & Cech, T. R. Human telomerase: biogenesis, trafficking, recruitment, and activation. *Genes Dev.* **29,** 1095–1105 (2015).

Schoeftner, S. & Blasco, M. A. Developmentally regulated transcription of mammalian telomeres by DNA-dependent RNA polymerase II. *Nat. Cell Biol.* **10,** 228–236 (2008).

Scott, G. K., Mattie, M. D., Berger, C. E., Benz, S. C. & Benz, C. C. Rapid Alteration of MicroRNA Levels by Histone Deacetylase Inhibition. *Cancer Res.* **66,** 1277–1281 (2006).

Sealey, D. C. F. *et al.* The N-terminus of hTERT contains a DNA-binding domain and is required for telomerase activity and cellular immortalization. *Nucleic Acids Res.* **38,** 2019–35 (2010).

Sfeir, A., Kabir, S., van Overbeek, M., Celli, G. B. & de Lange, T. Loss of Rap1 Induces Telomere Recombination in the Absence of NHEJ or a DNA Damage Signal. *Science* **327,** 1657–1661 (2010).

Sfeir, A. *et al.* Mammalian Telomeres Resemble Fragile Sites and Require TRF1 for Efficient Replication. *Cell* **138,** 90–103 (2009).

Shaham, L., Binder, V., Gefen, N., Borkhardt, A. & Izraeli, S. MiR-125 in normal and malignant hematopoiesis. *Leukemia* **26,** 2011–2018 (2012).

Shampay, J., Szostak, J. W. & Blackburn, E. H. DNA sequences of telomeres maintained in yeast. *Nature* **310,** 154–7 (1984).

Sharma, S. *et al.* REV1 and polymerase ?? facilitate homologous recombination repair. *Nucleic Acids Research* **40,** 682–691 (2012).

Shay, J. W. & Bacchetti, S. A survey of telomerase activity in human cancer. *European Journal of Cancer Part A* **33,** 787–791 (1997).

Shay, J. W., Reddel, R. R. & Wright, W. E. Cancer and Telomeres--An ALTernative to Telomerase. *Science* **336,** 1388–1390 (2012).

Shay, J. W. & Wright, W. E. Role of telomeres and telomerase in cancer. *Semin. Cancer Biol.* **21,** 349–53 (2011).

Shay, J. W. & Wright, W. E. Telomerase therapeutics for cancer: challenges and new directions. *Nature Reviews Drug Discovery* **5,** 577–584 (2006).

Shay, J. W. & Wright, W. E. Hayflick, his limit, and cellular ageing. *Nat. Rev. Mol. Cell Biol.* **1,** 72–76 (2000).

Singhapol, C. *et al.* Mitochondrial Telomerase Protects Cancer Cells from Nuclear DNA Damage and Apoptosis. *PLoS ONE* **8,** e52989 (2013).

Sitaram, R. T. *et al.* Wilms' tumour 1 can suppress hTERT gene expression and telomerase activity in clear cell renal cell carcinoma via multiple pathways. *Br. J. Cancer* **103,** 1255–1262 (2010).

Smogorzewska, A. *et al.* Control of human telomere length by TRF1 and TRF2. *Mol. Cell. Biol.* **20,** 1659–68 (2000).

Stahlhut, C. & Slack, F. J. MicroRNAs and the cancer phenotype: profiling, signatures and clinical implications. *Genome Med.* **5,** 111 (2013).

Stern, J. L., Zyner, K. G., Pickett, H. A., Cohen, S. B. & Bryan, T. M. Telomerase Recruitment Requires both TCAB1 and Cajal Bodies Independently. *Mol. Cell. Biol.* **32,** 2384–2395 (2012).

Strzelecka, M. *et al.* Coilin-dependent snRNP assembly is essential for zebrafish embryogenesis. *Nat. Struct. Mol. Biol.* **17,** 403–409 (2010).

Subhawong, A. P. *et al.* The alternative lengthening of telomeres phenotype in breast carcinoma is associated with HER-2 overexpression. *Mod. Pathol.* **22,** 1423–1431 (2009).

Suenaga, M. *et al.* Histone deacetylase inhibitors suppress telomerase reverse transcriptase mRNA expression in prostate cancer cells. *Int. J. cancer* **97,** 621–5 (2002).

Sun, Y.-M., Lin, K.-Y. & Chen, Y.-Q. Diverse functions of miR-125 family in different cell contexts. *J. Hematol. Oncol.* **6,** 6 (2013).

Sung, P. & Klein, H. Mechanism of homologous recombination: mediators and helicases take on regulatory functions. *Nature Reviews Molecular Cell Biology* **7,** 739–750 (2006).

Swuec, P. & Costa, A. Molecular mechanism of double Holliday junction dissolution. *Cell Biosci.* **4,** 36 (2014).

Szostak, J. W. & Blackburn, E. H. Cloning yeast telomeres on linear plasmid vectors. *Cell* **29,** 245–255 (1982).

Takai, K. K., Kibe, T., Donigian, J. R., Frescas, D. & de Lange, T. Telomere Protection by TPP1/POT1 Requires Tethering to TIN2. *Molecular Cell* **44,** 647–659 (2011).

Tang, W., Kannan, R., Blanchette, M. & Baumann, P. Telomerase RNA biogenesis involves sequential binding by Sm and Lsm complexes. *Nature* **484,** 260–264 (2012).

Teichroeb, J. H., Kim, J. & Betts, D. H. The role of telomeres and telomerase reverse transcriptase isoforms in pluripotency induction and maintenance. *RNA Biol.* **13,** 707–719 (2016).

Thomson, J. M. *et al.* Extensive post-transcriptional regulation of microRNAs and its implications for cancer. *Genes Dev.* **20,** 2202–2207 (2006).

Trionfini, P., Benigni, A. & Remuzzi, G. MicroRNAs in kidney physiology and disease. *Nat. Rev. Nephrol.* **11,** 23–33 (2015).

Tseng, C.-K. *et al.* Human Telomerase RNA Processing and Quality Control. *Cell Rep.* **13,** 2232–2243 (2015).

Turinetto, V. & Giachino, C. Multiple facets of histone variant H2AX: a DNA double-strand-break marker with several biological functions. *Nucleic Acids Res.* **43,** 2489–98 (2015).

Uringa, E.-J. *et al.* RTEL1 contributes to DNA replication and repair and telomere maintenance. *Mol. Biol. Cell* **23,** 2782–92 (2012).

Vaira, V. *et al.* miR-296 regulation of a cell polarity-cell plasticity module controls tumor progression. *Oncogene* **31,** 27–38 (2012).

Vega, L. R., Mateyak, M. K. & Zakian, V. A. Getting to the end: telomerase access in yeast and humans. *Nature Reviews Molecular Cell Biology* **4,** 948–959 (2003).

Venteicher, A. S. *et al.* A Human Telomerase Holoenzyme Protein Required for Cajal Body Localization and Telomere Synthesis. *Science* **323,** 644–648 (2009).

Venteicher, A. S. & Artandi, S. E. TCAB1: Driving telomerase to Cajal bodies. *Cell Cycle* **8,** 1329–1331 (2009).

Verheggen, C. & Bertrand, E. CRM1 plays a nuclear role in transporting snoRNPs to nucleoli in higher eukaryotes. *Nucleus* **3,** 132–137 (2012).

Vogan, J. M. & Collins, K. Dynamics of Human Telomerase Holoenzyme Assembly and Subunit Exchange across the Cell Cycle. *J. Biol. Chem.* **290,** 21320–35 (2015).

Voorhoeve, P. M. *et al.* A genetic screen implicates miRNA-372 and miRNA-373 as oncogenes in testicular germ cell tumors. *Advances in Experimental Medicine and Biology* **604,** 17–46 (2007).

Walsh, K. M. *et al.* Telomere maintenance and the etiology of adult glioma. *Neuro. Oncol.* **17,** 1445–52 (2015).

Wang, R. C., Smogorzewska, A. & De Lange, T. Homologous recombination generates t-loop-sized deletions at human telomeres. *Cell* **119,** 355–368 (2004).

Watson, J. D. Origin of concatemeric T7 DNA. *Nature: New biology* **239,** 197–201 (1972).

Wei, J. J. *et al.* Regulation of HMGA1 expression by MicroRNA-296 affects prostate cancer growth and invasion. *Clinical Cancer Research* **17,** 1297–1305 (2011).

Wilson, J. S. J. *et al.* Localization-dependent and -independent roles of SLX4 in regulating telomeres. *Cell Reports* **4,** 853–860 (2013).

Wu, L. *et al.* Pot1 Deficiency Initiates DNA Damage Checkpoint Activation and Aberrant Homologous Recombination at Telomeres. *Cell* **126,** 49–62 (2006).

Wu, R. A., Tam, J. & Collins, K. DNA-binding determinants and cellular thresholds for human telomerase repeat addition processivity. *EMBO J.* **36,** 1908–1927 (2017).

Wyatt, H. D. M., West, S. C. & Beattie, T. L. InTERTpreting telomerase structure and function. *Nucleic Acids Research* **38,** 5609–5622 (2010).

Xu, C. *et al.* MiR-296-5p suppresses cell viability by directly targeting PLK1 in non-small cell lung cancer. *Oncology Reports* **35,** 497–503 (2016).

Yao, M. C., Blackburn, E. & Gall, J. Tandemly repeated C-C-C-C-A-A hexanucleotide of Tetrahymena rDNA is present elsewhere in the genome and may be related to the alteration of the somatic genome. *Journal of Cell Biology* **90,** 515–520 (1981).

Yeager, T. R. *et al.* Telomerase-negative immortalized human cells contain a novel type of promyelocytic leukemia (PML) body. *Cancer Research* **59,** 4175–4179 (1999).

Yuan, P. *et al.* Telomerase Cajal body protein 1 depletion inhibits telomerase trafficking to telomeres and induces G1 cell cycle arrest in A549 cells. *Oncol. Lett.* **8,** 1009–1016 (2014).

Zaug, A. J., Podell, E. R., Nandakumar, J. & Cech, T. R. Functional interaction between telomere protein TPP1 and telomerase. *Genes Dev.* **24,** 613–622 (2010).

Zhang, D. *et al.* miR-1182 attenuates gastric cancer proliferation and metastasis by targeting the open reading frame of hTERT. *Cancer Lett.* **360,** 151–159 (2015).

Zheng, S. *et al.* Mutational analysis of Encephalitozoon cuniculi mRNA cap (guanine-N7) methyltransferase, structure of the enzyme bound to sinefungin, and evidence that cap methyltransferase is the target of sinefungin's antifungal activity. *Journal of Biological Chemistry* **281,** 35904–35913 (2006).

Zhong, F. L. *et al.* TPP1 OB-fold domain controls telomere maintenance by recruiting telomerase to chromosome ends. *Cell* **150,** 481–494 (2012).

Zhong, F. *et al.* Disruption of telomerase trafficking by TCAB1 mutation causes dyskeratosis congenita service Disruption of telomerase trafficking by TCAB1 mutation causes dyskeratosis congenita. *Genes and Development* **25,** 11–16 (2011).

Zhou, N., Fei, D., Zong, S., Zhang, M. & Yue, Y. MicroRNA-138 inhibits proliferation, migration and invasion through targeting hTERT in cervical cancer. *Oncol. Lett.* **12,** 3633–3639 (2016).

Zhu, X. D. *et al.* ERCC1/XPF Removes the 3??? Overhang from Uncapped Telomeres and Represses Formation of Telomeric DNA-Containing Double Minute Chromosomes. *Molecular Cell* **12,** 1489–1498 (2003).

Zhu, Y. *et al.* Cloning and characterization of PIMT, a protein with a methyltransferase domain, which interacts with and enhances nuclear receptor coactivator PRIP function. *Proc. Natl. Acad. Sci.* **98,** 10380–10385 (2001).

Zinn, R. L., Pruitt, K., Eguchi, S., Baylin, S. B. & Herman, J. G. hTERT Is Expressed in Cancer Cell Lines Despite Promoter DNA Methylation by Preservation of Unmethylated DNA and Active Chromatin around the Transcription Start Site. *Cancer Res.* **67,** 194–201 (2007).